Università degli Studi di Cagliari

DOTTORATO DI RICERCA IN NEUROSCIENZE

Ciclo XXX

"Influence of Amphetamine-type stimulants in the Central Nervous System: abuse and neurotoxicity"

Settore scientifico disciplinare di afferenza

BIO/14- Farmacologia

Presentata da: Dott.ssa Liliana Contu

Coordinatore Dottorato: Prof. Antonio Argiolas

Tutor: Prof.ssa Micaela Morelli

Esame finale anno accademico 2016 – 2017

Thanks to
University of Cagliari
and
National Institute on Drug Abuse (Baltimore).

Index

List of abbreviations

The following abbreviations have been used in the present report:

ABC	Avidin–biotin–peroxidase complex
ADHD	Attention-Deficit/Hyperactivity Disorder
AKT	Protein Kinase B
AMPK	AMP-activated protein kinase
AMPH	Amphetamine
AP1	Activator protein
AMPT	α-methyl-p-tyrosine
aPKC	Atypical protein kinase c
ATS	Amphetamine type stimulants
BBB	Blood brain barrier
BDNF	Brain-derived neurotrophic factor
bZIP	Basic region leucine zipper
cAMP	Cyclic AMP
Cav2.2	Voltage-gated calcium channels
2C-B	4-bromo-2,5-dimetossi-feniletilamina
CBP	CREB-binding protein
CNS	Central nervous system
CPu	Caudate-putamen or striatum
CREB	Cyclic AMP response element binding
Ct	Control group
D1	Dopamine receptor 1
D2	Dopamine receptor 2
DA	Dopamine
DAB	Diaminobenzidine
DAT	Dopamine transporters
Dexras	Dexamethasone-induced Ras-related protein
DOPAC	3,4-Dihydroxyphenylacetic acid
Egr	Early growth response protein
Egr-1 or Zif268	Early growth response gene 1
Egr-2	Early growth response gene 2
Egr-3	Early growth response gene 3
ELK1	ETS domain-containing protein
EMCDDA	European agency of drugs abuse
FR-1	Fixed ratio
Fra2	Fos-related antigen 2
Fra1	Fos-related antigen 1
Gαi	G-alpha proteins of the i class
GFAP	Glial fibrillary acidic protein

GLU	Glutamate
GPCR	G protein receptors
GTP	Guanosine-5'-triphosphate
H_2O_2	Hydrogen peroxides
HHA	3, 4-dihydroxyamphetamine
HHMA	3, 4-dihydroxymethamphetamine
HMA	4-hydroxy-3-methoxyamphetamine
HMMA	4-hydroxy-3-methoxymethamphetamine
HVA	Homovanillic acid
5-HT	Serotonin
Iba-1	Ionized calcium binding adaptor molecule 1
IEGs	Immediate-early genes
IgG	Immunoglobulin G
i.p.	Intraperitoneal injection
ISPAD	Italian population survey on alcohol and other drugs
Jun	Jun family members
KO	Knockout
L-dopa	Levodopa
mA	Milliampere
MAO	Monoamine oxidase
MAPK	Mitogen-activated protein kinase
MBDB	Methylenedioxy-N-methyl-α-ethylphenylethylamine
MDA	Methylenedioxyamphetamine
MDEA	Methylenedioxyethylamphetamine
MDMA	3,4 methylenedioxymethamphetamine or ectasy
METH	Methamphetamine
METH SA	Methamphetamine self-administration
MPP^+	1-methyl-4-phenylpyridinium
MPTP	1-methyl-4-phenyl-1,2,3,6-tetrahydropyridine
M-SR	Shock-resistant
M-SS	Shock-sensitive
mTORC1	Mammalian target of rapamycin complex 1
NA	Norepinephrine or noradrenaline
NAc	Nucleus accumbens
NE	Norephedrine
NET	Noradrenaline transporter
NIDA	National Institute on drug abuse
NO	Nitric oxide
NPS	New psychoactive substances
NR	Nuclear hormone receptor
Nr4A	Nuclear receptor subfamily 4, group A
NR4A1 or Nur77	Nuclear receptor subfamily 4, group A1

NR4A2 or Nurr1	Nuclear receptor subfamily 4, group A2
NR4A3 or NOR-1	Nuclear receptor subfamily 4, group A3
O_2^-	Superoxide radicals
•OH	Hydroxyl radicals
$ONOO^-$	Reactive peroxynitrite
o.s.	Oral somministration
PCR	Polymerase Chain Reaction
PD	Parkinson's disease
β-PEA	β-phenethylamine
PI3K	Phosphatidylinositol 3-kinase
PIP3	Inositol triphosphate
PKA	Protein kinase A
Rhes	Ras Homolog Enriched in striatum
$Rhes^{-/-}$	Rhes Knockout
$Rhes^{+/+}$	Rhes Wild-type
ROS	Reactive oxygen species
SA	Self-administration
s.c.	Subcutaneous injection
SERT	Serotonin transporters
SNc	Substantia nigra pars compacta
STP/DOM	2,5-Dimethoxy-4-METHylamphetamine
TH	Tyrosine hydroxylase
TH (+)	Tyrosine hydroxylase positive
TrkB	Tyrosine kinase receptor type 2
UNODC	United Nations Office on Drugs and Crime
VMAT2	Vesicular monoamine transporter 2
VTA	Ventral tegmental area
WDR	World Drug Report
Y	Yoked group
Y-SR	Yoked group shock resistance
Y-SS	Yoked group shock sensitive

1. Introduction

1.1 Amphetamine type stimulants: Definitions and epidemiology

Amphetamines are synthetic drugs characterized by their psychostimulant effects on the central nervous system (CNS), and include a wide range of substances such as alpha-methylphenethylamine or amphetamine (AMPH), N-methylamphetamine or methamphetamine (METH) and 3,4 methylenedioxymethamphetamine (MDMA) also known as “ecstasy”.

All these drugs are included in Amphetamine type stimulants *(ATS)* group and they were medically used during the 19th and the 20th century for the treatment of asthma and congestion, treatment of obesity as well as to alleviate fatigue during World War II (Kalant, 1966; Rasmussen et al., 2008; Fischman et al., 2001). Nowadays, ATS (excluding MDMA) are the second most widely abused drug in the world after cannabis (United Nations Office on Drugs and Crime (UNODC) 2017 report), with up to 1.2% of the adult population (15-64 years old) consuming ATS (**Figure 1**), (World Drug Report (WDR), 2012).

Fig. 1

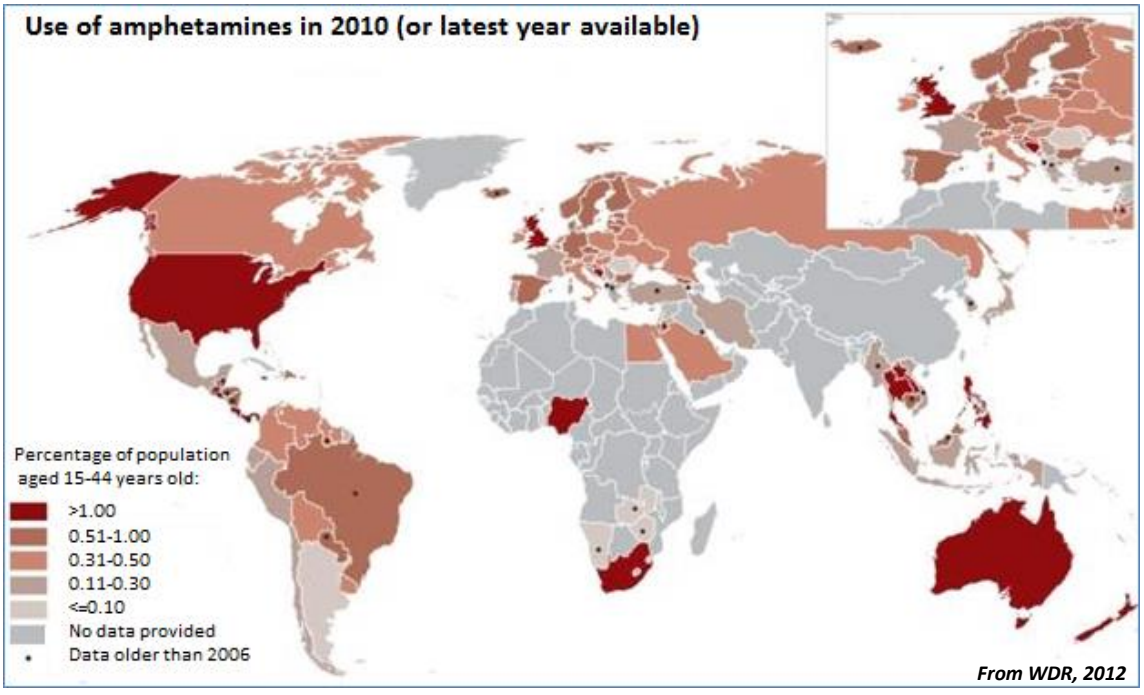

Use of ATS drugs in the World expressed in percentage of population between 15-44 years old.

According to the 2015 WDR, the global market for synthetic drugs continues to be dominated by the increase of METH pills in East and South-East Asia; meanwhile the use of crystalline (highly purified form) METH is growing in various regions of North America. In Europe, several countries have recently seen the decline of MDMA, since new psychoactive substances (NPS) like mephedrone were introduced as substitutes (UNODC 2015 report). According to National Institute on Drug Abuse (NIDA) estimates for 2015, 4.1% of the people at 8th graders, 6.8% of 10th graders, and 7.7% of 12th graders used ATS during the past year (NIDA 2015 report). In Italy, the project called ISPAD (Italian population survey on alcohol and other drugs), reckons that 160.000 people (0.4%) used ATS drugs, with an adult abuse increase (35-44 years old) and a little reduction in the under 35 (Institute of clinical physiology of Cnr 2014 report). European agency of drugs abuse (EMCDDA), in the 2017, located Italy at 17th and 16th position, respectively, in Europe for the abuse of ATS and MDMA in young adults (15-34 years old), (**Figure 2**).

Fig. 2

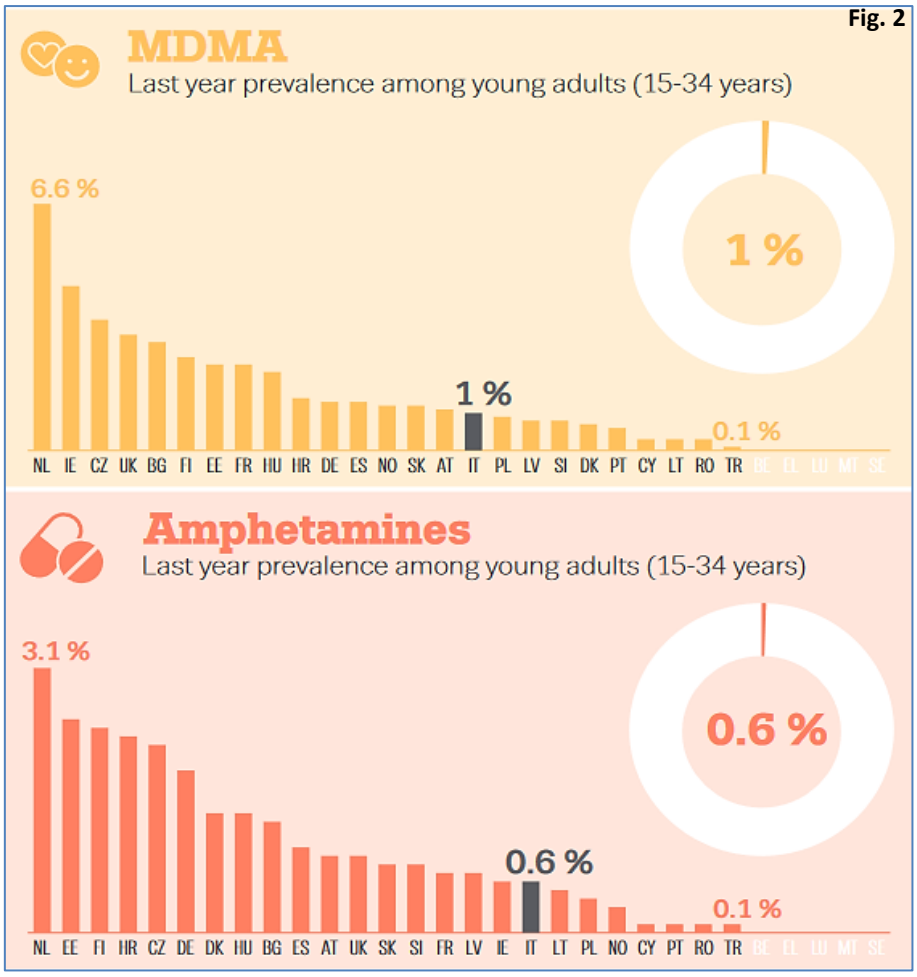

European dashboard of drugs use prevalence (%) in young adults (15-34 years old) and ranking versus European States. Countries with no data available are marked in white. ***From EMCDDA 2017.***

1.2 Molecular structure of ATS

The ATS, structurally, are a group of substances (UNODC report 2006) related to the compound known as *β-phenethylamine* (β-PEA), a naturally neurotransmitter in the body (Irsfeld et al., 2013).

Fig. 3

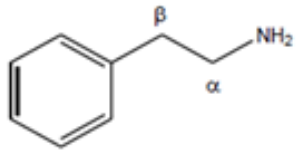

Structure of β -PEA

The structure of β-PEA is presented in the image (**Figure 3**), with characteristics like phenyl ring, carbonyl side-chain and amino moiety. All ATS have similar pharmacological properties on CNS, (Daéid, 2005). Specifically, they act by increasing the production of neurotransmitters such as dopamine (DA), (it enhances the sense of wellbeing and pleasure), (Di Chiara et al., 2007); norepinephrine (NA) (activating wakefulness and motivation) and serotonin (5-HT); see below for further details in the following paragraphs.

Structural modifications on the aromatic ring of β-PEA create multiple synthetic derivatives with different pharmacological properties (Moffat et al., 2004).

Fig. 4

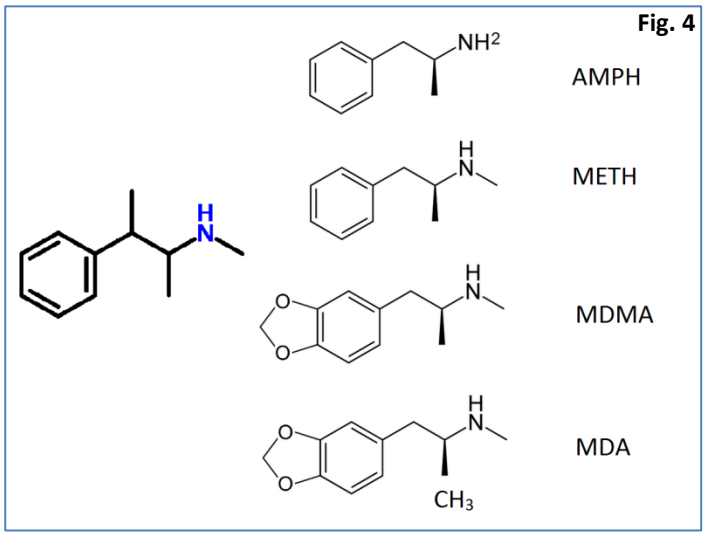

Comparative structures of β-PEA derivatives

For example, ring substituted amphetamines such as MDMA and Methylenedioxyamphetamine (MDA) are associated with low stimulant and, at the same time, hallucinogenic effects; whilst substitutions at the N-terminus, such as METH, are associated with similar psychomotor and anorectic effects to AMPH (**Figure 4**), (Carvalho et al., 2012).

The ATS, in terms of structural characteristics, can be classified into three major sub-groups defined by their substitution patterns on the aromatic ring (King, 2009):

i. No substitution on aromatic ring (e.g. AMPH, METH, fenethylline).
ii. Methylenedioxy-substitution on aromatic ring (e.g. MDA, MDMA, 3, 4-methylenedioxy-N-methyl-α-ethylphenylethylamine (MBDB).
iii. Other substitution patterns, usually including one or more alkyloxy group (e.g. 2, 5-dimethoxy-4-bromophenethylamine or 2C-B; 2, 5-Dimethoxy-4 methylamphetamine (STP/DOM).

The above-mentioned first group acts like psychostimulants, whereas the two other groups resemble the structure of the hallucinogenic Mescaline, which has a methylenedioxy group (–O–CH2–O–) attached to positions 3 and 4 of the phenyl structure and thus it has both stimulant and hallucinogenic effects, such as MDMA, MDA and methylenedioxyethylamphetamine (MDEA), (Kalant et al., 2001).

1.3 Methamphetamine

1.3.1 Generality

In 1893, Nagayoshi Nagai, in Japan, first synthesized METH, a variant of AMPH from the precursor chemical Ephedrine (derived from the plant Ephedra sinica), (Nagai & Kamiyama, 1988; Meredith et al., 2005). METH was used during the World War II (1940), to keep troops awake and improve their endurance (Meredith et al., 2005; McGuinness, 2006), whereas the Japanese Kamikaze pilots were heavily administrated before their suicide missions. In 1971, U.S.A law restricted METH, although it continues to be orally taken today in the USA as a second-line treatment for a number of medical conditions, including the attention deficit hyperactivity disorder (ADHD) and the refractory obesity (Mariani et al., 2007; Bray 1993). METH abuse is a serious problem in the USA, Mexico, South America, the Middle East, the Arabian Peninsula, Asia, and Australia (WDR 2000; WDR 2015). METH is a very strong stimulant, as a consequence, even if swallowed at low doses, it can cause an elevated mood and increase alertness, concentration, and energy, at higher doses it can induce psychosis, rhabdomyolysis (a condition in which damaged skeletal muscle tissue breaks down rapidly) and may lead to kidney failure (Rusyniak, 2011). The users feel more complex psychological effects including euphoria, dysphoria, changes in libido, insomnia or wakefulness, self-confidence, sociability, irritability, restlessness, obsessive behaviors as well as anxiety, depression, psychosis, suicide, and violent behaviors (Westfall & Westfall, 2010; O'Connor, 2012). These effects can last for several hours because the elimination half-life of METH ranges from 10 to 12 hours (Schepers et al., 2003). One of the reasons, METH has overtook cocaine in worldwide usage, is that it has a longer half-life (12 hours compared to 90 minutes) and therefore a much longer lasting effects (Meredith et al., 2005).

Human studies show that the metabolism of METH is regulated by the polymorphic cytochrome P450 isozyme CYP2D6 (CP450-2D6), (de la Torre et al., 2012) with formation of two major metabolites: para-hydroxymethamphetamine and AMPH, respectively, from different concurrent pathways (N-demethylation, aromatic hydroxylation and aliphatic hydroxylation at the methylene group next to the benzene ring), (Caldwellet et al., 1972). AMPH can be further metabolized into para-hydroxyamphetamine, N-hydroxyamphetamine and Norephedrine (NE). METH is less readily metabolized in men than in the guinea pigs or rats, but all three species excrete NE derivatives like false neurotransmitters and are involved in the undesirable effects of the chronic intake of METH

(Caldwellet et al., 1972; Brodie et al., 1970). The involvement of the polymorphic P450-2D6 may contribute to inter-individual variability in metabolism (Lin et al., 1997).

1.3.2 Neurotoxicity of Methamphetamine

Neurotoxicity is the capacity of chemical, biologic, or physical agents to cause adverse functional or structural changes in the CNS. Various hypotheses regarding the mechanism responsible for METH-induced neurotoxicity, have been proposed, including high release of monoamines (DA, 5-HT), DA quinones formation synthesized by oxidation of the catechol ring of DA, excitatory amino acid glutamate (GLU) release and hyperthermia (Cadet et al., 2003; Miyazaki et al., 2006). It is likely that interactions between these factors trigger neurotoxicity induced by METH.

METH enters DAergic and 5-HTergic neurons via DA transporters (DAT), serotonin transporters (SERT) and passive diffusion (Rothman and Baumann, 2003, Fleckenstein et al., 2007). Within these neurons, then, METH enters the synaptic vesicles through vesicular monoamine transporter 2 (VMAT2), disrupt the vesicle proton gradient via changes in pH balance and causes DA and 5-HT release into the cytoplasm in rats (Brown et al., 2002; Hansen et al., 2002; Riddle et al., 2002; Halpin et al., 2014). This increase of DA and 5-HT release in the cytoplasm induces a strong efflux of these neurotransmitters from neurons (Sulzer et al., 2005) that causes significant potential-independent action from neurotransmitter efflux (Yamamoto et al., 2010).

Moreover, METH provokes persistent decreases in the levels of DAT and SERT expression (Halpin et al., 2014). A role of DAT in METH toxicity is also supported by studies using DAT knockout mice (KO) that are protected against drug-induced DA depletion in brain region like caudate-putamen (CPu), (Fumagalli et al., 1998). In particular, CPu coordinates multiple aspects of cognition, including motor- and action-planning, decision-making, motivation, reinforcement, and reward perception (Yager et al., 2015). Further studies have recently shown that the administration of the DAT inhibitor, methylphenidate, 1 hour after METH injection, could reverse the decreases in vesicular DA uptake, reductions in VMAT2 ligand binding and decreases in VMAT2 immunoreactivity in vesicular subcellular fractions, 6 hours after injections of the methylphenidate (Hansen et al., 2002).

In DAergic neurons, the rate limiting enzyme for DA synthesis is the tyrosine hydroxylase (TH), an important biomarker used to characterize DA neuron degeneration. Indeed, the α-methyl-p-tyrosine (AMPT) an inhibitor of TH, blocks DA synthesis and assures protection against METH toxicity (Axt et al., 1990). In addition, METH can cause death of DA neurons in the CPu, frontal and parietal cortices, hippocampus and olfactory bulb of rat (Deng et al., 1999; 2001).

Furthermore, in the cytoplasm, DA auto-oxidizes to form toxic DA quinones with generation of reactive oxygen species (ROS) as superoxide radicals (O_2^-) and hydrogen peroxides (H_2O_2) via quinone cycling. Subsequent formation of hydroxyl radicals (•OH), through interactions of O_2^- and H_2O_2 with transition metals, leads to oxidative stress, mitochondrial dysfunctions and peroxidative damage to presynaptic membranes. All these steps reveal an imbalance between the systemic manifestation of ROS and a biological system's ability to readily detoxify the reactive intermediates (e.g. Glutathione, coenzyme Q10, bioflavonoids) or to recover from the resulting damage (proteins, lipids and nucleic acids damage) in rat brains after METH administering (Yamamoto et al., 1998, Kuhn et al., 2006).

Secondary to increases in extracellular DA and 5-HT, GLU has also been implicated in METH-induced neurotoxicity (Sonsalla et al., 1991; Mark et al., 2004) by its increased release in the brain (Abekawa et al., 1994; Mark et al., 2004; Nash and Yamamoto, 1992). Excessive GLU release develops a series of events forming parts of excitotoxicity mechanism. This excitotoxicity leads to a rise of intracellular calcium levels and consequently the activation of calcium-dependent proteolytic enzymes (e.g. calpain), free radical as ROS and nitric oxide (NO) production. Specifically, the increase of NO levels can lead directly to cell damaging or to a reaction with O_2^-, causing the development of highly reactive peroxynitrite (-$ONOO^-$), (Radi et al., 1991). These effects occur primarily in the CPu, but are also seen in the cortex, thalamus, hypothalamus, and hippocampus of mice (Ares-Santos et al., 2012; Granado et al., 2010; 2011; Guilarte et al., 2003; Krasnova & Cadet, 2009; Ricaurte et al., 1980), (**Figure 5).** Besides, excitotoxicity leads to the activation of apoptotic pathways, ultimately culminating in cellular damage (Nicholls, 2004). Recently, it has been shown that Somatostatin, an inhibitor of GLU neurotransmission, has the ability to reduce METH-induced cell death in the CPu (Afanador et al., 2013).

Fig. 5

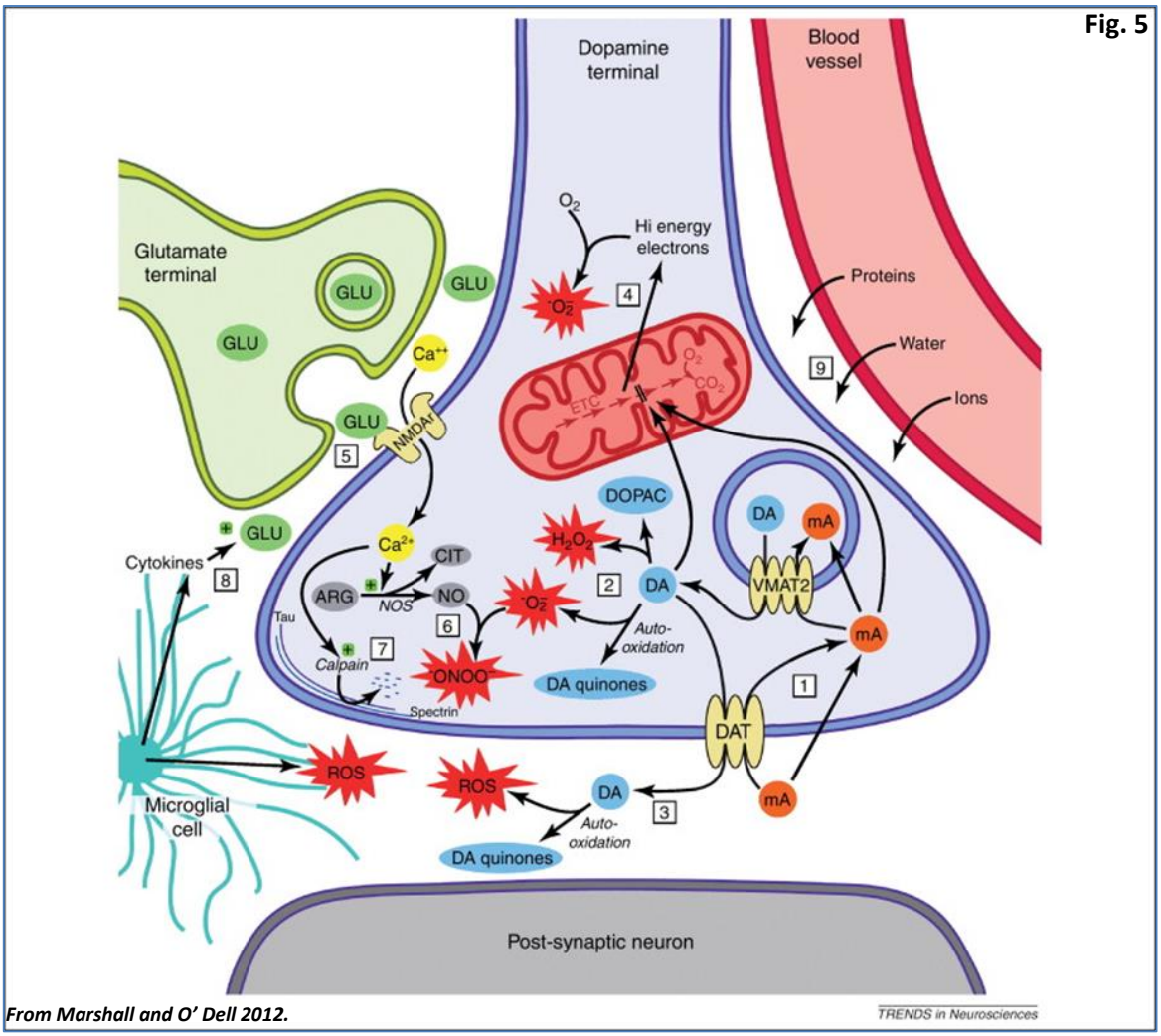

From Marshall and O' Dell 2012.

Mechanisms of METH neurotoxicity. *METH (mA in the graph) enters DAergic terminals, as shown in the right side of the diagram (1), causing efflux of DA from intraneuronal vesicles. This DA is broken down intracellularly, producing reactive species (2) such as hydrogen peroxide (H_2O_2) and superoxide ($-O_2^-$), and is transported to extracellular spaces (3) where it is also oxidized producing reactive oxygen species (ROS). High intracellular concentrations of DA and METH can inhibit the electron transport chain (ETC) in mitochondria (4), causing leakage of high-energy electrons which trigger the formation of superoxide. METH-induced increases in GLU release, seen on the left side of the diagram (5), stimulate NMDA receptors (NMDAR) on DAergic terminals to cause increases in intracellular Ca^{2+}. These Ca^{2+} increases stimulate nitric oxide synthase (NOS) activity, increasing the production of nitric oxide (NO), which can combine with superoxide to form highly-damaging peroxynitrite ($-ONOO^-$), (6). High intracellular Ca^{2+} also stimulates proteolytic enzymes such as calpain (7) which can break down structural proteins such as spectrin and tau, damaging terminal integrity. METH also stimulates microglia to release ROS and cytokines (8) which further increase extracellular GLU levels. Finally, METH causes leakage of the blood brain barrier (BBB), allowing plasma proteins to enter the brain (9), followed by water and ions, causing brain edema and further physiological disruption of neurotransmission.*

Additionally, METH use/abuse can trigger a different mechanism of neurotoxicity: the hyperthermic conditions (**Figure 6**). Hyperthermia is the medical term that refers to the elevated body temperature deriving from a thermoregulation mechanism failure; it occurs when a body produces or absorbs more heat than it dissipates (Gao et al., 2014). This condition usually occurs at temperatures over 40 Celsius degrees or 104 Fahrenheit degrees. At these temperatures, organ dysfunctions ensue and may include liver failure, kidney failure, cerebral edema (swelling of the brain), and 5-HT syndrome may occur (a predictable consequence of excess 5-HTnergic activity at CNS and peripheral 5-HT receptors). Each one of these events can cause death (Rahmani et al., 2011). At low doses, METH does not have significant effects on body temperature, but can produce lethal hyperthermia upon exposure to high doses (Krasnova & Cadet, 2009). METH provokes hyperthermia through a variety of mechanisms involving numerous systems (increase in heat shock protein expression, vasoconstriction, and piloerection in animals), (Kiyatkin et al., 2010; Kousik et al., 2011; Kikuchi-Utsumi et al., 2013). Furthermore, METH induces damage to DAergic nerve terminals in rats and mice, as mentioned above, and this is also associates with elevated body temperature (Bowyer et al., 1994; Miller & O'Callaghan, 2003). Indeed, hyperthermia alone induced by high ambient temperatures did not deplete striatal DA in the absence of METH (Bowyer et al., 1994).

However, it should be noted that the contribution of monoamines in METH hyperthermia can vary depending on environmental conditions and species. For example, depletion of monoamines by pretreatment with the AMPT can attenuate the hyperthermic effects of METH in rats, but not in mice (Metzger et al., 2000; Sandoval et al., 2000; Thomas et al., 2008). This suggests that monoamines may be important, but cannot be considered as the only METH mechanisms provoking hyperthermic effects.

Fig. 6

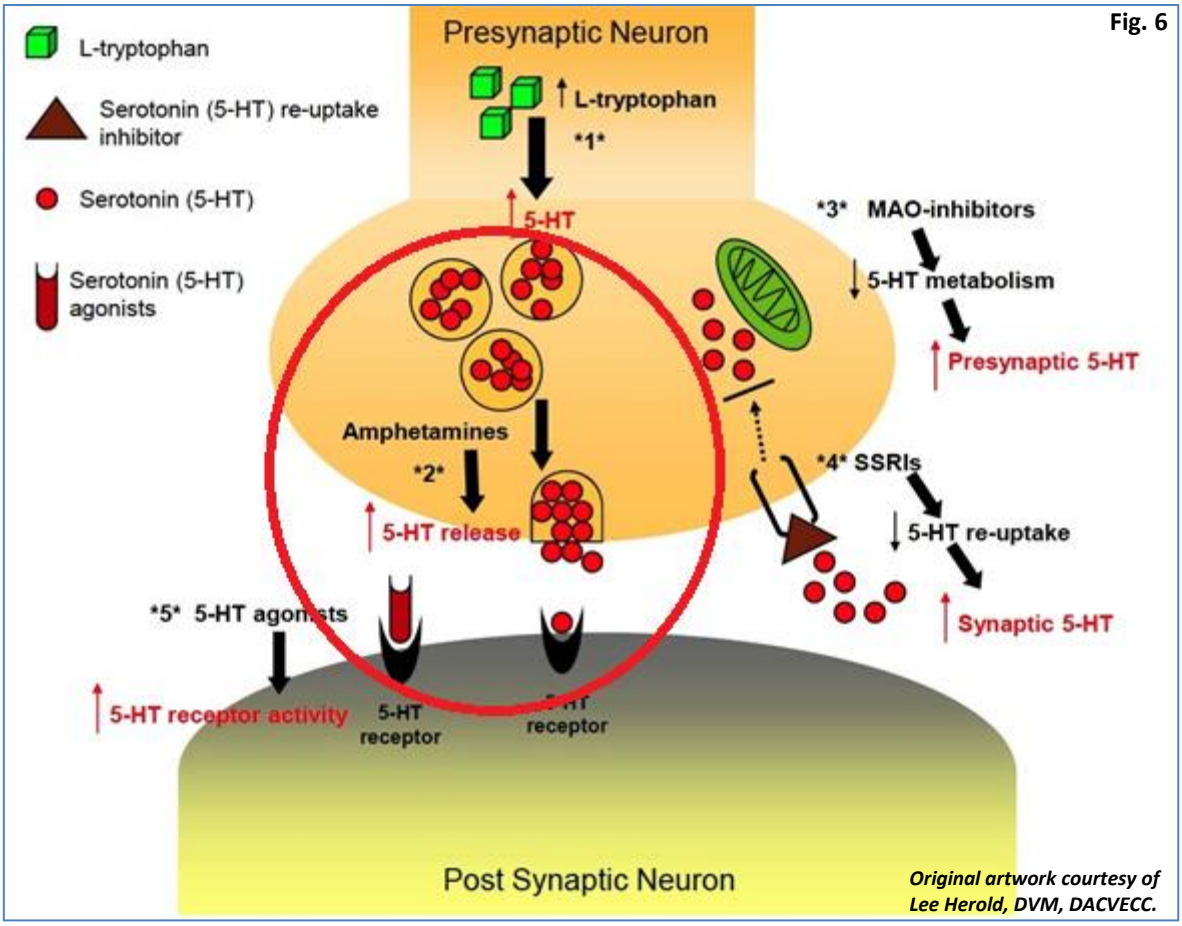

***Mechanisms of serotonin syndrome**.*1* Increased ingestion of L-tryptophan will proportionally increase 5-HT (serotonin) formation. *2* Amphetamines and other drugs increase the release of stored 5-HT. *3* Inhibition of 5-HT metabolism by monoamine oxidase (MAO) inhibitors will increase presynaptic 5-HT concentration. *4* Impairment of 5-HT transport into the presynaptic neuron by uptake blockers (including SSRIs, TCAs) increases synaptic 5-HT concentration. *5* Direct 5-HT agonists can stimulate postsynaptic 5-HT receptors.*

1.3.3. Methamphetamine abuse

METH, elicits euphoria, wakefulness, increased levels of energy and mental alertness as described above.

Repeated exposure to this substance can lead to addiction. According to MediLexicon's Medical Dictionary, the “Addiction” is a neuropsychiatric disorder given by interactions between repeated exposure to the drug and biological (genetics, neuroadaptive changes) and environmental factors (stressful life events, drug availability). Substances addiction can sometimes lead to serious problems in the course of a life-time with a transition from impulsive to compulsive drug use, facilitating a state of uncontrollable and chronic relapse (Koob & Le Moal, 2008). Alongside these common risk factors, a high level of impulsivity induced by METH can increase the vulnerability to addiction through the reduction of inhibitory control over these emotive states (Jentsch & Taylor, 1999).

The progression of drug abuse has been depicted as a downward spiral comprising three stages (Koob & Le Moal, 1997):

- binge/intoxication: compulsion to seek and take the drug, loss of control in limiting intake;
- preoccupation/anticipation: start of negative emotional states (e.g. dysphoria, anxiety, irritability);
- withdrawal/negative affect: characterized by preoccupation and anticipation that persists even after prolonged withdrawal (signs and symptoms that result from either the sudden removal of a drug or the abrupt decrease in its regular dosage), (Koob et al., 2010).

Self-administration (SA) studies represent one of the oldest methods for studying addiction (Panlilio et al., 2007). SA laboratory models described the physiological, behavioral, and cognitive aspects of drug effects, and translated them into a measurable indicator of abuse liability, drug-taking behavior itself. The role of SA drug models is based on the assumption that drugs act as reinforces increased the likelihood of the behavior that results in their intake (Altman et al., 1996). It is assumed that drugs have functional similarities to other reinforces such as food studied by Skinner in the 1930s (Panlilio et al., 2007).

Thus, SA is considered viewed as an operant response (a learning behavior that can be modified by its own consequences and it is often referred to as purposeful or voluntary behavior) reinforced by the effects of the drug. By mean of this procedure, an animal performs a response (e.g. pressing a lever in

an operant chamber) that produces a delivery of the drug (typically delivered through an intravenous catheter).

Compared to other addiction models, this procedure provides the most direct point-to-point correspondence with addictive behavior similar to that occurs in the natural environment. Accordingly, this method has a high degree of validity (Panlilio et al., 2007).

The main disadvantage of SA procedures is their time-consumption and relative expensiveness in comparison with other methods. In addition, long-term studies using intravenous routes in rodents are limited by the duration of the implanted catheters (Panlilio et al., 2007).

Recent studies have highlighted how SA of drugs is facilitated by stressful factors that increase the activity of neurobiological systems (e.g. studies focused on DAergic projections from the midbrain to the nucleus accumbens (NAc), which is considered to be one of the major substrates of drug-strengthening effects), (Nestler 1992; Robinson et al., 1993; Koob et al., 1988).

Brain stress systems are thought to play a significant role, above all, in generating the negative emotional state characteristic of drug dependence, with dysregulation of stress systems, also underlying the persistence of drug-seeking and relapse (Koob, 2008). The concept of stress is very vague, and the term is often used with different meanings. It seems relevant, therefore, to define stress in the context of experimental research. Models of stress are mainly based on the enforced exposure to stimuli or situations that are normally avoided by the individual (Hyman 2001). This is the reason why stress, as analyzed in animals, probably corresponds to the internal status induced by the exposure to threatening and aversive stimuli. This isn't probably the most comprehensive definition of stress, but it well reflects what is generally studied in experimental stress research.

Brain stress systems, during the progression to drug dependence, suggest that individuals may be predisposed to develop addictive disorders, perpetuate and/or worsen addictive disorders once established. The most direct procedure to evaluate the reinforcing properties of a substance during a stress situation is to test whether animals work to obtain the substance (Lynch et al., 2010).

One of the most commonly stress type employed for studying the relationship between drug abuse and stress stimuli is the electric footshock in association with SA. Electric footshock is a complex stressor with both physical (e.g. sleep deprivation, water deprivation, heat stress) and emotional components (e.g. crowding, loud sound), (Bali et al., 2015). It has been employed as an important

tool to develop different animal models in the field of psychopharmacology (Bali et al., 2015). The electric footshock paradigm includes acute or chronic exposures of shocks of varying intensity and duration on an electrified grid floor in an electric footshock apparatus (Shaham et al., 1995).

Many studies have demonstrated that re-exposure to drugs and drug-related stimuli reinstate drug seeking in rats and monkeys. For these reasons the ability of footshock stress to induce restoration of drug seeking was originally illustrated by Shaham and colleagues (1995) in rats with a history of intravenous heroin SA (Shaham et al., 1995; Kupferschmidt et al., 2011).

1.3.4. Methamphetamine and Parkinson disease (PD)

In light of the METH-induced DAergic neurotoxicity and DA loss observed in experimental animals, it has been speculated for several years that METH abuse may predispose consumers to developing neurodegenerative disorders like Parkinson's disease (PD), (Rusyniak, 2011; Guilarte 2001; Thrash et al., 2009).

PD was first described by James Parkinson and consists of a motor syndrome including bradykinesia (slowness of initiation of voluntary movement), akinesia (inability to initiate voluntary movement), rigidity (resistance to externally imposed joint movements), postural abnormalities and tremor (Mazzoni 2012; DeMaagd et al., 2015). The principal neuropathological characteristic of PD is the progressive death of the pigmented neurons of the Substantia Nigra pars compacta (SNc), (Hassler, 1938; Costa and Caltagiorne 2009) and a significant loss of DA in the CPu (Wilson et al., 1996). Biochemical and neuroimaging studies in human METH users have shown decreased levels of DA and DAT in the CPu and in other areas of the brain, changes similar to those observed in PD patients (Volkow et al., 2001; Granado et al., 2013). For these reasons different studies have documented the idea that METH might increase the risk of developing PD (Thrash et al., 2009; Guilarte 2001). Callaghan's group, in 2012, found that the risk of developing PD was 75% higher among METH abusers than in a group of control subjects; this probability was also higher in the METH abusers compared with cocaine abusers (Cardoso et al., 1993).

1.3.5. Methamphetamine and Immediate early genes family (IEGs)

METH causes substantial changes in gene expression in some brain regions including the cortex, the dorsal CPu, and the midbrain (Cadet et al., 2009). These molecular changes include transient increases and decreases in the expression of various transcription factors, neuropeptides, and genes that participate in several biological functions (cell cycle, cell differentiation, signaling transduction), (Jayanthi et al., 2005).

METH users display biochemical and behavioral effects, which involve the activation of DAergic and GLUergic pathways as described in previous paragraphs. These effects are associated with transcriptional changes in the CPu and NAc evaluated within a short or longer time as well as after cessation of drug taking. Indeed, after a few hours from withdrawal, there was an increased expression of genes that participate in transcription regulation such as cyclic AMP (cAMP) response element binding (CREB), ETS domain-containing protein (ELK1), brain-derived neurotrophic factor (BDNF), tyrosine kinase receptor type 2 (TrkB) and synaptophysin in rats (Cadet et al., 2015; Martin et al., 2012).

The transcription of all these genes is controlled by many regulation steps (transcription, post-transcriptional modification, mRNA degradation) and the specific pathways determine the timing of gene expression induced as a response to cell-extrinsic (e.g. temperature, stress factors) and cell-intrinsic signals (e.g. transcription factors), (Bahrami et al., 2016). Indeed, a complex set of interactions between genes, proteins and other components of the expression system (e.g. activators or repressors) determine when and where specific genes are activated and the amount of protein or RNA products which are synthesized (Brown 2002).

In detail, acute METH injections increase the expression of specific group of genes that respond very rapidly to regulatory signals (Thiriet et al., 2001; Wang et al., 1995): the Immediate early genes (IEGs):

- Activator protein 1 (AP1): Fos and Jun family.
- Early growth response protein (Egr) family.
- Nuclear receptor subfamily 4, group A (Nr4A) family.

The protein Fos plays a key role in cellular events, including proliferation, differentiation and survival, and is also regulated by post-translational modification such as phosphorylation by different kinases

like mitogen-activated protein kinase (MAPK), which influence protein stability and DNA-binding activity (O'Donnell et al., 2012). Expression of the Fos mRNA peaks 30–60 minutes after stimulation, and returns to basal level after 90 minutes (Greenberg & Ziff, 1984). Compounds that act directly to release DA (such as cocaine and ATS) also increase expression of c-Fos and other IEGs in CPu via DA receptors (D1), (Robertson et al., 1989; Graybiel et al., 1990; Young et al., 1991; Moratalla et al., 1992) and in the cortex during withdrawal phase in rats (Krasnova et al., 2013, Cornish et al., 2012).

Two more Fos family protein are Fos-related antigen 1 (Fra1), expressed at significant levels in proliferating cells (Bergers et al., 1995), and Fos-related antigen 2 (Fra2), known to play a critical role in the progression of human tumors (Rani et al., 2014).

Moreover, Jun family members, described in literature are: c-Jun (Maki et al., 1987), JunB (Ryder et al., 1989), and JunD (Ryder et al., 1989; Hirai et al., 1989). These Jun family proteins can form homodimers. Generally, Jun family genes are expressed at moderately high levels in adult tissues; c-Jun is also expressed throughout organogenesis, whereas JunB is not expressed until late in gestation (Foletta et al., 1997).

Moreover, Jun family members form with Fos family the AP-1, with the role of transcriptional factor, which binds the region promoter of numerous mammalian genes (Curran & Franza, 1988). AP-1 transcription factor is assembled through the dimerization of a characteristic basic region leucine zipper (bZIP domain) in the Fos and Jun subunits, and whole complex AP-1 is able to activate or suppress the expression of many genes involved in proliferation, differentiation, and survival (Hess et al., 2004).

Moreover, IEGs family include the Early growth response gene 1 (Egr1) also known as Zif-268, which encodes a nuclear phosphoprotein, known as Krox24 (Kukushkin et al., 2005). Egr1 is involved in the regulation of cell growth and differentiation in response to signals such as mitogens, growth factors, and stress stimuli in rats and mice (Bae et al., 2002; Liu et al., 2001; Zhang et al., 2003). The four members of this family are Egr1, Egr2, Egr3 and Egr4. Several studies demonstrated that induction of the expression of Egr1 and other IEGs in striatal neurons is blocked by the selective D1 antagonist, SCH23390 (Moratalla et al., 1992). This pharmacological result completes anatomical studies that document the induction of Egr1 expression in a subpopulation of striatal neurons with a large number of D1 receptors (Okuno 2011; Gerfen et al., 1995).

Further IEGs are the nuclear hormone receptor (NR) superfamily, which includes the orphan NR4A subgroup, comprising Nur77 (NR4A1), Nurr1 (NR4A2) and NOR-1 (NR4A3). These IEGs are induced by signals, including fatty acids, stress, growth factors, cytokines, peptide hormones, neurotransmitters, inflammatory cytokines and physical stimuli (Tetradis et al., 2001; Kagaya et al., 2005).

Owing to the many interactions and complexity that these IEGs have in the cellular mechanisms and in its expression, few studies have been conducted on transcriptional gene effects by drugs of abuse (Grzanna & Brown, 2007) and in particular few studies have demonstrated important changes of these IEGs during METH use (McCoy et al., 2011).

1.4 MDMA

1.4.1 Generality

The German pharmaceutical company Merck synthesized MDMA, in 1912, in order to produce and to patent a possible appetite suppressor (Freudenmann et al., 2006). In an effort to determine the psychoactive properties of the drug, Shulgin (1995) tested it on himself and discovered that MDMA, in addition to wakefulness effect of ATS, also produced a number of very different effects, such as an increased willingness to communicate and feelings of love, empathy and closeness to others (Kalant 2001).

MDMA is chemically related to the ATS, and belongs to the family of phenethylamines, as mescaline, but it is not an hallucinogen. MDMA is an illicit drug that stimulates the transporter-mediated release of monoamine transmitters: 5-HT, NA, and DA from nerve cells (Verrico et al., 2007). MDMA is metabolized by hepatic mechanisms in humans and other mammals through two pathways. Through the main pathway, MDMA by the O-demethylenation produces (±) 3, 4 dihydroxymethamphetamine (HHMA) and by the O-methylation generates (±) 4-hydroxy-3-methoxymethamphetamine (HMMA). On the other hand, in the minor pathway, MDMA is N-demethylated to form (±) MDA, a potent and efficacious monoamine-releasing agent (Johnson et al., 1986). MDA is further metabolized to (±) 3, 4-dihydroxyamphetamine (HHA) and (±) 4-hydroxy-3-methoxyamphetamine (HMA), (**Figure 7**).

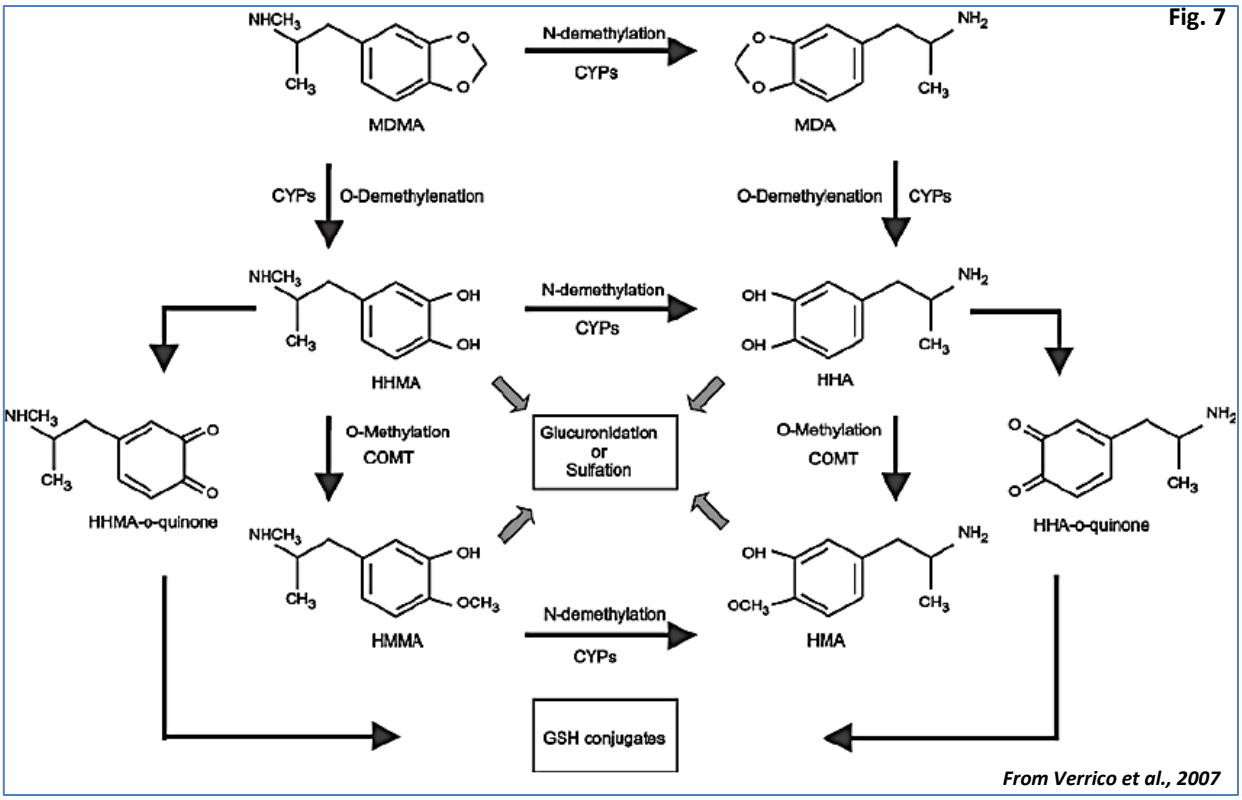

MDMA metabolism in humans and rats. *Thick arrows represent major pathways of biotransformation, and thin arrows indicate minor pathways. The main cytochrome P450 isoforms responsible for specific reactions in humans and rats are noted. COMT, catechol-O-methyltransferase.*

1.4.2 Neurotoxicity of MDMA

The pharmacology of MDMA involves two brain neurotransmitters: 5-HT and DA as previously discussed for METH.

The selective effects of MDMA on 5-HT neurons are species-dependent. The 5-HT neuron-selective toxicity of MDMA has been attributed to its higher affinity, uptake, or releasing capacity at the SERT, compared with DAT or Noradrenaline transporter (NET), (Rudnick & Wall 1992).

MDMA acts in the brain through different neurochemical mechanisms. MDMA enters the neuron through SERT. Settled inside the neuron, it inhibits the VMAT2. Accordingly, 5-HT (localized in synaptic vesicles) is released and it is accumulated in the cytosol. In addition, MDMA is able to reverse the direction of SERT. The result is a dramatic release of 5-HT from the cytosol to the synaptic space with an intensification of the postsynaptic receptor activity and its reuptake inhibition, (**Figure 8**). In addition, to an excessive receptor response, long term effect lead to a depletion of 5-HT (O'Shea et al., 1998).

In rats, a single dose of MDMA (10 mg/kg) produces a biphasic effect, with acute depletion of 5-HT mostly after 3–6 hours since its administration, and a recovery within 24 hours; whereas, administration of multiple doses of MDMA (≥20 mg/kg) can induce further decreases in 5-HT biomarkers (e.g. [(11) C] SB207145 to quantify 5-HT4 receptor) and SERT levels, that are still present 1 week later (Schmidt 1987).

Moreover in rats, 5-HT depletion, was found 7 days after a single high dose of MDMA (10 mg intraperitoneally (i.p.)), and after a multiple moderate doses of MDMA (4 mg i.p. twice-da y for 4 days), but not after a single moderate dose (4 mg i.p.) or a multiple moderate doses of MDMA distanced over time (4 mg i.p. twice-weekly for 8 weeks), (O'Shea et al., 1998).

5-HT neurons of the primate brain are more susceptible to MDMA-induced changes when compared to rats (Ricaurte & McCann 1992). In effect, in the cerebral cortex of monkeys, 5-HT depletion occurs at low doses of repeated MDMA respect to the cortex of rats and persists for longer periods after injections (Banks et al., 2008); whereas, in mice, MDMA selectively affects DA neurons, while sparing 5-HT neurons in comparison with rats (Xie et al., 2004; Stone, DM et al., 1987), with a reduction in DAT and TH immunoreactivity in DAergic cerebral regions, directly related to the number of MDMA administrations (Granado et al., 2008, Costa et al., 2017; Green et al., 2003; Costa et al., 2013).

Indeed, in contrast to the substantial numbers of investigations on the pharmacological effects of MDMA in rats, rather few studies have been conducted into the effects of MDMA in mice. Some early

studies on the neurotoxic actions of MDMA in mouse brain demonstrated a very different profile to that seen in rats, namely long-term neurotoxic loss of striatal DA (Logan et al., 1988).

With regard to DA biochemistry, there is good evidence that MDMA administration produces an acute release of DA. The striatal content of both DA and its metabolites, homovanillic acid (HVA) and 3, 4-Dihydroxyphenylacetic acid (DOPAC), is reduced 3 hours after the last of three injections of MDMA (O'Shea et al., 2001). Furthermore, a recent study provided direct evidence for MDMA-induced DA release by using in vivo microdialysis, which confirmed that the extracellular DA concentration in the CPu increased after MDMA administration (Colado et al., 2001; Camarero et al., 2002). A single injection of MDMA only produced a modest rise in the extracellular DA concentration, but the rise was magnified and sustained by the two subsequent doses of MDMA (Colado et al., 2001; Camarero et al., 2002). Furthermore, it would seem that DA acts as an intermediary in the damage effects of MDMA on the 5-HTergic system. This conclusion is based on the observation that pretreatment with GBR 12909, a selective inhibitor of DA, (Stone et al., 1988) or reserpine, enhanced the MDMA-induced increase in the extracellular DA concentration and prevents MDMA toxicity on 5-HT neurons (Koch & Galloway, 1997). This observation is identical to that seen by Mechan et al. (2002) in rats and indicates that MDMA may enter the nerve terminal by diffusion and not via the DA uptake site (Camarero et al., 2002).

Furthermore, similarly to METH, MDMA-induced toxicity is associated with the production of ROS and reactive NO species and a subsequent production of oxidative/nitrosamine stress. The free radicals can originate from several molecular pathways (oxidative deamination of monoamine, metabolic pathways, cathecolamines autoxidation, and hyperthermia) and their harmful effect causing potential biological damage such as lipoperoxidation and cellular death. Indeed, MDMA increases hydroxyl radical production in a dose-dependent manner (20 and 40 mg/kg i.p.), (Górska et al., 2014) as well as increases the release of DA and 5-HT in the CPu mice (Gołembiowska et al., 2013).

Fig. 8

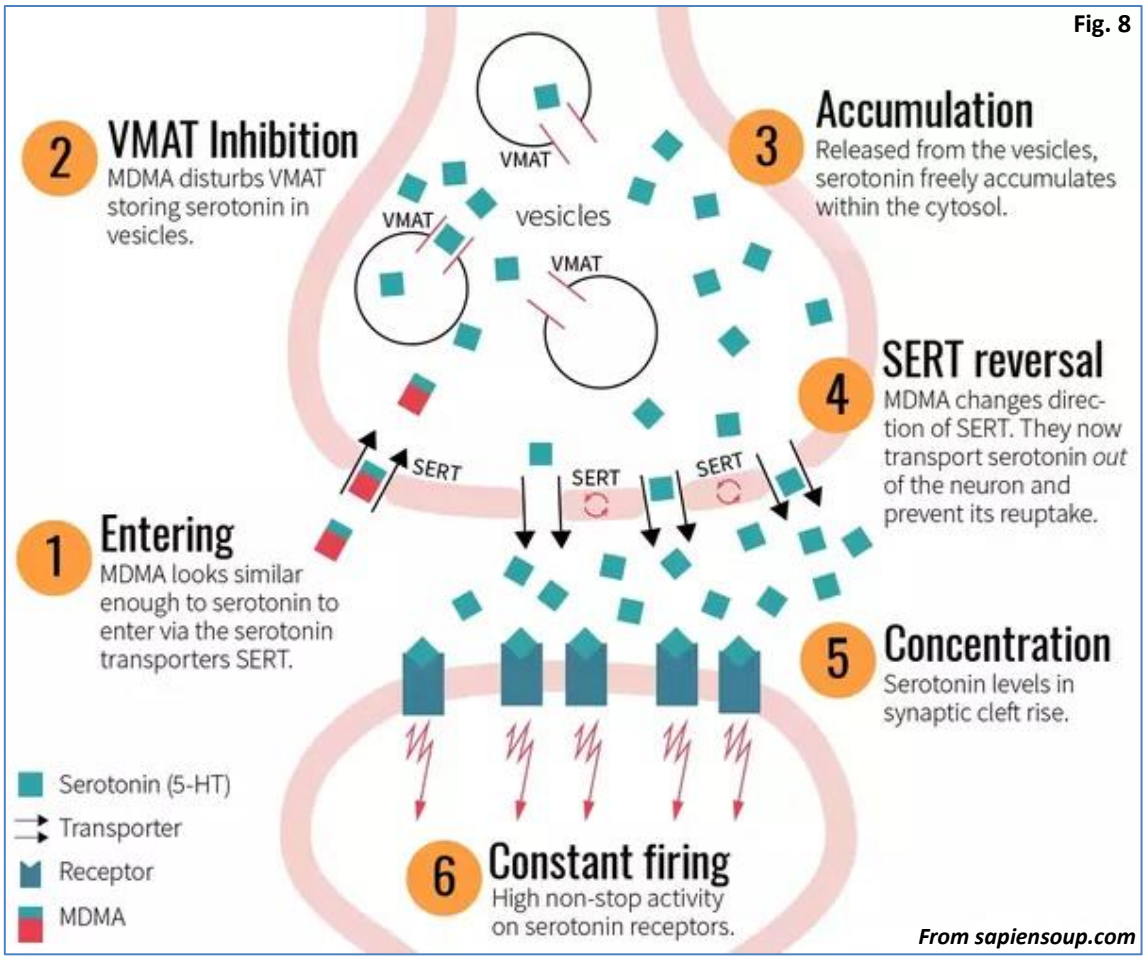

ATS act as "false neurotransmitters". *They are transported into the cytoplasm by presynaptic transports and then occupy VMAT2 causing an increase in extra-vesicular cytosolic DA/5-HT levels. This increase in transmitter's concentration reverses the transport of the transmitter into the extracellular space.*

1.4.3 Hyperthermia

MDMA, as seen for METH, is responsible of another neurotoxic effect: the hyperthermia.

This effect is influenced by dose, ambient temperature and housing conditions (Colado et al., 1995; Green et al., 2004). The first published study to assess the effects of MDMA on body temperature in humans was a 'phase-1 pilot study' (Grob et al., 1996).

The mechanism of MDMA-induced hyperthermia is complex, and involves not only 5-HT and DA systems but also adrenergic transmission (Sprague et al., 1998). The increased release of these monoamines induced by MDMA administration may stimulate receptors involved in thermoregulation (Shankaran & Gudelsky 1999). Further support for a possible relationship among hyperthermia and neurotoxicity derives from experimental animals, where MDMA increases body temperature and this enhances the generation of toxic drug metabolites, which are known to increase oxidative stress (Cadet et al., 2007) and glial cell activation (Miller & O'Callaghan 1994; Connor et al., 2004).

MDMA-induced brain hyperthermia was strongly potentiated during social interaction in mice, where crowding amplifies both glia activation and DAergic neurotoxicity (Kiyatkin et al., 2016; Frau et al., 2016); on the contrary, high environmental temperature exacerbates only glia activation (Frau et al., 2016). A similar potentiating of brain hyperthermia during social interaction had been previously shown with MDMA as compared to METH (Brown et al., 2004), but such an effect was absent for cocaine (Blech-Hermoni & Kiyatkin, 2004). Furthermore, the thermogenesis induced by MDMA in laboratory animals involved molecular mediators in the hypothalamic-pituitary-thyroid axis, sympathetic nervous system, and uncoupling proteins (Dao et al., 2014).

1.4.4 Ras Homolog Enriched in Striatum (Rhes)

Ras homolog enriched in striatum (Rhes) is a 266 aminoacid protein belonging to Ras superfamily, a monomeric G protein family. Rhes protein in rat shares 62% identity with mouse Dexamethasone-induced Ras-related protein (Dexras), a brain-enriched member of the Ras family. These two proteins have a common C-terminal tail, which differentiates them from the conventional Ras family members (Falk et al., 1999). In fact, as proteins belonging to the Ras family, Rhes contains a region that binds to Guanosine-5'-triphosphate (GTP) and a CAAX, region that can be farnesylated (post-translational-modifies proteins), (Rubio et al., 1999). The farnesylation of the CAAX domain is an important event, because it allows this protein to locate at the plasma membrane level and to perform its functions (cell growth, differentiation, and survival processes).

The expression of this Rhes protein in the CPu is postnatal and decreases in adulthood of rodent (Bernal et al., 1995). Its expression is controlled by thyroid hormones that influence normal functions and brain development by activating or suppressing different genes (Spano et al., 2004). Studies in hypothyroid rats showed that Rhes mRNA dropped, and its expression recovered normal levels, when animals were treated with T3 (Vargiu et al., 2001) or T4 hormone (Falk et al., 1999). At CPu level, Rhes is able to alter the intracellular transduction mechanisms induced by stimulation of D1 and D2 receptors in mice (Quintero et al., 2008). Specifically Rhes is able to counteract the activation of the cAMP/protein kinase A (PKA) intracellular signal pathway, whose genesis depends on the DA binding to D1 receptors (Ghiglieri et al., 2014). PKA is a family of enzymes, whose activity is dependent on cellular levels of cAMP. PKA is also known as cAMP-dependent protein kinase, and it has several functions within cell, including regulation of glycogen, sugar, and lipid metabolism. The administration of a pure agonist of D1 receptors, such as SKF 81297, or a pure antagonist of D2 receptors, such as haloperidol, results in a marked increase in PKA target protein phosphorylation (such as AMPA receptor) in KO Rhes ($Rhes^{-/-}$) mice compared to control mice (Errico et al., 2008); this confirms how Rhes influences this transduction pathway.

Furthermore, Rhes protein plays an important role in the regulation of Phosphatidylinositol-4,5-bisphosphate 3-kinase-Protein kinase B (PI3K-Akt), an intracellular signaling pathway which is important for cell cycle regulation. In non-stimulated cells, Rhes is located on the plasma membrane, whereas PI3K and Akt are found in the cytosol. During signal transduction, PI3K is located close to the activated receptor, and it binds to the C-terminal portion of the Rhes. This process is essential to

allow the conversion of inositol triphosphate (PIP3). At the same time, PIP3 binds Akt facilitating translocation on the plasma membrane, where it is phosphorylated and activated (Bang et al., 2012).

It has also been found that Rhes can modulate the mammalian target of rapamycin complex 1 (mTORC1). The mTORC1 is a multifunctional kinase complex that facilitates the absorption of nutrients, metabolism and cell growth (Harrison et al., 2013). When Rhes is at the level of the plasma membrane (after farnesylation of the CAAX domain), in its active state, it is able to bind directly to the catalytic site of mTOR performing striatal functions (Long et al., 2005), (**Figure 9**).

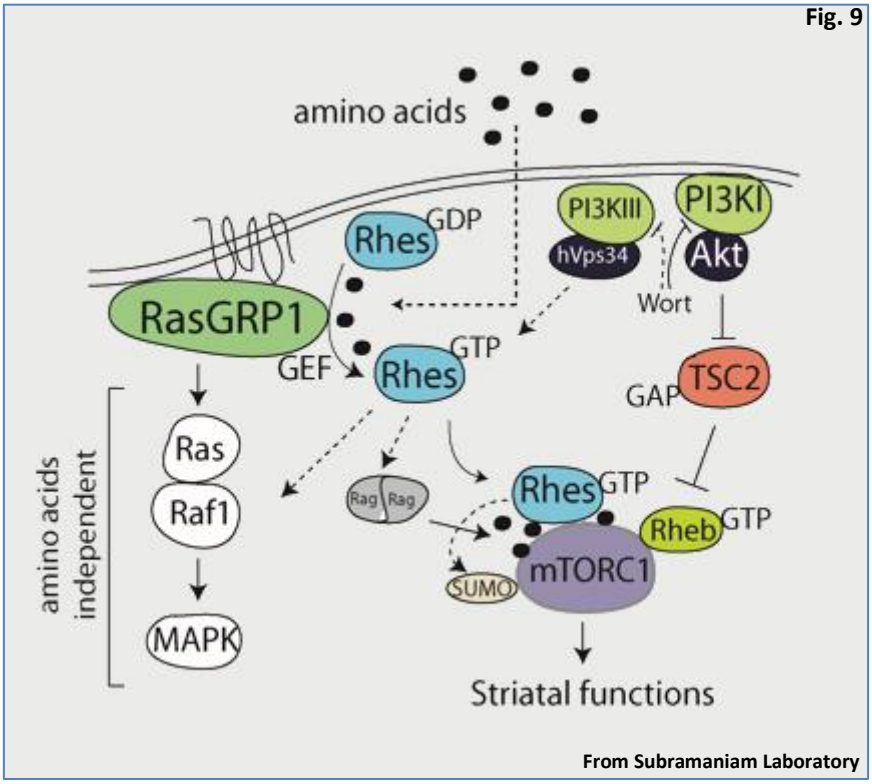

Model of how Rhes GTPase activates mTORC1 in CPu.

However, subsequent studies have shown that in addition to this striatal enrichment, Rhes mRNA is also expressed in other brain areas and tissues, despite to a lesser extent, in SNc and ventral tegmental area (VTA) of mouse midbrain (Pinna et al., 2016).

An important role of the protein Rhes, as described above, is the influence in the modulation of the activity and the motor coordination (Pinna et al., 2016); indeed, it seems that the lack of this protein triggers subtle alterations in motor performance and coordination during aging in male mice (Pinna et al., 2016). Furthermore recent results obtained by Shahani's laboratory has shown the implication of Rhes, which acts as a brake on increased motor activity induced by the release of DA after ATS abuse (Shahani et al., 2016).

1.4.5 MDMA and Parkinson Disease

Similarly to METH, MDMA has been implicated in the appearance of PD, and a few studies explained in detail this implication. However, one of the first studies showing signs of PD between MDMA users (Mintzer et al., 1999) remained controversial because the patients selected for this study showed already a family history of PD (Baggott et al., 1999; Borg 1999). In 2002, NIDA-sponsored researchers demonstrated that MDMA was thought to be able to damage DA neurons in primates speculated that this drug could even lead to PD (Ricaurte et al., 2002). After this publication, several more cases of PD in MDMA users emerged (Kuniyoshi & Jankovic 2003; O'Suilleabhain & Giller 2003), (**Figure 10**).

Fig. 10

Human case studies of "parkinsonism" in ecstasy* users	Mintzer et al.	Rapidly progressive bradykinesia and postural instability (no tremor) in 29-years-old male Ectstasy* user; normal MRI, fdg-pet; not responsive to levodopa/pramipexole
	Kuniyoshi and Jankovic	Trihexyphenidyl-responsive resting tremor plus? in 19-year old male Ectasy* user; normal MRI; family history of parkinsonism
	O'Suilleabhain and Giller	Bradykinesia, resting and postural tremor, and rigidity in 38-year old male Ectsasy* user; normal MR; at least partially responsive to levodopa and subthalamic nuclei stimulation

Superscript numbers correspond to the list of References.
*Self-reported use of ecstasy without forensic confirmation to prove actual use of the drug.
DA, dopamine; MRI, magnetic resonance imaging; FDG-PET, 18-fluorodeoxyglucose positron emission tomography; striatal, caudate/putamen.

A study of the long-term effects of stimulant MDMA, as well as cocaine and METH suggests that there is an abnormal morphology in the SNc (it appears abnormally enlarged) in these individuals (Todd et al., 2013). This alteration represents a major risk factor for developing PD in later life (Todd et al., 2013).

Interestingly, the MDMA is able to normalize motor activity in marmoset lesioned with the toxin 1-methyl-4-phenyl-1, 2, 3, 6-tetrahydropyridine (MPTP), an important neurotoxicity model of PD (Fox et al., 2010). This is controversial because, as mentioned above, the development of PD has also been linked to MDMA abuse (Todd et al., 2013). At the same time, MDMA has been reported to reduce dyskinesia (abnormal involuntary movements) in PD patients taking Levodopa (L-dopa, the precursor of DA), achieving a successful restoration of the normal function (Morton, 2005). Despite a potential role for dyskinesia treatment in PD, MDMA collateral effects add a great risk for PD patients, and it cannot be considered as a potential treatment. Indeed, PD patients have an increased risk of

psychological side effects (e.g. hallucinations, confusion and depression) from many medical supplies, and although MDMA reduced tremor and dyskinesia and improved mobility, it also interfered with thought processes (Morton 2005). These studies open the way for investigation of the use of MDMA analogues in the treatment of dyskinesia. Searching for MDMA analogues or other agents that interact with the 5-HT system to mimic the beneficial effects of MDMA (while minimizing cognitive side effects) will be key to advances in this area.

1.4.6. Metformin

Metformin is a biguanide derivative that has been used since the 1960s for patients to treat diabetes mellitus (brand name Glucophage, Glucophage XR, Glumetza, Riomet).

Studies have demonstrated that metformin protects the liver from ischemia reperfusion-injury by increasing antioxidant enzyme activity through the lowering of mitochondrial ROS formation, as well as by reducing post-ischemic inflammation (Cahova et al., 2015; Abd-Elsameea et al., 2014). Some recent experimental and clinical studies have suggested that metformin has anti-inflammatory properties (Saisho 2015; Cameron 2016). Inflammation is a widely encompassing term referring to the complex biological response of the immune system to tissue damage (e.g. microglia, a type of neuroglia (glial cell) located in the brain and spinal cord), toxic proteins (e.g. metabolites of DA), infection, or abnormal molecular signals (e.g. oxidations). CNS immune response is thought to be orchestrated principally by microglia with lesser contributions by neurons, oligodendrocytes, and astrocytes (Tansey et al., 2007). Metformin has anti-inflammatory properties, not only in the peripheral tissues, but also in the brain; indeed, it has been shown that this drug crosses the blood brain barrier (BBB) and can accumulate in the brain of rodents (Towler & Hardie, 2007; Łabuzek et al., 2010). Treatment with metformin is capable to reduce key astrocyte and microglial markers such as glial fibrillary acidic protein (GFAP), ionized calcium binding adaptor molecule 1 (Iba-1) and inflammation markers such as interleukin 1 (IL-1) in the PD model induced by MPTP injection (Lu et al., 2016), (**Figure 11**).

Fig. 11

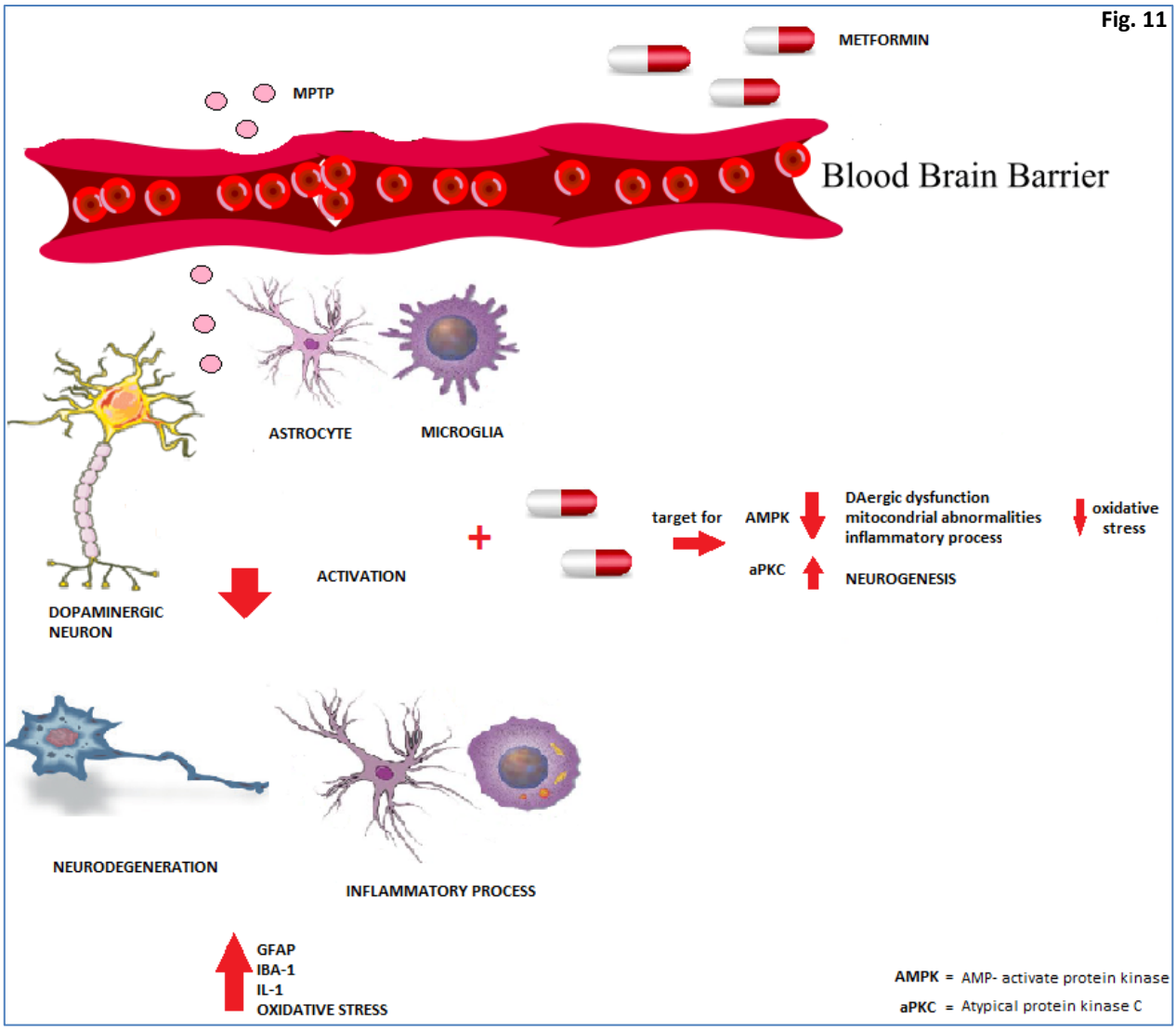

Effects of metformin in PD model induced by MPTP injection.

However, Patil's studies demonstrated that, despite the decrease in inflammatory parameters, metformin fail to decrease death of DAergic neurons in the SNc, but even increases neuronal damage in this structure, probably through inhibition of mitochondrial complex I (a very large enzyme catalyzing the first step of the mitochondrial electron transport chain) and finally, increases the vulnerability of these neurons (Patil et al., 2014).

Furthermore, Kuan's laboratory showed how the risk of developing PD, was 2.27 times higher in participants who took metformin than who didn't take it (Kuan et al., 2017). Nevertheless, according to the authors, this neurological disease isn't supposed to be directly related to metformin but rather to some unknown factor that links the assimilation of metformin to the development of PD (Kuan et al., 2017; Ismaiel et al., 2016).

2. Aims of study

In order to better understand the molecular mechanism that control the compulsive drug use, in the Cadet's laboratories (NIDA, Baltimore) we have used the SA paradigm in association with footshocks to induce negative consequences during METH SA. We investigated whether the compulsive METH taking under punishment can increase the expression of IEGs in the rat NAc and PFC, that are important areas involved in reward, memory, executive function, motivation and contribute to some of the differences in the circuit of addiction (Volkow & Morales 2015; Volkow et al., 2012; Adinoff 2004).

In the second and third study, performed at the University of Cagliari, we focused on MDMA treatment in mice in order to clarify the role played by this drug on neurotoxicity and motor behavior resulting from MDMA administration.

Specifically, in the second study, considering the influence of the Rhes protein on the age-related survival of DA neurons in the SNc, the different response to AMPH of $Rhes^{-/-}$ mice (Vitucci et al., 2016) and the differential incidence of PD between the male and female human population (Smith & Dahodwla 2014), we have investigated the basal and the MDMA-induced neurotoxic effects in $Rhes^{-/-}$ mice, male and female at different ages. Moreover, in an attempt to link neurochemical changes with behavioural modifications, this study investigated the motor activity.

The third study investigated the possible neuroprotective effect of metformin, against short and long-term neurotoxicity induced by MDMA, together with its role on MDMA-induced hyperthermia.

3. Materials and methods

3.1 Experiment I: METH self-administration

Animals

Male Sprague–Dawley rats (Charles River, Raleigh, NC, USA), are used for the SA experiments with a weight of 350–400 g before surgery, at National Institutes on Drug Abuse, in Baltimore. All rats are group housed (two per cage) for one week before surgery, and housed individually after surgery. Rats were maintained in the animal facility under a reversed 12:12 hours light/dark cycle with regular food and water freely available. All animal treatments and procedures were approved by the National Institute of Drug Abuse Animal Care and Use Committee and followed the Guide for the Care and Use of Laboratory Animals (ISBN 0-309-05377-3).

Rats are divided in three groups: Control group (Ct), METH group (METH) and the yoked group (Y). Y group is a control rats were yoked to the shocked animals so that each time animals in the METH SA group received a contingent shock, these rats also received a non-contingent shock and a saline infusion. Footshocks caused the separation into two METH subgroups: METH shock-resistant (M-SR) and METH shock-sensitive (M-SS); and into two Y subgroups: yoked shock-resistance (Y-SR) and yoked shock-sensitive (Y-SS).

Intravenous Surgery and SA phase

Rats were anesthetized with ketamine and xylazine (50 and 5 mg/kg, i.p., respectively) and a silastic catheters was inserted into the jugular vein (Bossert et al., 2009; Theberge et al., 2013). Catheters were attached to a modified 22-gauge cannula that was mounted to the rats' skulls with dental cement. Buprenorphine was injected (0.1 mg/kg, s.c.) after surgery to relieve pain and allowed the rats to recover for 5 days before METH SA. During the recovery and training phases, catheters were flushed every 24–48 hours with gentamicin (Butler Schein; 5 mg/ml) and sterile saline. One week after surgery, rats were trained in SA chambers located inside sound-attenuating cabinets and controlled by a Med Associates system. Each chamber was equipped with two levers located 8.5 cm above the grid floor. Moreover, chambers of the SA rats were equipped with a pellet dispenser and receptacle located near the active lever activated by infusion pump for the METH or Ct, respectively. Presses on the other inactive (stationary) lever had no reinforced consequences. Catheters were connected in the METH or Ct group of rats to a modified cannula (PlasticsOne) attached to a liquid

swivel (Instech) via polyethylene-50 tubing that was protected by a metal spring. On the first day of training, rats were brought to the SA rooms, in which rats were chronically housed. Rats were trained to SA experiment during 3 hours/day for three sessions (sessions were separated by 30 min). These drug access and reinforcement schedule conditions are based on previous incubation studies with heroin and METH (Theberge et al., 2012; Theberge et al., 2013). Rats were trained in six days and one off day, in order to prevent loss of body weight during the training phase (under our training conditions of 9 hours daily sessions, rats lose weight after each training day and regain the lost weight during the off days), (Shepard et al., 2004; Theberge et al., 2013). Weight loss is a common side effect of METH use by humans (Mooney et al., 2009; Neale et al., 2009) or laboratory animals (Krasnova et al., 2010) because of the drug's anorexic effects (Saito et al., 1995). In order to prevent drug overdose, the number of METH infusions were limited to 35 per session, for a maximum total of 105 available METH infusions each day.

Punishment phase

Following the maintenance phase of METH SA or Ct group, electric generators were activated and rats were subjected to contingent punishment procedures. During this phase, 50% of active lever-presses resulted in the concurrent delivery of a footshock lasting 0.5-s through metal grid floors. Throughout the punishment phase, rats continued METH SA every day (9-hours/day) on a fixed ratio (FR-1) reinforcement schedule. The initial footshock session was set at 0.18 milliampere (mA) and amplified by 0.06 mA increments to a final intensity of 0.36 mA. The total days with footshocks were 8. This contingent footshock regiment led to the separation of two distinct METH SA phenotypes M-SR vs. M-SS. Animals was classified as M-SS whether they reduced their intake by 70%.

Tissue collection

For the SA paradigm, rats were euthanized at 2 hours after the last SA session. Their brains were quickly removed from the skull, NAc and prefrontal cortex (PFC) were dissected on ice, snap frozen on dry ice, and stored at −80°C until used in quantitative polymerase Chain Reaction (PCR) experiments. Total RNA was isolated using Qiagen RNeasy Mini kit (Qiagen, Valencia) and used to measure the expression of members of several classes of IEGs. Individual total RNA obtained from rats was reverse-transcribed with oligo dT primers and RT for PCR kit (Clontech, Palo Alto, CA). PCR experiments were done using the Chroma4 RT-PCR Detection System (BioRad Hercules, CA USA) and iQ SYBR Green Supermix (BioRad) according to the manufacturer's protocol. Sequences for gene-

specific primers corresponding to PCR targets were obtained using LightCycler Probe Design software (Roche). The primers were synthesized and HPLC-purified at the Synthesis and Sequencing Facility of Johns Hopkins University (Baltimore, MD).

Statistic

Statistical analysis of SA data was conducted separately for the escalation, maintenance, and footshock phases of our experiment. Repeated measures ANOVAs were used for multiple comparisons and Student's t-test were used to determine if two sets of data are significantly different from each other groups. The null hypothesis was rejected at $p<0.05$.

3.2. Experiment II: MDMA in Rhes mice

Animals and Treatment

Regarding MDMA experiments on Rhes mice, adult (3-month-old) and elderly (12-month-old) male and female $Rhes^{+/+}$ and $Rhes^{-/-}$ mice without PGK-neo cassette (Sciamanna et al., 2015), backcrossed to F11 generation to the C57BL/6J strain, were used. Experimental procedures were approved by the Ethics Committee of the University of Cagliari in compliance with the European Communities Council Directives (2010/63/EU; L.276; 22/09/2010).

Adult (3-month-old) and elderly (12-month-old) male and female $Rhes^{+/+}$ and $Rhes^{-/-}$ mice were treated with vehicle (saline solution) or MDMA (4×20 mg/kg, 2 hours intervals, i.p.). Animals were sacrificed 48 hours after the last administration of MDMA. Immunohistochemical evaluation was performed in a group of mice different from that used for motor activity.

Tissue collection

After MDMA treatment, mice were anesthetized and transcardially perfused with paraformaldehyde (4% in 0.1 M phosphate buffer, pH 7.4) for immunohistochemistry studies. Fifty µm sections from the CPu (A: 1.10 mm; 0.74 mm; 0.38 mm from bregma) and SNc (A: −2.92 mm; −3.28 mm; −3.64 mm from bregma) were cut coronally on a vibratome and immunoreacted with TH antibodies (polyclonal rabbit anti-TH, 1:1000, Millipore, Temecula, CA, USA). After washing, the sections were incubated in biotinylated secondary antibody (goat anti-rabbit immunoglobulin G, IgG for TH). For visualization, the avidin–peroxidase protocol (ABC, Vector Laboratories, UK) was applied, using DAB (Sigma-Aldrich, Milan, Italy) as chromogen (Costa et al., 2013). Sections were mounted on gelatin-coated slides, dehydrated, and coverslipped. Moreover, an additional set of SNc sections was stained with Nissl staining to evaluate cell death in this area.

For the analysis of TH immunoreactivity in the CPu, images were digitized in gray scale and captured at 5× magnification. Analysis was performed in three sections, according to the Mouse Brain Atlas (Paxinos & Franklin, 2008). The density of immunoreacted fibers was determined quantitatively using the Image J program (U.S. National Institutes of Health, USA). Sections were captured in black and white 8-bit monochrome and the density of fibers was determined in fixed regions using a threshold level that was kept constant across all images. No significant differences in the density of

immunoreacted fibers were seen between the three sections, thus values from different levels were averaged.

Stereological analysis of total number and density of TH (+) neurons in the SNc were counted on both hemispheres, using software (Stereologer) linked to a motorized stage on a light microscope (Casu et al., 2004). The SNc region was outlined at low magnification (2×), and sampling of cells was achieved using automatically randomized sampling and an optical dissector (50×50×15 µm). Cells were sampled with a 40× objective through a defined depth with a guard zone of 2 µm. Coefficient of error ranged from 0.05 to 0.1 (Casu et al., 2004).

Behavioral test

Measurement of motor activity was carried out in a quiet, isolated room kept at the constant temperature of 21 ± 1°C. Each mouse was placed individually in a cage (length, 47 cm; width, 27 cm; height, 19 cm) equipped with two pairs of infrared photocell emitters and detectors located along the long axis (Opto-Varimex; Columbus Instruments, Columbus, OH, USA). Two kinds of motor activity were registered: horizontal locomotion along the long axis of the cage, which caused interruption of different beams, and total motor activity, including horizontal locomotion plus vertical activity (stereotypes), the latter causing interruption of the same infrared beam. Mice were habituated to the cages for 1 hour before the first vehicle or MDMA administration. Activity counts were taken every 15 min, for a total of four evaluations (cumulative time: 1 hour), starting after each injection.

Statistic

Statistical analysis was performed with Statistica for Windows (StatSoft, Tulsa, OK, USA). Data from motor activity measurements were analyzed with a two-factor analysis of variance (ANOVA) for repeated measures, followed by Newman–Keuls's post hoc test. Data from the immunohistochemical analysis were statistically compared by means of a two-factor ANOVA (genotype × treatment), followed by Newman–Keuls's post hoc test. Moreover, a two-tailed t-test was applied to verify the presence of significant differences between male and female mice. Results are expressed as mean ± S.E.M. for every analysis performed. Results were considered significant at $p<0.05$.

3.3 Experiment III: Metformin plus MDMA in mice

Animals and Treatment

Regarding metformin plus MDMA experiments adult (3-month-old) male C57BL/6J mice (Charles River, Milan, Italy) were treated with vehicle (saline solution, i.p.), metformin (Sigma-Aldrich, Milan, Italy) (2x200 mg/kg, 11 hours interval by oral somministration), MDMA (4X20 mg/kg, 2-hours intervals, i.p.), or MDMA plus metformin (2X200 mg/kg, 1 hour before the first MDMA administration and 4 hours after the last). On the second and third day, mice receive vehicle or metformin (1X200 mg/kg). 48 hours and 7 days after the last administration of MDMA, mice were anesthetized for immunohistochemical studies. Experimental procedures were approved by the Ethics Committee of the University of Cagliari in compliance with the European Communities Council Directives (2010/63/EU; L.276; 22/09/2010).

MDMA–HCl was synthesized at the Department of Life and Environmental Sciences of the University of Cagliari, as described elsewhere (Frau et al., 2013). In all experiments performed in this study, MDMA was dissolved in saline and administered i.p. in a volume of 10 ml/kg. Metformin, obtained from Sigma (Sigma-Aldrich, Milan, Italy), was dissolved in distillated water and administered orally (o.s.) in a volume of 10 ml/kg.

Tissue collection

For immunohistochemical studies, 48 hours and seven days after the last administration of MDMA, mice were anesthetized with chloral hydrate (400 mg/kg, i.p.) and transcardially perfused with paraformaldehyde (4% in 0.1 M phosphate buffer, pH 7.4). Sections for immunohistochemistry and Cresyl Violet for Nissl Staining from the CPu and SNc (50 µm thick) were coronally cut on a vibratome. Free-floating sections were incubated overnight with TH and DAT primary antibodies (polyclonal rabbit anti-TH, 1:1000, Millipore; monoclonal rat anti-DAT, 1:1000, Millipore, USA). The primary antibodies were prepared in phosphate buffer solution plus Triton containing normal goat serum. After washing, the sections were incubated in proper biotinylated secondary antibodies (Vector Laboratories, UK). For visualization, the avidin–peroxidase protocol (ABC, Vector Laboratories, UK) was applied, using DAB (Sigma-Aldrich, Milan, Italy) as chromogen. After washing, the sections were mounted on gelatin-coated slides, air-dried, dehydrated in ascending concentrations of ethanol, and

cleared with xylene (Frau et al., 2011). SNc sections were stained with cresyl violet for the Nissl staining to evaluate cell death in this area.

For TH and cresyl violet-stained cell immunohistochemistry in the SNc, three sections were sampled (anterior–posterior: -2.92 to -3.28 mm from bregma) according to the atlas of Paxinos and Franklin (2001). Images were digitized (PLA686 video camera, Pixelink, Canada) under constant-light conditions. A blind experimenter counted the stained cells manually. The number of TH (+) cells and Nissl stained neurons was obtained separately for each SNc level. Thereafter, in order to obtain an average value from all levels analyzed, the number of cells/level from each mouse was normalized with respect to the vehicle. Values from the three levels were than averaged to generate a mean. Analysis of TH and DAT (+) fibers in the CPu for each mouse, three sections from the CPu (anterior–posterior: 1.10 to 0.62 mm from bregma) was analyzed for TH and DAT immunoreactivity. Images were digitized with a video camera (Pixelink PL-A686) in gray scale for both TH and DAT (+) striatal analyses. The analyses were performed using the Scion Image analysis program. The average gray values from white matter were subtracted from each section to correct for background immunoreactivity. For each level of CPu, the obtained value was first with respect to vehicle, and values from different levels were averaged thereafter. Temperature Recording Body temperature was measured using a rectal probe (BRET-3) connected to a digital thermometer [MicroTherma 2T Hand Held Thermometer (2Biological Instruments, Besozzo, Varese, Italy)].

Temperature Recording

Body temperature was measured using a rectal probe (BRET-3) connected to a digital thermometer (MicroTherma 2T Hand Held Thermometer (2Biological Instruments, Besozzo, Varese, Italy)). Baseline temperature was recorded prior to the first metformin or vehicle administration, to ascertain that there wasn't differences in this parameter occurred among the experimental groups and then 1 hour after each administration of metformin, MDMA or vehicle. Temperature was recorded by holding each mouse at the base of its tail while the probe was inserted approximately 1 cm into the rectum for 4-5s, until stable rectal temperature was maintained for 3s at an ambient temperature of 21 ± 1 °C.

Statistic

For immunohistochemical experiments, results were statistically analyzed by two-way analysis of variance (ANOVA) followed by Tukey's post hoc test. For temperature recording, the results were

statistically compared with ANOVA repeated measures, followed by Tukey's post hoc test, for comparison between experimental groups. The results were considered significant at $p<0.05$.

4. Results

4.1 Experiment I: METH Self-administration

- **METH SA caused rapid escalation and maintenance of METH intake**

All METH-trained rats significantly escalated their intake of the drug during the first 21 days (**Figure 12**). Animal was divided in three groups: control group (Ct), saline YS group and METH group. Data are mean ± SEM of number of METH infusions (0.1 mg/kg/infusion). METH group showed significant increase of infusion as comparison to Ct group and to saline Y group on the same day (**Figure 12**); moreover a significant increase in the METH group as comparison to first days of METH, was found (**Figure 12**).

Fig. 12

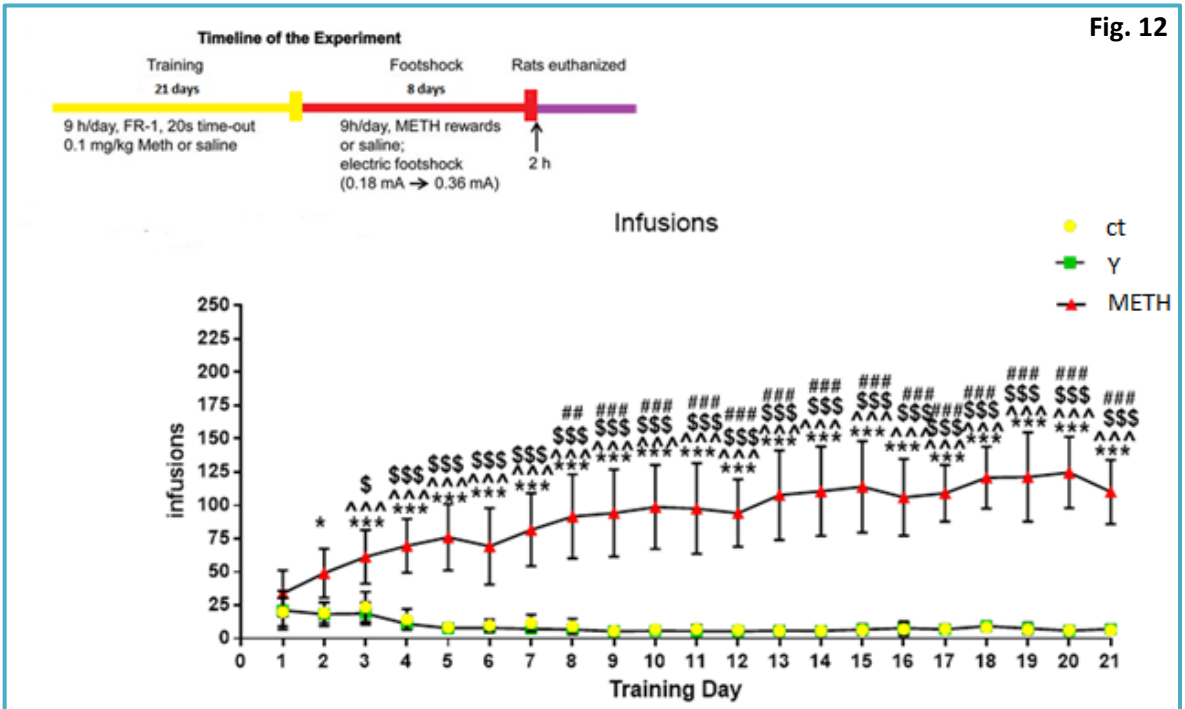

Escalation of METH intake during the training phase of the experiment. *N=10 (Ct), N=15 (METH SA group) and N=19 (Y group). Data are mean ± SEM of number of METH infusions (0.1 mg/kg/infusion) for 21 days. Data were analyzed by two-way ANOVA for repeated measures showed a significant treatment effect, time effect, and time × treatment interaction, followed by Tukey's multiple comparison tests. *p<0.05 and ***p<0.0001 vs. Ct group on the same day; ^^^p<0.0001 vs. Saline Y group on the same day; $p<0.05 and $$$p<0.0001 vs. METH group on day 1 and 2; #p<0.05; ###p<0.0001 vs. METH group on day 3.*

Furthermore, we have measured the number of active and inactive lever presses during the 9 hours daily SA sessions. During training (21 days of SA), active lever-presses were reinforced on an FR-1 20s timeout reinforcement schedule; reward delivery was paired with a 5-s tone-light cue. In METH group, rats showed a significant increase in the number of active lever, as compared to Ct group and to Y group on the same day, but as well as within METH group as compared to first days of METH (**Figure 13**). The number of inactive lever is similar for Ct, Y group and METH group (**Figure 13**).

Fig. 13

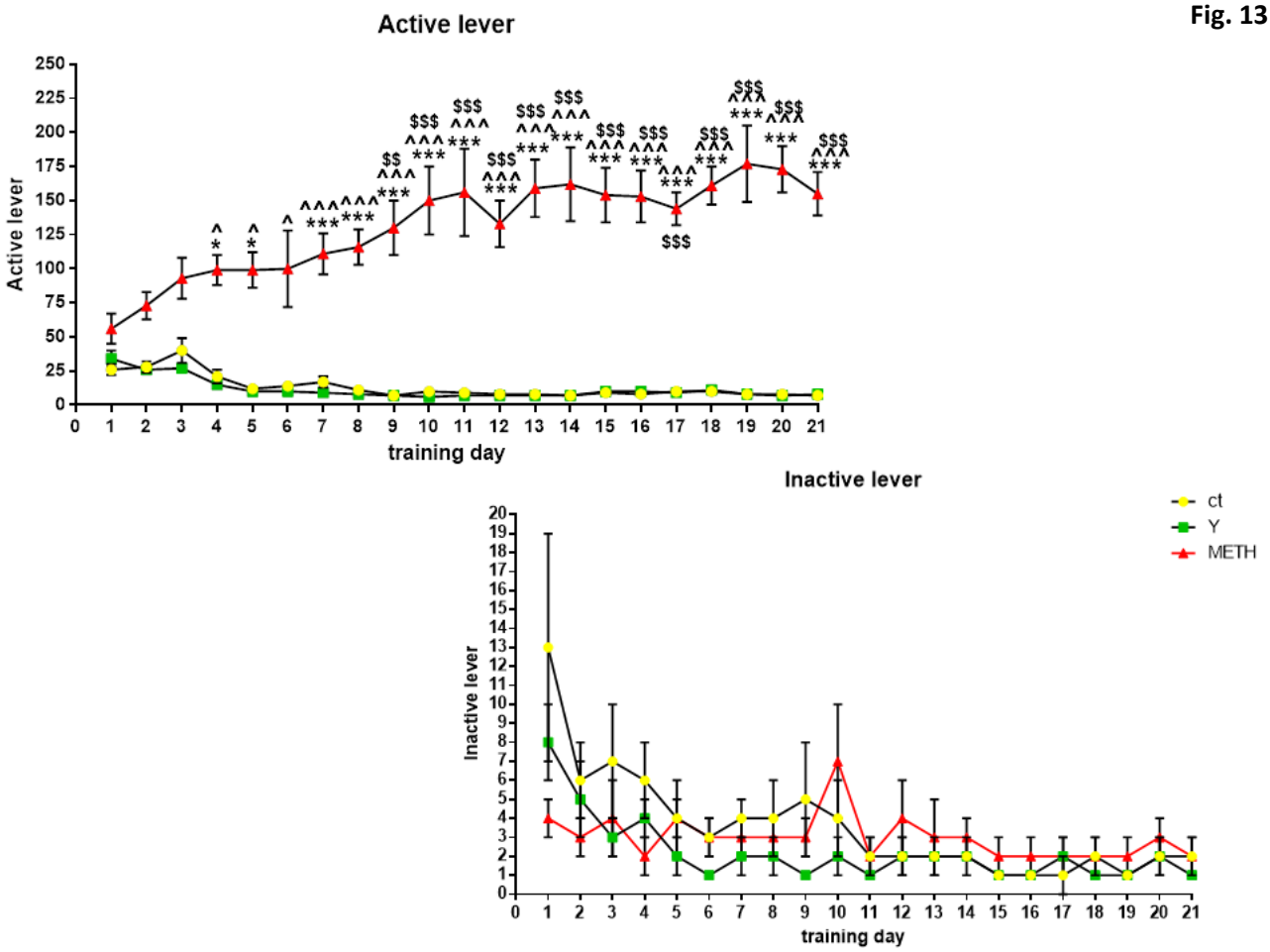

Average of number of lever presses in both active (drug SA option) and inactive (no programmed consequences) lever-presses. *N=10 (Ct), N=15 (METH group) and N=19 (Y group). Data are mean ± SEM of average number of lever presses in both active (drug SA option) and inactive (no programmed consequences) lever-presses during the 9 hours daily SA sessions for 21 days. Data were analyzed by two-way ANOVA for repeated measures showed a significant treatment effect, time effect, and time × treatment interaction, followed by Tukey's multiple comparison tests. Active lever: *p<0.05,***p<0.0001 vs Ct group on the same day; ^p<0.05 and ^^^p<0.0001 vs Y group on the same day, $$p<0.005 and $$$p<0.0001 vs METH group on day 1 and 2.*

- **Behavior during Footshock phase**

During 8 days were administered footshocks, we have considered only two groups of animals: Ct group and METH group. The initial footshock session was set at 0.18 mA and amplified by 0.06 mA increments to a final intensity of 0.36 mA. Results showed that METH group had a significant numbers of METH infusion, as compared to Ct group on the same day (**Figure 14**).

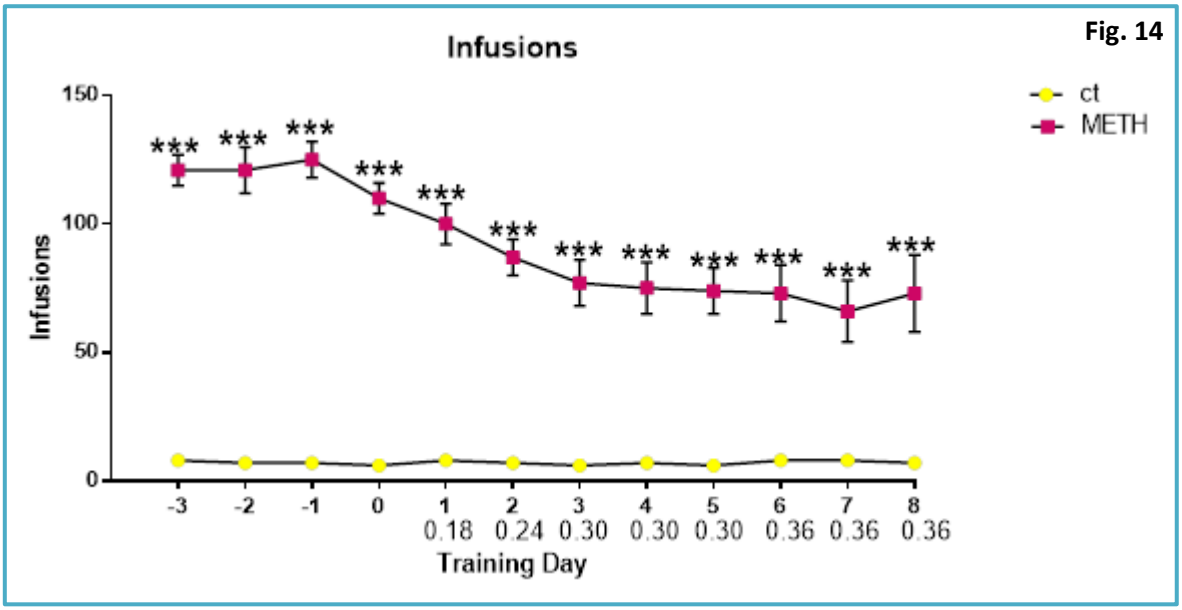

Fig. 14

Number of infusions during footshocks phase. *N=10 (Ct group), N=15 (METH group). In the graph, we have putted also 4 days before the start of footshocks to better understand the behavior during footshocks phase. Data were analyzed by ANOVA for repeated measures showed a significant treatment effect, time effect, and time × treatment interaction, followed by Tukey's multiple comparison tests. ***p<0.0001 vs. Ct group on the same day.*

We have seen the same result in the number of active lever, where METH group showed a significant increase, as compare to Ct group on the same day, whereas the number of inactive lever was low in both groups (**Figure 15**).

Fig. 15

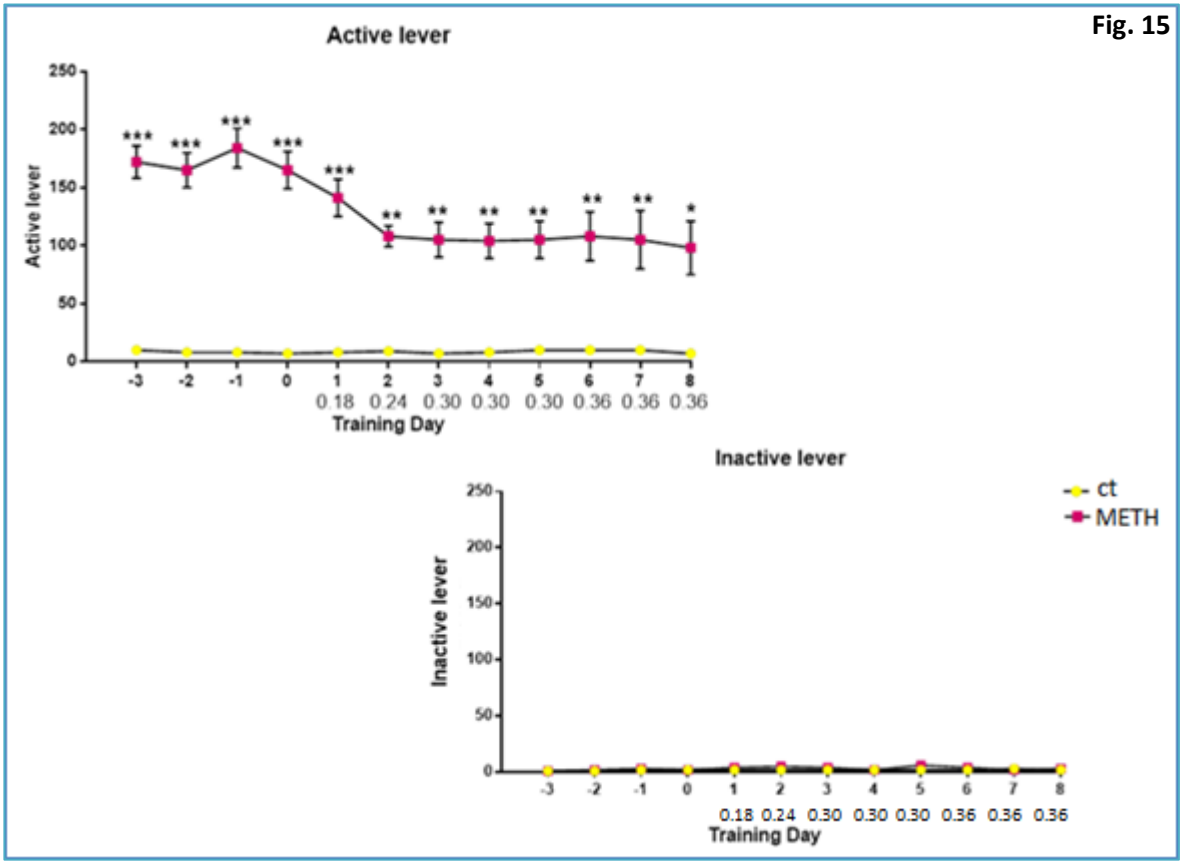

Active and inactive lever during footshock phase. *N=10 (Ct group), N=15 (METH group). Average of number of lever presses in both active (drug SA option) and inactive (no programmed consequences) lever-presses during the 9 hours daily self-administration sessions for 21 days. Data were analyzed by ANOVA for repeated measures showed a significant treatment effect, time effect, and time × treatment interaction, followed by Tukey's multiple comparison tests. *p<0.05, **p<0.005 and ***p<0.0001 vs. Ct group on the same day.*

- **Mild footshocks segregate METH self-administering rats into animals with distinct addiction profiles.**

During the punishment phase, footshock intensity was increased gradually from 0.18 mA to 0.36 mA over a period of 8 days. The shocks differentiated METH-trained animals into two phenotypes. One group continued to compulsively press the lever for METH (shock-resistant (M-SR)), whereas the other group progressively decreased their intake (shock-sensitive (M-SS)).

We classified 8 rats as M-SR, because they showed less than 30% decrease in the number of METH infusions from pre-shock level during the last three sessions of the punishment phase. In contrast, we classified 7 animals as M-SS, because they showed more than 70% suppression of drug infusions relative to pre-shock levels. Although both groups (M-SR and M-SS) increased their METH intake as compare to Ct group on the same day (**Figure 16**). The M-SR rats continued to take infusions of METH significantly higher rate than the M-SS group on the same day (**Figure 16**). Moreover, within the M-SS group, we have found significantly decrease of METH infusions as compared to day -3 (**Figure 16**).

Fig.16

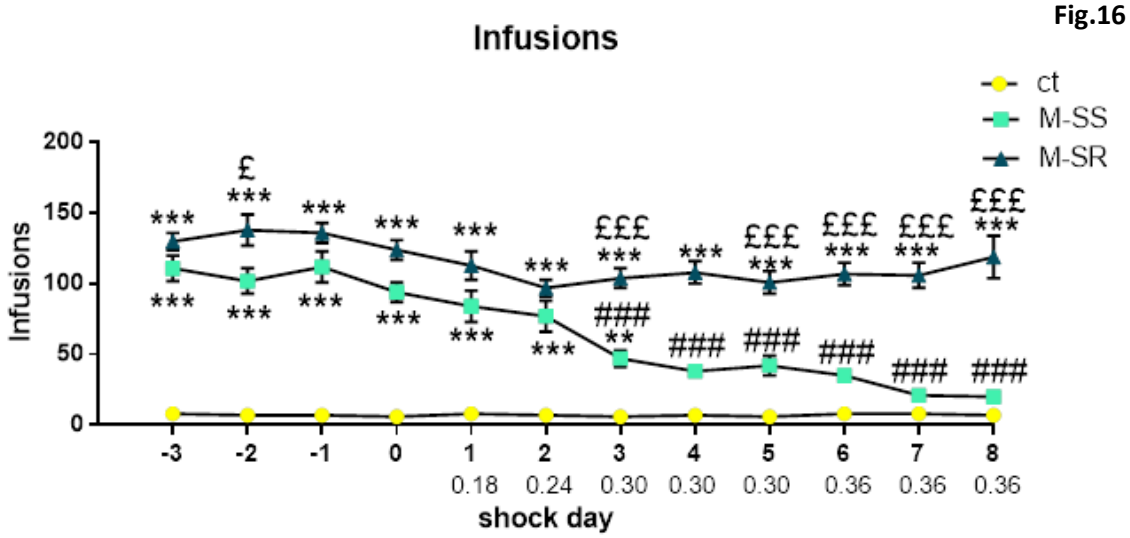

Infusions during Footshocks and the segregation of the METH-trained animals into two phenotypes. *N=7 (SS group) and N=8 (SR group). In the graph we have putted four days before the start of footshocks to better understand the behavior during footshock phase. As the level of footshocks increased, reinforced responding decreased in M-SS, but not in M-SR rats. During the footshock phase, shock intensity was increased from 0.18 to 0.36 mA, with 50% of rewarded lever presses being accompanied by footshocks. **p<0.005, ***p<0.0001 vs. Ct group on the same day; $^{£}$p<0.05 and $^{£££}$p<0.0001 vs. M-SS group on the same day; $^{###}$p<0.0001 vs. M-SS on day -3.*

We have seen the same result in the number of active lever (**Figure 17)**. M-SR group showed a significant increase in the number of active lever pressed, as compare to M-SS group and to Ct group on the same day (**Figure 17)**. M-SS group showed a significant increase, as compare to Ct group on the same day (**Figure 17**).

Fig. 17

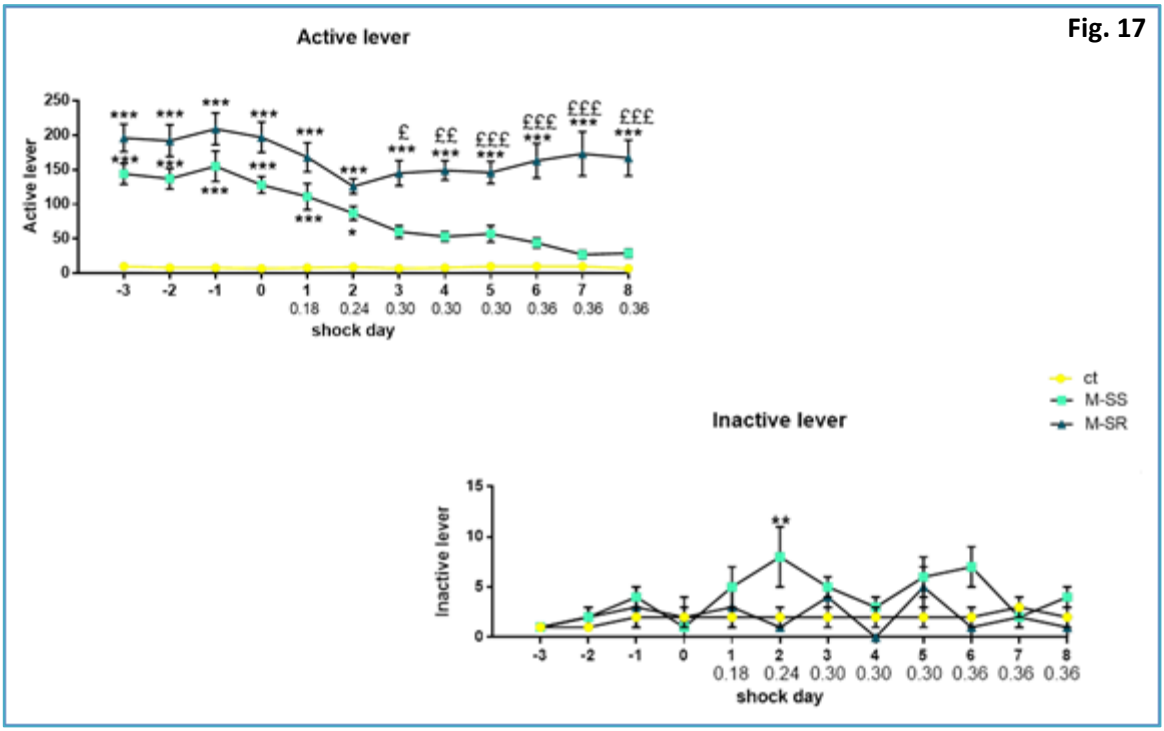

Average of number of lever presses in both active (drug SA option) and inactive (no programmed consequences) lever-presses. *N=7 (M-SS), N=8 (M-SR). Data are mean ± SEM of average number of lever presses in both active (drug SA option) and inactive (no programmed consequences) lever-presses during the 9-hours daily SA sessions for 8 days. Data were analyzed by ANOVA for repeated measures showed a significant treatment effect, time effect, and time × treatment interaction, followed by Tukey's multiple comparison tests. Active lever : *p<0.05 and ***p<0.0001 vs. Ct group on the same day; $^{£}$p<0.05, $^{££}$p<0.005 and $^{£££}$p<0.0001 vs. M-SS group on the same day. Inactive lever **p<0.005 vs. Ct group on day -3 and -2.*

Evaluation of footshocks during last 8 days of SA, showed a suppression of number of shocks in shock-sensitive (M-SS) rats, but not in shock-resistant (M-SR) (**Figure 18**). Significant differences in METH infusion between M-SS and M-SR phenotypes were observed (**Figure 18**).

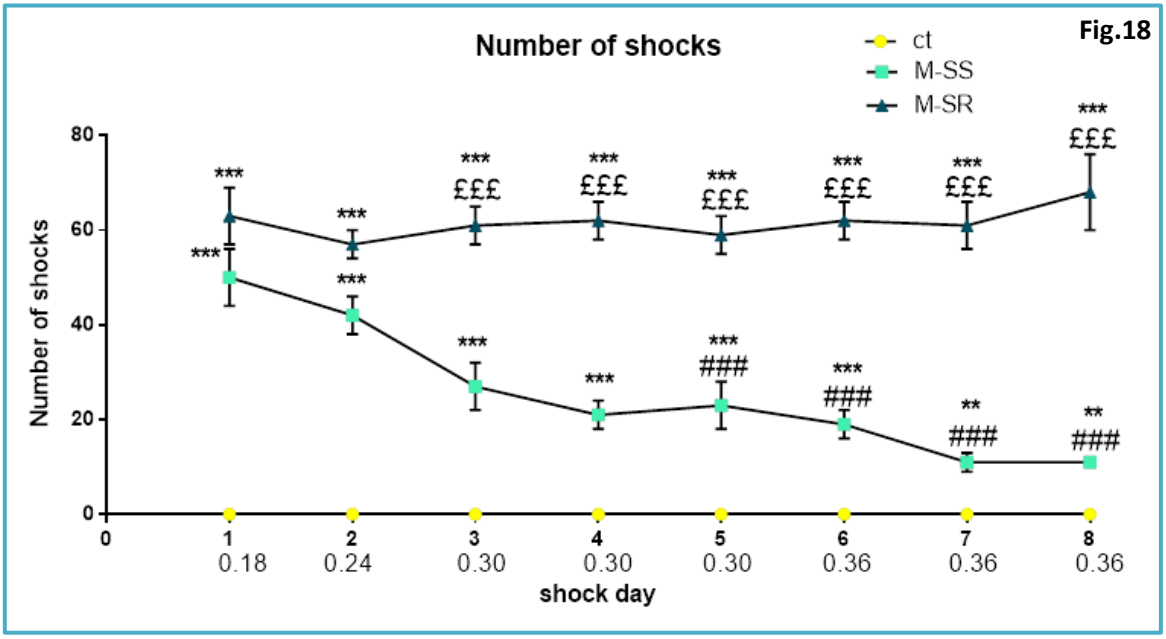

Footshocks during last 8 days of SA. *N=7-8 per group. Suppression of number of shocks in shock-sensitive (SS) rats but not in shock-resistant (SR) compulsive METH takers. During the footshock phase, shock intensity was increased from 0.18 to 0.36 mA, with 50% of rewarded lever presses being accompanied by footshocks. Significant differences in METH infusion between M-SS and M-SR phenotypes were observed. Data analyzed by ANOVA for repeated measures, followed by Turkey's multiple comparison test. **p<0.005 and ***p<0.0001 vs. Ct group on the same day; £££p<0.0001 vs. M-SS on the same day; ###p<0.0001 vs. M-SS on day 1.*

- **Effects of chronic METH treatment on the expression of Fos members of AP1 family in PFC.**

The figure 19 shows the effects of METH on the mRNA levels for AP1 family in PFC (**Figure 19**). METH infusion (0.1 mg/kg) for 9 hours daily didn't caused substantial increases in c-Fos expression in different groups considered (control, Y-SR, Y-SS, M-SR and M-SS) **(Figure 19)**. We have found a significant decrease in Y-SR and Y-SS group for Fos-B in comparison to Ct group (**Figure 19**). Moreover, in M-SS group, we have found a significant increase in Fos-B mRNA, as compared to Y-SS group. Regarding Fra1 mRNA, we have seen a significant increase in M-SS group in comparison to Y-SR group (**Figure 19**).

Fig. 19

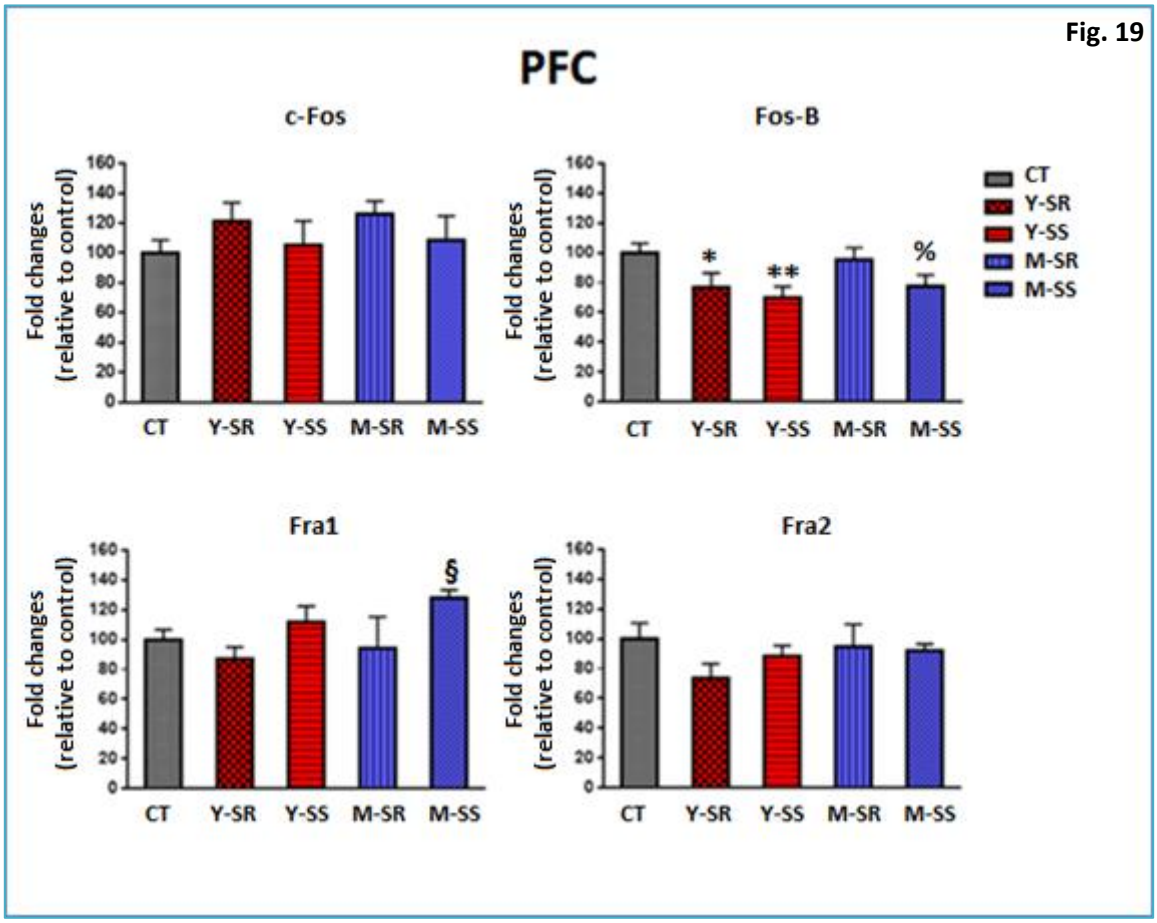

Expression of Fos members of AP1 family in PFC. *N=7-10 per group. The rats were euthanized 2h after the last session of SA. Total RNA was extracted from the PFC and used in quantitative PCR assays. Values from the 5 groups were compared by ANOVA followed by Fisher's PLSD. Graphs show a significant changes decrease in Fos-B and Fra-1 expression. *p<0.05 and **p<0.005 vs. Ct group; $^{\%}$p<0.05 vs. Y-SS group; §p<0.05 vs. Y-SR group.*

- **Effects of chronic METH treatment on the expression of Fos members of AP1 family in NAc.**

The figure 20 shows the effects of METH on the mRNA levels for AP1 family in NAc (**Figure 20**). METH infusion (0.1 mg/kg) caused substantial increases in c-Fos expression in M-SR group, as compared to Ct group, to Y-SR group, to Y-SS and to M-SS group (**Figure 20**). In FosB mRNA, we have seen a significant increase in M-SR group as comparison to Ct group, to Y-SR, to Y-SS and to M-SS group (**Figure 20**). In Fra2 mRNA, results showed a significant increase in M-SR group in comparison to Ct group, to Y-SR group, to Y-SS and to M-SS (**Figure 20**).

Fig.20

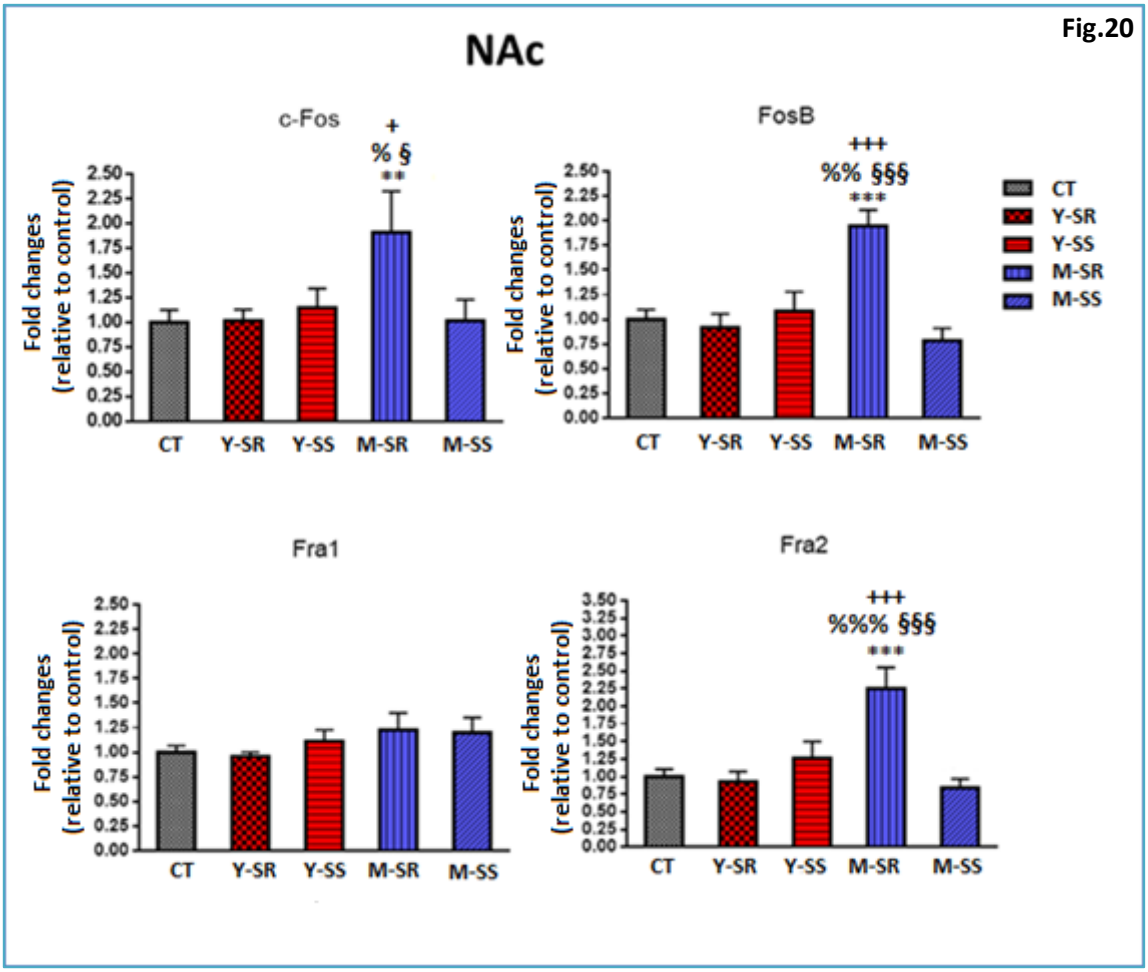

Effects of chronic METH treatment on the expression of AP1 family in NAc. *N=7-10 per group Values from the 5 groups were compared by ANOVA followed by Fisher's post hoc test analyses.*p<0.5, **p<0.001 and ***p<0.0001 vs. Ct group; $^{\%}$p<0.05, $^{\%\%}$p<0.005 and $^{\%\%\%}$p<0.0001 vs. Y-SS group; $^{+}$p<0.05 and $^{+++}$p<0.0001 vs. M-SS group; §p<0.05 and §§§p<0.0001 vs. Y-SR group.*

- **Effects of chronic METH treatment on the expression of Jun members of AP1 family in PFC.**

The figure 21 illustrates the effects of METH on the expression of the Jun members of AP1 family of IEGs. The chronic METH did not cause any changes in c-Jun, JunB and JunD mRNA levels in all groups (**Figure 21**).

Fig.21

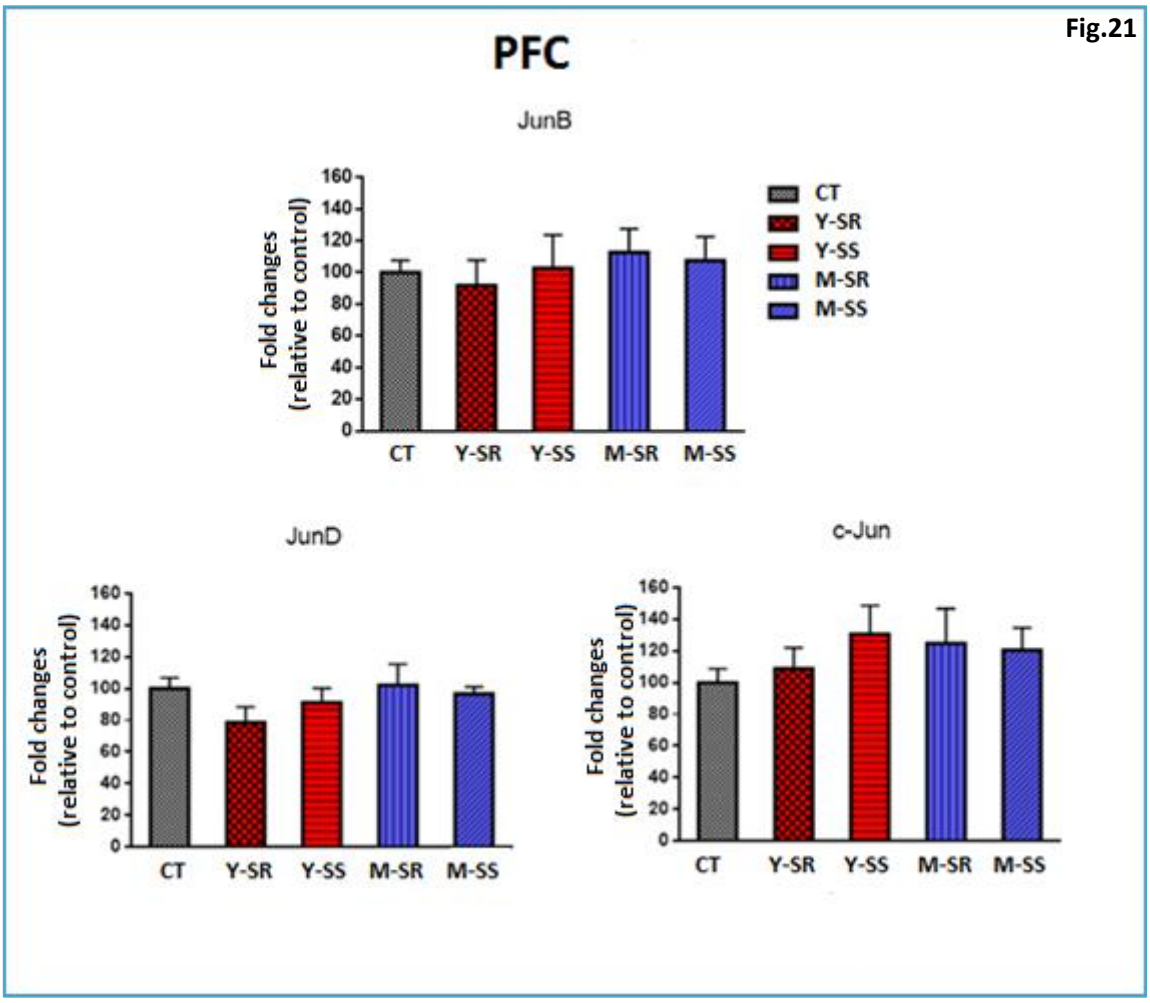

Effects of chronic METH treatment on the expression of Jun members of AP1 family of IEGs in PFC*. N=7-10 per group. Values from the 5 groups were compared by ANOVA followed by Fisher's post hoc test analyses. METH did not cause any changes in Jun mRNA levels family.*

- **Effects of chronic METH treatment on the expression of Jun members of AP1 family in NAc.**

The figure 22 shows the effects of METH on the mRNA levels for AP1 family in NAc (**Figure 22**). METH caused increases of JunB expression in M-SR group as compared to Ct group, to Y-SR group, to Y-SS group and to M-SS group (**Figure 22**). In JunD expression, the graph showed a significant decrease in M-SS group, as compared to Y-SS group (**Figure 22**). In c-Jun mRNA, we have seen a significant increase in M-SR group as comparison to Y-SR group and to Y-SS (**Figure 22**).

Fig.22

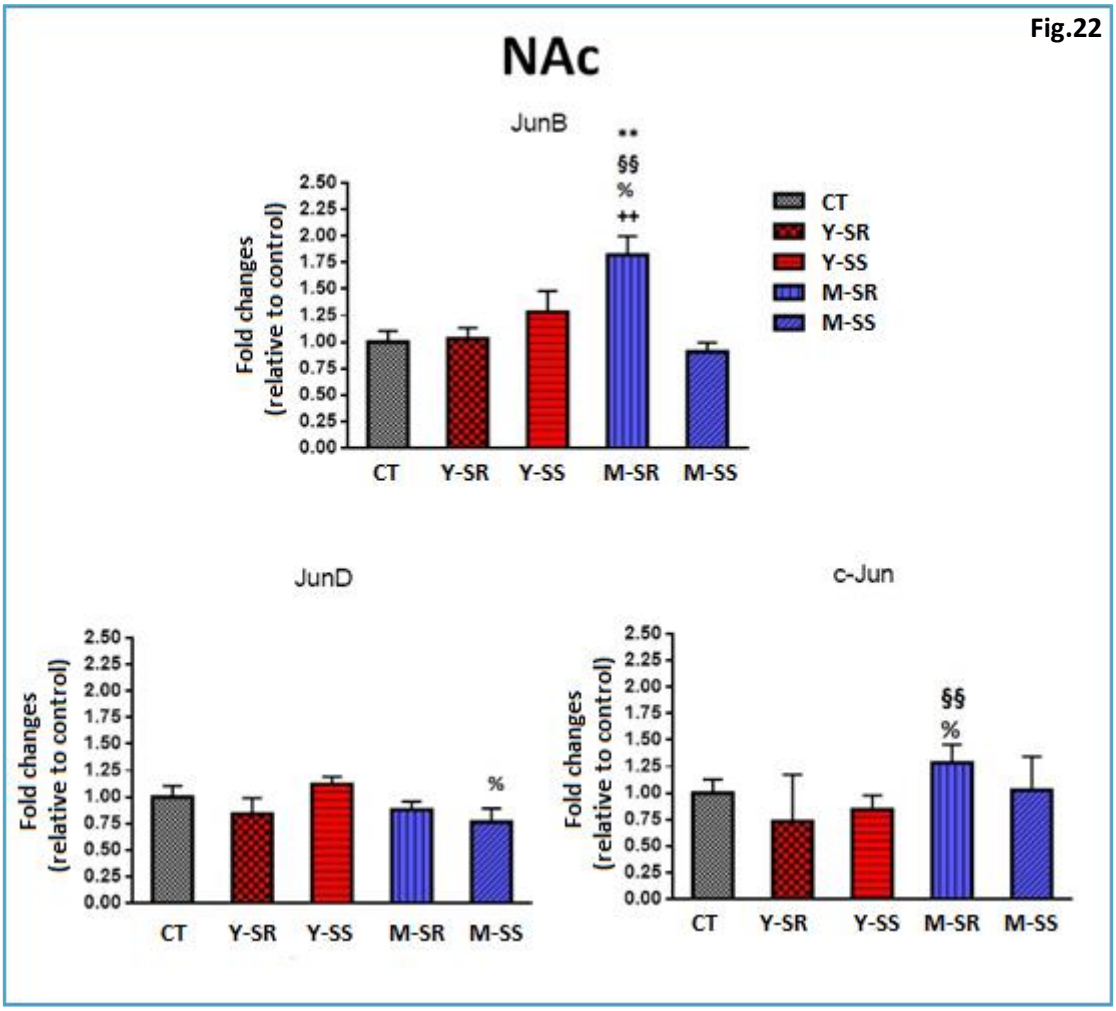

Effects of chronic METH treatment on the expression of Jun members of AP1 family in NAc. *N=7-10 per group. Values from the 5 groups were compared by ANOVA followed by Fisher's post hoc test analyses. **p<0.005 vs. Ct group; §§p<0.005 Y-SR group; %p<0.05 Y-SS group; ++p< 0.005 M-SS.*

- **The effects of METH on the early growth response (Egr) family of IEGs in PFC.**

The METH infusion caused significant change Egr2 gene in M-SR group in PFC, as compared to Y-SR group and to M-SS group (**Figure 23**). In contrast, the METH infusion didn't cause expression values in the Egr1 and Egr3 (**Figure 23**).

Fig.23

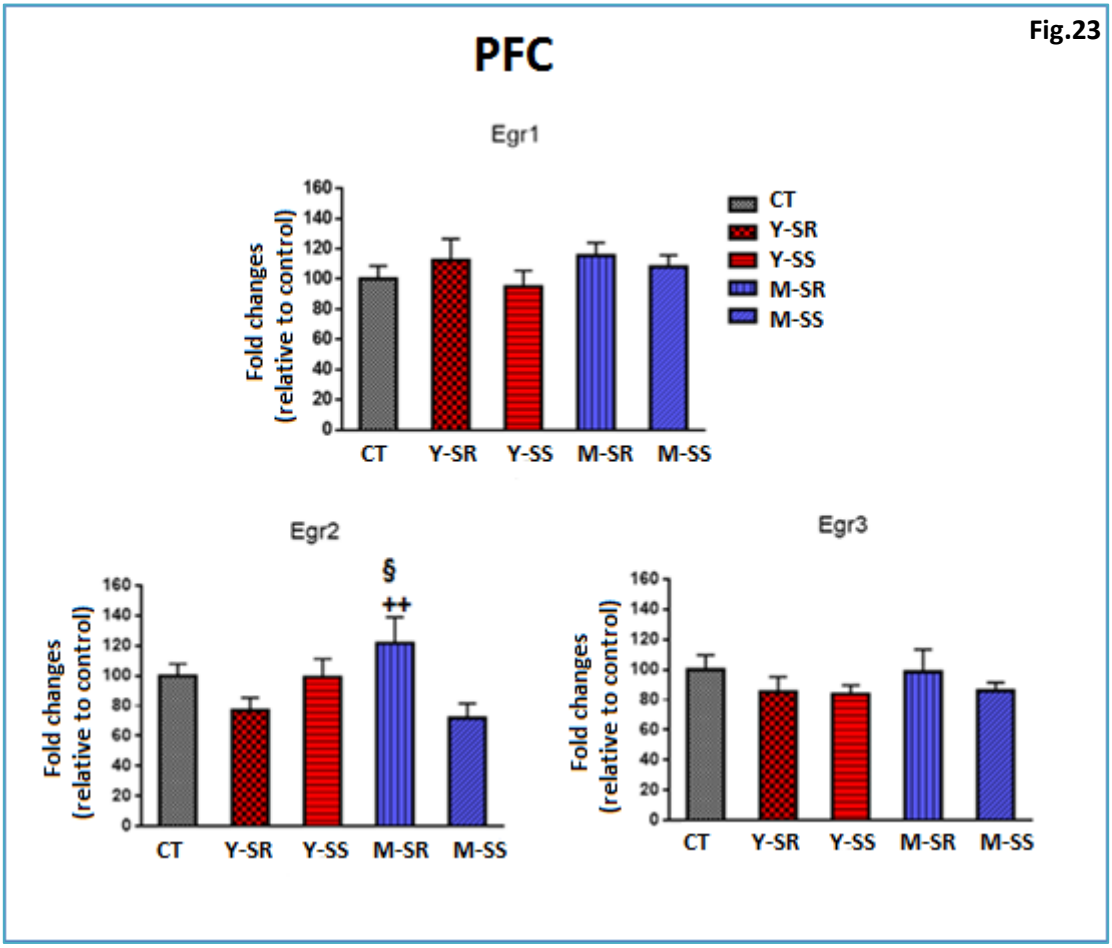

Effects of chronic METH treatment on the expression of Egr members of IEGs. *N= 7-10 per group. METH caused significant changes in Egr2 M-SR group. The rats were euthanized 2 hours after the last session of SA. Total RNA was extracted from the PFC and used in quantitative PCR assays. Values from the 5 groups were compared by ANOVA followed by Fisher's post hoc test analyses when ANOVA was significant.* $^{\S}p<0.05$ *vs. Y-SR group;* $^{++}p<0.005$ *vs. M-SS group.*

- **The effects of METH on the early growth response (Egr) family of IEGs in NAc.**

The picture 24 shows the effects of METH on the Egr mRNA levels in NAc (**Figure 24**). METH infusion caused Egr1 increases in M-SR group, as compared to Ct group, to Y-SR, to Y-SS group and to M-SS group (**Figure 24**). In Egr2 mRNA, we have seen a significant increase in M-SR group as comparison to Ct group, to Y-SR, to Y-SS and to M-SS group (**Figure 24**). Egr3 showed significant increase in M-SR group compared to M-SS (**Figure 24).**

Fig.24

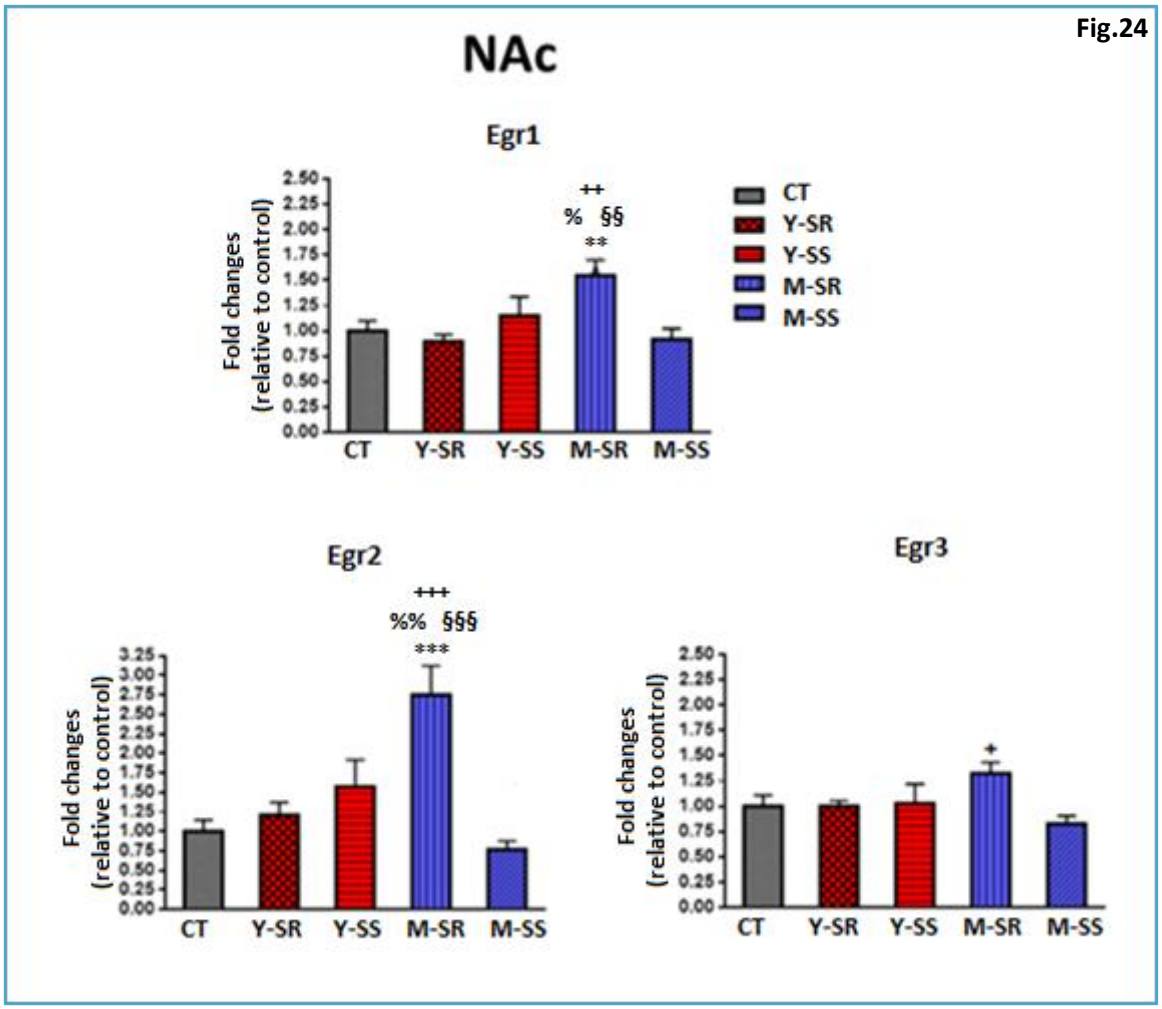

Effects of METH on the early growth response (Egr) family in NAc*. N= 7-10 per group. Graph shows the effects of METH on the mRNA levels Egr. Values from the 5 groups were compared by ANOVA followed by Fisher's post hoc test analyses when ANOVA was significant. **p<0.005 and ***p<0.0001 vs. Ct, §§p<0.005 and §§§p<0.0001 vs. Y-SR; $^{\%}$p<0.05 and $^{\%\%}$p<0.005 vs. Y-SS group; $^{++}$p<0.005 and $^{+++}$p<0.0001 vs. M-SS.*

- **Effects of METH on the members of the nuclear receptor subfamily 4 (NR4A) in PFC.**

Figure 25 shows effects of METH on the members of the Nr4A family of transcription factors (**Figure 25**). METH infusions caused significant increases in NR4A1 in Y-SR group in comparison to Ct group, and a significant increase of Nr4A3 mRNA level in M-SR group in comparison to the M-SS group (**Figure 25**).

Fig.25

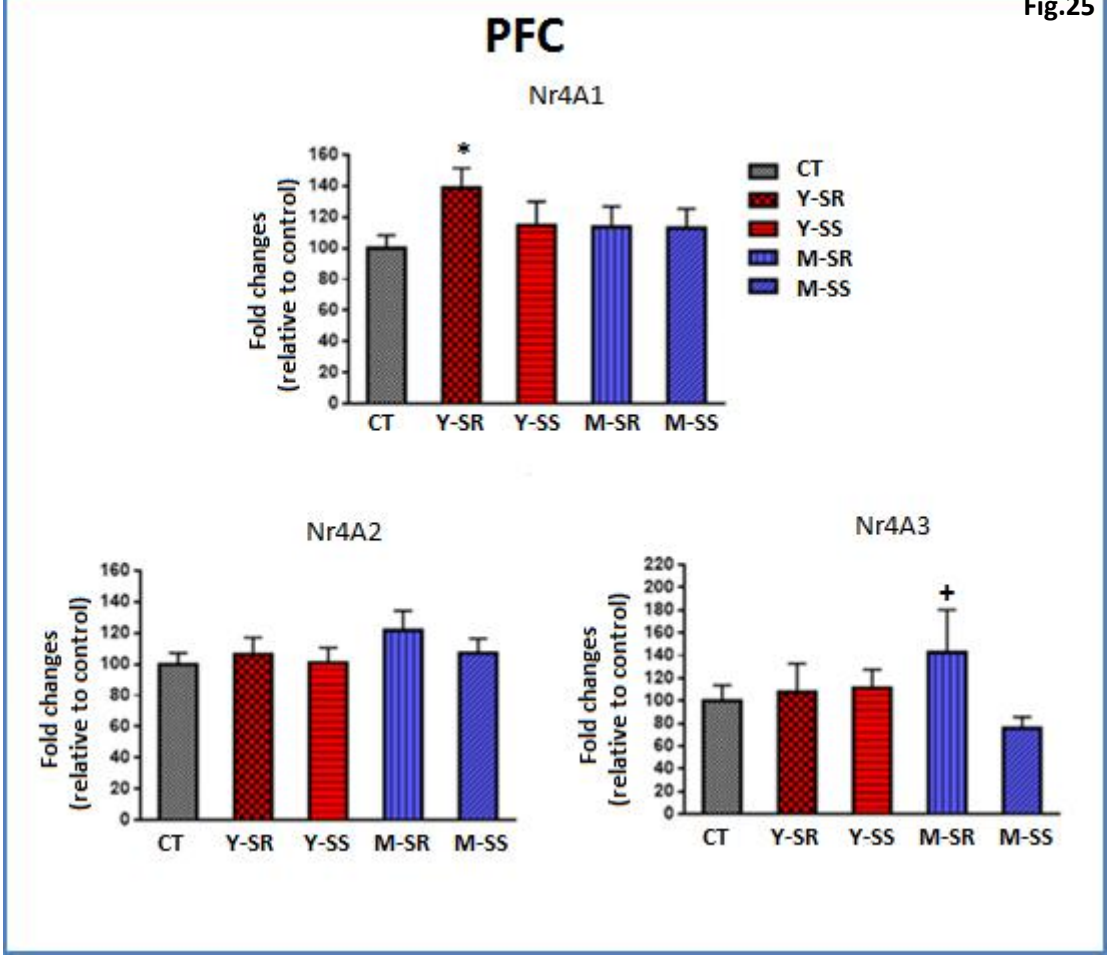

Effects of chronic METH treatment on the expression of Egr family members of IEGs*. N=7-10 per group. Graphs show significant changes for NrA1 and Nr4A3. The rats were euthanized 2 hours after the last session of SA. Total RNA was extracted from the PFC and used in quantitative PCR assays. Values from the 5 groups were compared by ANOVA followed by Fisher's post hoc test analyses when ANOVA was significant.*p<0.05 vs. Ct group; $^{+}$p<0.05 vs. M-SS group.*

- **Effects of METH on the members of the nuclear receptor subfamily 4 (NR4A) in NAc.**

Figures 26 shows changes in the mRNA expression of Nr4A1, with an increase in M-SR group, as compared to Ct group, to Y-SR, to Y-SS group and to M-SS group (**Figure 26**). In Nr4A2 expression, M-SR group showed a significant increase, as compared to Ct group, to Y-SR and to Y-SS (**Figure 26**). Evaluation of mRNA expression for Nr4A3 showed a significant increase in M-SR group, as compare to Ct group, to Y-SR and to Y-SS and to M-SS group (**Figure 26**).

Fig.26

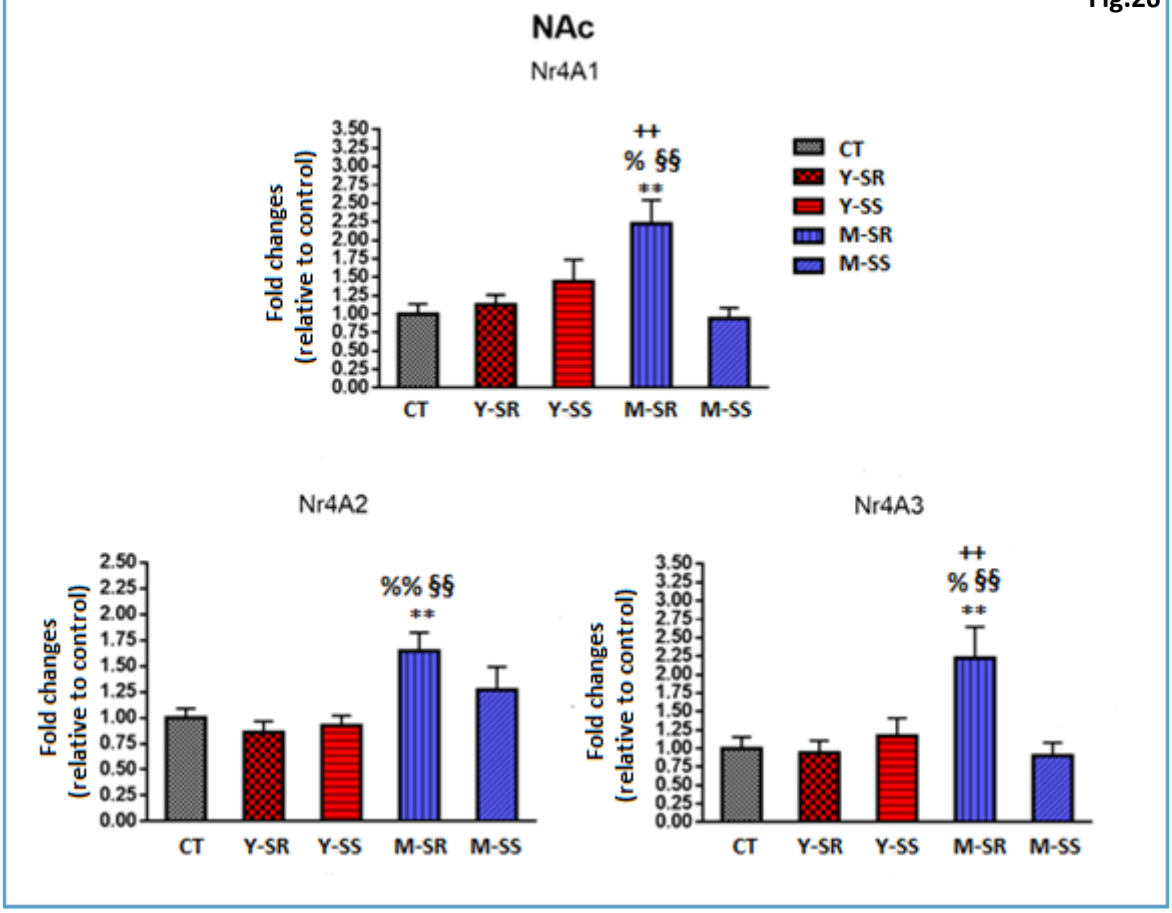

Effects of METH on the members of the nuclear receptor subfamily 4 (NR4a) in NAc. *N=7-10 per group. The rats were euthanized 2 hours after the last session of SA. Total RNA was extracted from the NAc and used in quantitative PCR assays. Values from the 5 groups were compared by ANOVA followed by Fisher's post hoc test analyses when ANOVA was significant. **p<0.005 vs. Ct group; §§p<0.005 Y-SR; $^{\%}$p<0.05 and $^{\%\%}$p<0.005 vs. Y-SS; $^{++}$p<0.005 vs. M-SS group).*

4.2 Experiment II: MDMA in Rhes mice

- **TH immunohistochemistry in vehicle-treated Rhes WT and Rhes KO mice**

Adult and elderly $Rhes^{-/-}$ male mice showed a significant decrease in both the density of TH (+) fibers in CPu, and the total number of TH (+) neurons in SNc, as compared with controls $Rhes^{+/+}$ male mice (**Figure 27**).

In SNc, adult and elderly $Rhes^{-/-}$ female mice showed a significant decrease in the total number of TH (+) neurons, as compared with controls $Rhes^{+/+}$ female mice (**Figure 27**). Moreover, elderly $Rhes^{-/-}$ female mice showed a decrease in TH immunoreactivity in CPu, as compared to vehicle-treated $Rhes^{+/+}$ female mice (**Figure 27**).

In adult age, $Rhes^{-/-}$ male mice showed a significant decrease in the number of TH (+) neurons in SNc, as compared to $Rhes^{-/-}$ female mice (**Figure 27**); whereas, in elderly age, $Rhes^{-/-}$ male mice showed a significant increase, as compared to $Rhes^{-/-}$ female mice (**Figure 27**). However, elderly $Rhes^{-/-}$ male mice showed a significant decrease in TH immunoreactivity in CPu, as compared to $Rhes^{-/-}$ female mice (**Figure 27**).

In addition, adult $Rhes^{+/+}$ female mice showed a significant decrease in the TH (+) fibers in CPu, as compared with adult $Rhes^{+/+}$ male mice, whereas in elderly age $Rhes^{+/+}$ female mice showed a significant increase in TH immunoreactivity in CPu, as compared to elderly $Rhes^{+/+}$ male mice (**Figure 27**).

In SNc, adult $Rhes^{+/+}$ female mice showed a significant increase in TH (+) neurons, as compared to adult $Rhes^{+/+}$ male mice. At elderly age $Rhes^{+/+}$ female mice showed a significant decrease in TH (+) neurons in SNc, as compared to elderly $Rhes^{+/+}$ male mice (**Figure 27**).

Fig. 27

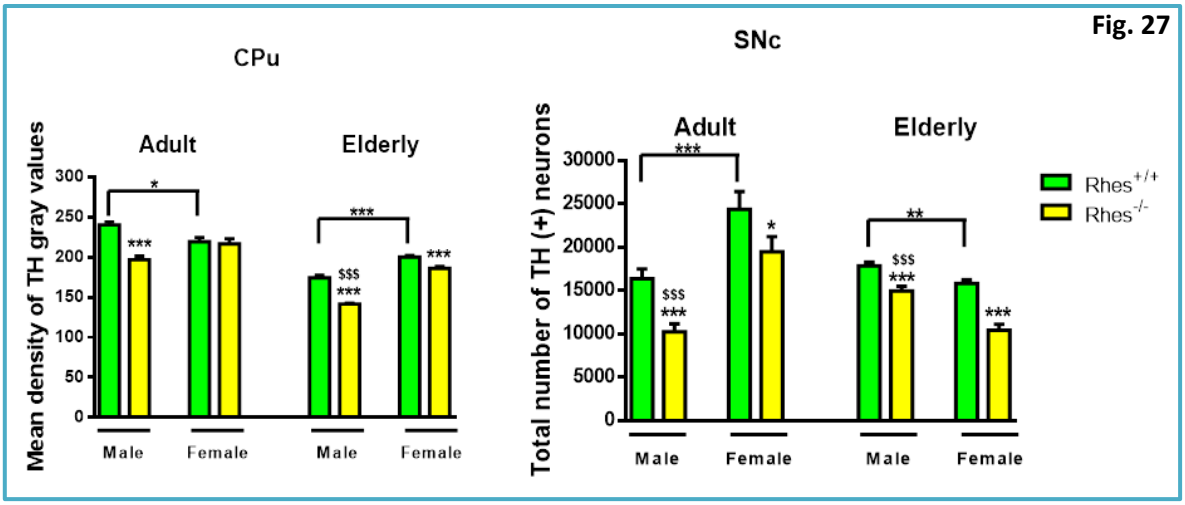

TH immunohistochemistry in vehicle-treated Rhes$^{+/+}$ and Rhes$^{-/-}$ mice. *Representative histograms of the CPu (left panel) and SNc (right panel) immunostained for TH of adult and elderly male and female Rhes$^{+/+}$ and Rhes$^{-/-}$ mice. The histograms in the left panel show the mean density of gray values of TH (+) fibers in the CPu, whereas the histograms in the right panel show the number of TH (+) neurons in SNc, calculated with the stereological analysis. Values are expressed as mean ± S.E.M. Number of mice per group: Rhes$^{+/+}$ adult male: n=5 and female n=8; Rhes$^{+/+}$ elderly male: n=9 and female n=6; Rhes$^{-/-}$ adult male: n=5 and female n=9; Rhes$^{-/-}$ elderly male: n=8 and female n=6. *p<0.05 and ***p<0.001 compared with Rhes$^{+/+}$ mice;* $^{\$\$\$}$p<0.001 *compared with female Rhes$^{-/-}$ mice by Newman-Keuls post hoc test.*

- **DA neuron degeneration (TH immunoreactivity) after MDMA treatment in adult mice**

Adult MDMA-treated Rhes$^{+/+}$ male mice showed a significant decrease in both the density of TH (+) fibers in CPu and in the total number of TH (+) neurons in SNc, as compared with vehicle-treated Rhes$^{+/+}$ male mice (**Figure 28**). We obtained similar results in MDMA-treated Rhes$^{-/-}$ male mice with a significant decrease in TH immunoreactivity, as compared with vehicle-treated Rhes$^{+/+}$ male mice in both SNc and CPu (**Figure 28**).

As described above, vehicle-treated Rhes$^{-/-}$ male mice showed a significant decrease in both the density of TH (+) fibers in CPu and in the total number of TH (+) neurons in SNc, as compared to vehicle-treated Rhes$^{+/+}$ male mice (**Figure 28**).

Furthermore, MDMA-treated male Rhes$^{-/-}$ mice showed a significant decrease in TH immunoreactivity in CPu, compared to vehicle-treated Rhes$^{-/-}$ male mice and compared to Rhes$^{+/+}$ MDMA-treated **(Figure 28)**. On the other side, in adult female we didn't find any significant change (**Figure 28**).

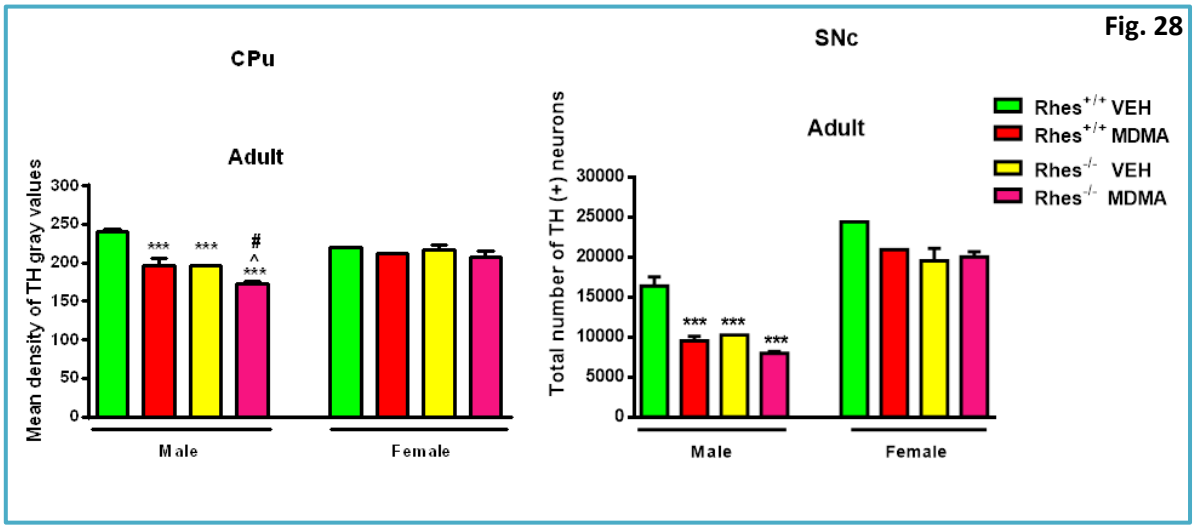

TH immunohistochemistry in MDMA treatment in Rhes$^{+/+}$ and Rhes$^{-/-}$ mice. *Representative sections and histograms of the CPu and SNc immunostained for TH of adult male and female Rhes$^{+/+}$ and Rhes$^{-/-}$ mice vehicle or treated with MDMA (4×20 mg/kg, i.p.). The histograms in the left panel show the mean density of gray values of TH (+) fibers in the CPu, whereas the histograms in the right panel show the number of TH (+) neurons in SNc, calculated with the stereological analysis. Values are expressed as mean ± S.E.M. Number of mice per group: vehicle Rhes$^{+/+}$ adult male: n=5 and female n=8; vehicle Rhes$^{-/-}$ adult male: n=5 and female n=8; MDMA treated Rhes$^{+/+}$ male: n=5 and female n=9. MDMA treated Rhes$^{-/-}$ male: n=5 and female n=9. *p<0.05 and ***p<0.001 compared with vehicle treated Rhes$^{+/+}$ mice; ^p<0.05 compared with vehicle-treated Rhes$^{-/-}$ mice; $^{\#}$p<0.05 compared to MDMA-treated Rhes$^{+/+}$ by Newman-Keuls post hoc test*

- ***DA neuron degeneration (TH immunoreactivity) after MDMA treatment in elderly mice***

Elderly MDMA-treated Rhes$^{+/+}$ male and female mice showed a significant decrease in both the density of TH (+) fibers in CPu and in the total number of TH (+) neurons in SNc, as compared with vehicle-treated Rhes$^{+/+}$ mice (**Figure 29**).

As describe above, vehicle-treated Rhes$^{-/-}$ male and female mice showed a significant decrease in TH immunoreactivity in CPU and SNc, as compared to vehicle-treated Rhes$^{+/+}$ mice (**Figure 29**).

Furthermore, MDMA-treated Rhes$^{-/-}$ male and female mice showed a significant decrease in the density of TH (+) fibers in CPu and in the total number of TH (+) neurons in SNc, as compared to vehicle-treated Rhes$^{+/+}$ mice (**Figure 29**).

MDMA-treated Rhes$^{-/-}$ male and female mice showed a significant decrease in TH immunoreactivity both in CPu and SNc, as compared with vehicle-treated Rhes$^{-/-}$ mice (**Figure 29**).

MDMA-treated Rhes$^{-/-}$ male and female mice showed a significant decrease in TH immunoreactivity in CPU and SNc, as compared to corresponding MDMA-treated Rhes$^{+/+}$ mice (**Figure 29**).

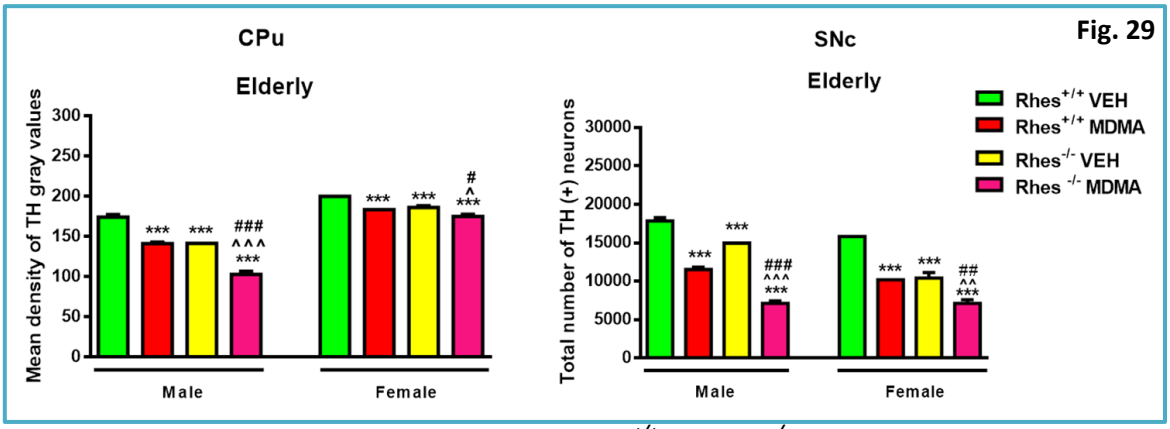

TH immunohistochemistry in MDMA treatment in Rhes$^{+/+}$ and Rhes$^{-/-}$ mice. *Representative sections and histograms of the CPu and SNc immunostained for TH of elderly male and female Rhes$^{+/+}$ and Rhes$^{-/-}$ mice vehicle or treated with MDMA (4×20 mg/kg, i.p.). The histograms in the left panel show the mean density of gray values of TH (+) fibers in the CPu, whereas the histograms in the right panel show the number of TH (+) neurons in SNc, calculated with the stereological analysis. Values are expressed as mean ± S.E.M. Number of mice per group: vehicle Rhes$^{+/+}$ adult male: n=9 and female n=6; vehicle Rhes$^{-/-}$ adult male: n=8 and female n=6; MDMA treated Rhes$^{+/+}$ male: n=9 and female n=6. MDMA treated Rhes$^{-/-}$ male: n=8 and female n=5. *p<0.05 and ***p<0.001 compared with vehicle treated Rhes$^{+/+}$ mice; $^{\#}$p<0.05, $^{\#\#}$p<0.005 and $^{\#\#\#}$p<0.001 compared with MDMA-treated Rhes$^{+/+}$ mice. $^{\wedge}$p<0.05, $^{\wedge\wedge}$p<0.005 and $^{\wedge\wedge\wedge}$p<0.001 compared with vehicle-treated Rhes$^{-/-}$ by Newman-Keuls post hoc test.*

- **Nissl staining in the SNc of MDMA-treated Rhes$^{-/-}$ mice**

Results on TH where confirmed by Nissl (+) cells staining in SNc, in both adult (male: -20%; female: -19%) and elderly mice (male: -25%; female: -23%), as compared with the respective Rhes$^{+/+}$ mice. Treatment with MDMA of Rhes$^{-/-}$ male mice potentiated the loss of Nissl (+) cells in adult male (-31%), but not in female mice; whereas MDMA administration to elderly Rhes$^{-/-}$ mice induced the loss of Nissl-positive cells, that was potentiated in both gender (male: -39%; female: -2%) (Data not shown).

- **Motor activity evaluation after MDMA treatment**

MDMA induced a significant increase in both locomotor and total motor activity (locomotor plus stereotypies) of Rhes$^{+/+}$ and Rhes$^{-/-}$ male and female mice, as compared with the respective vehicle for the 1st, 2nd, 3rd and 4th administration (**Figures 30**). Moreover, the increase observed in the motor activity of MDMA-treated Rhes$^{-/-}$ male, but not female, mice was significant as compared with MDMA-treated Rhes$^{+/+}$ male mice, for the 1st and 2nd administration (**Figures 30**). In contrast, a significant decrease in both the total motor activity and locomotor activity was observed in MDMA-treated Rhes$^{-/-}$ female mice as compared with MDMA-treated Rhes$^{+/+}$ female mice after the 4th administration (**Figure 30**).

Fig. 30

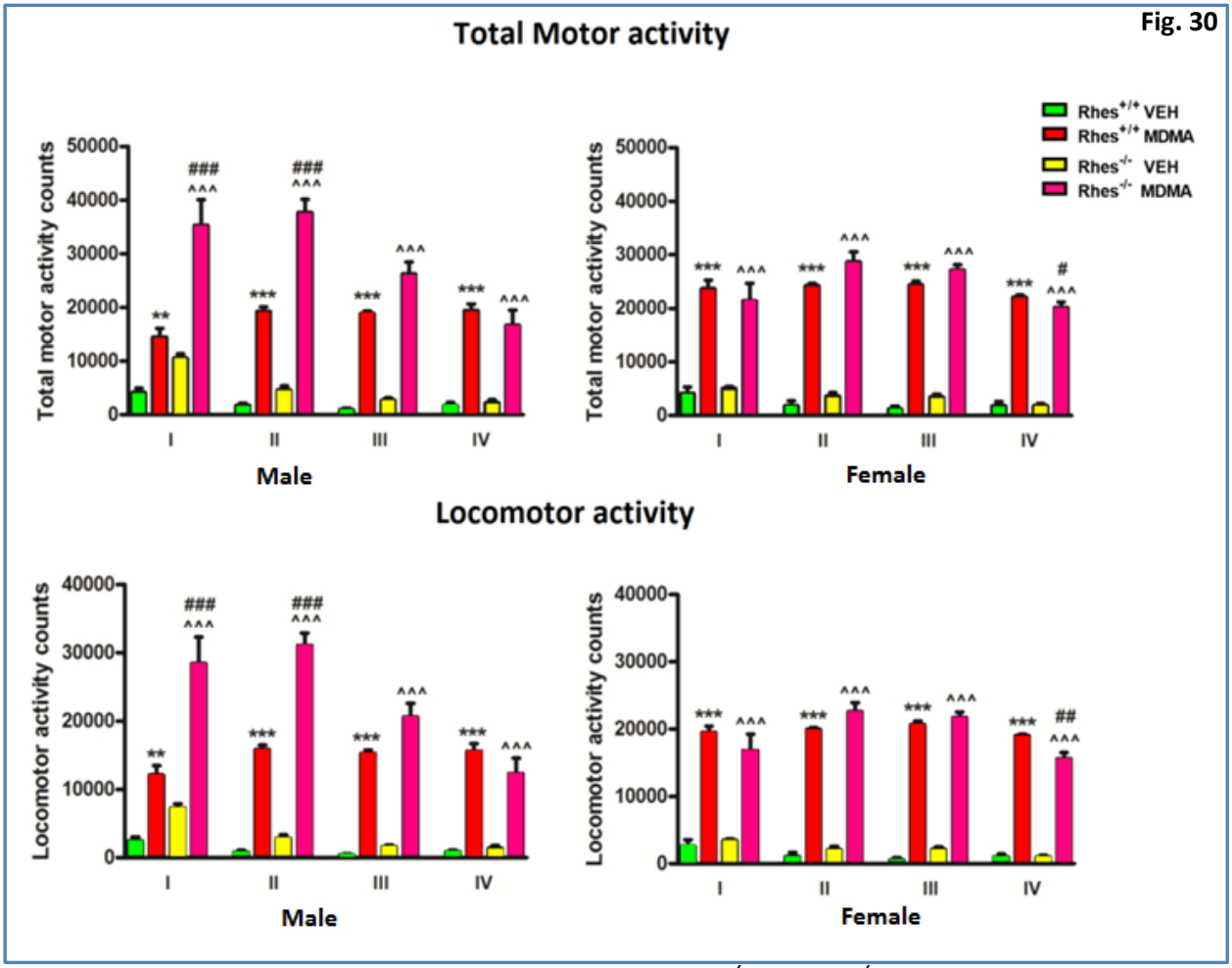

Effect of MDMA on motor activity in adult male and female Rhes$^{+/+}$ and Rhes$^{-/-}$ mice. *The histograms show the total motor and locomotor activity counts registered over the course of the treatment of adult mice, reported as total counts calculated for each MDMA administration. Activity counts were taken every 15 min for a total of 4 evaluations (cumulative time: 1 hour) within each MDMA administration (I, II, III, IV). Mice were treated with vehicle (saline, male Rhes$^{+/+}$ n=6 and Rhes$^{-/-}$ n=6; female Rhes$^{+/+}$ n=5; Rhes$^{-/-}$ n=5) or MDMA (4 × 20 mg/kg, i.p., male Rhes$^{+/+}$ n=6 and Rhes$^{-/-}$ n=5; female Rhes$^{+/+}$ n=4; Rhes$^{-/-}$ n=5). Values are expressed as mean ± S.E.M. **p<0.005 and ***p<0.0001 vs. vehicle-treated Rhes$^{+/+}$ mice; ^^^p<0.001 vs. vehicle-treated Rhes$^{-/-}$ mice; ###p<0.001 vs. MDMA-treated Rhes$^{+/+}$ mice by Newman-Keuls post hoc test.*

4.3 Experiment III: MDMA plus Metformin in mice

- **TH immunoreactivity and Nissl Staining in SNc: metformin with neuroprotective effects**

Mice belong to metformin group show an unchanged number of TH (+) neurons in the SNc, compared with vehicle group (**Figures 31, 32**). In line with previous results, the acute MDMA treatment induced a significant short- and long-term loss of TH (+) neurons in the SNc as measured by TH immunoreactivity. Nissl staining confirmed a reduction in the number of neurons in the SNc of MDMA-treated mice by about 30%, compared with the vehicle group (**Figure 32**). Metformin treatment during MDMA administration prevented the MDMA-induced decrease in TH (+) neurons in the SNc of mice sacrificed at 48 hours and 7 days after the last MDMA administration (**Figure 32**). Finally, the analysis of Nissl (+) neurons demonstrated a recovery in the number of neurons in the SNc of mice treated with MDMA plus metformin, compared with the MDMA group (**Figure 32**).

Fig. 31

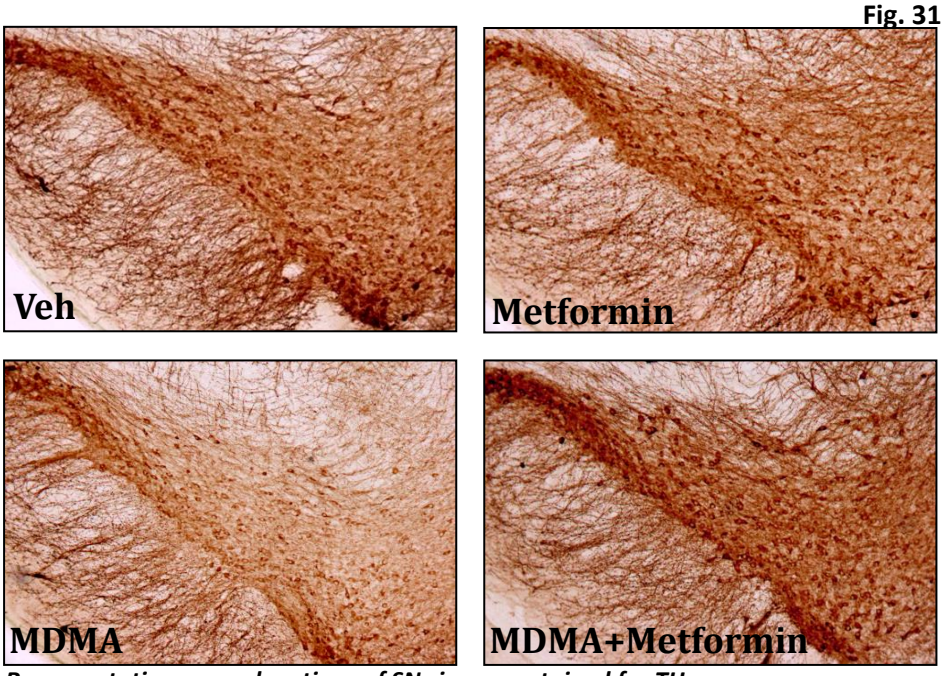

Representative coronal sections of SNc immunostained for TH

Fig. 32

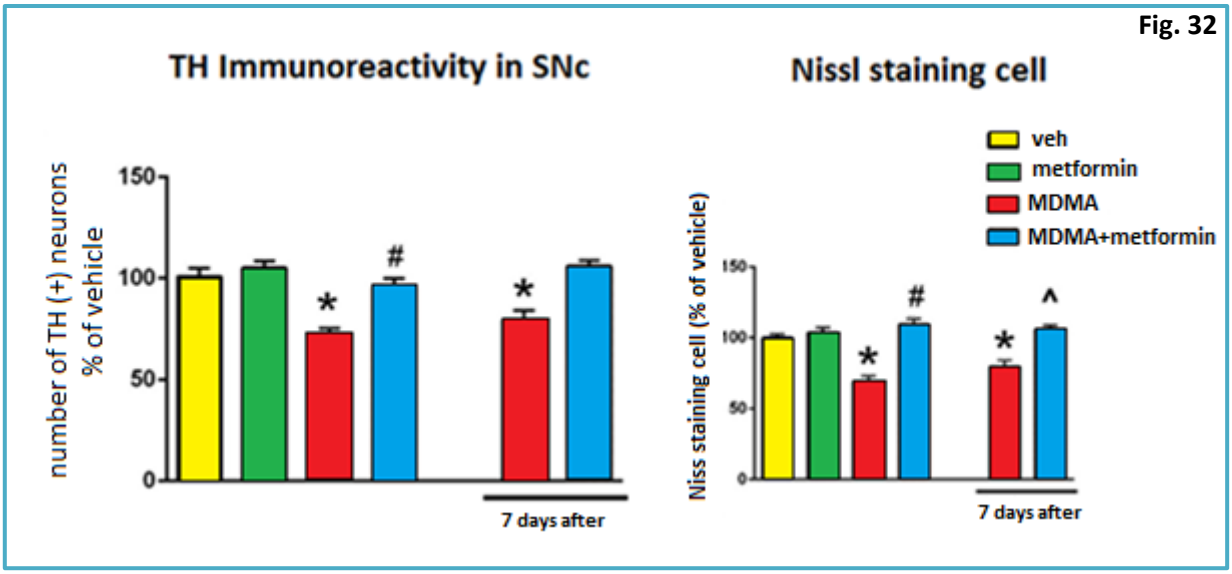

Immunoreactivity for TH in the SNc. *Mice were treated with vehicle (n=7), metformin (2X200 mg/kg, o.s., n=7), MDMA (4X20 mg/kg, i.p., n=11), and MDMA plus metformin (n=12), and sacrificed 48 h and 7 days after the last MDMA administration. The graphs show the number of TH (+) neurons in the SNc and the Nissl stained cells expressed as a percentage with respect to vehicle-treated mice. *p<0.05 compared with vehicle-treated mice. $^{\#}$p<0.05 compared with MDMA-treated mice sacrificed at 48 hours. ^p<0.05 compared with MDMA-treated mice sacrificed at 7 days. Data were statistically compared with two-way ANOVA, followed by Tukey's post hoc test.*

- **TH and DAT immunoreactivity in CPu: metformin prevents the loss of dopaminergic fibers**

In the CPu the density of TH (+) fibers is unvaried in metformin group, compared with vehicle group, whereas in the MDMA-treated at 48 hours and 7 days, there was a decrease in TH (+) fibers compared with vehicle group **(Figures 33, 34)**. The metformin prevented the TH (+) fibers loss induced by MDMA at 48 hours and 7 days after the last dose of MDMA **(Figures 34).**

Similarly to the TH results, the density of DAT (+) fibers was not decreased in the CPu of metformin-treated mice compared with vehicle group at 48 hours and 7 days after drug administration **(Figure 34)**. Confirming the striatal degeneration, the DAT immunohistochemistry showed a decrease of DAT (+) fibers induced by MDMA administration at 48 hours and 7 days after the last MDMA dose **(Figure 34)**. It is notable that the significant decrease of DAergic fibers in the MDMA-treated group sacrificed at 7 days is smaller than that observed at 48 hours, as demonstrated by the two-way ANOVA **(Figure 34)**. However, this analysis proved the short- and long-lasting neuroprotective effect of metformin, preventing the MDMA-induced DAT decrease **(Figure 34)**.

Fig. 33

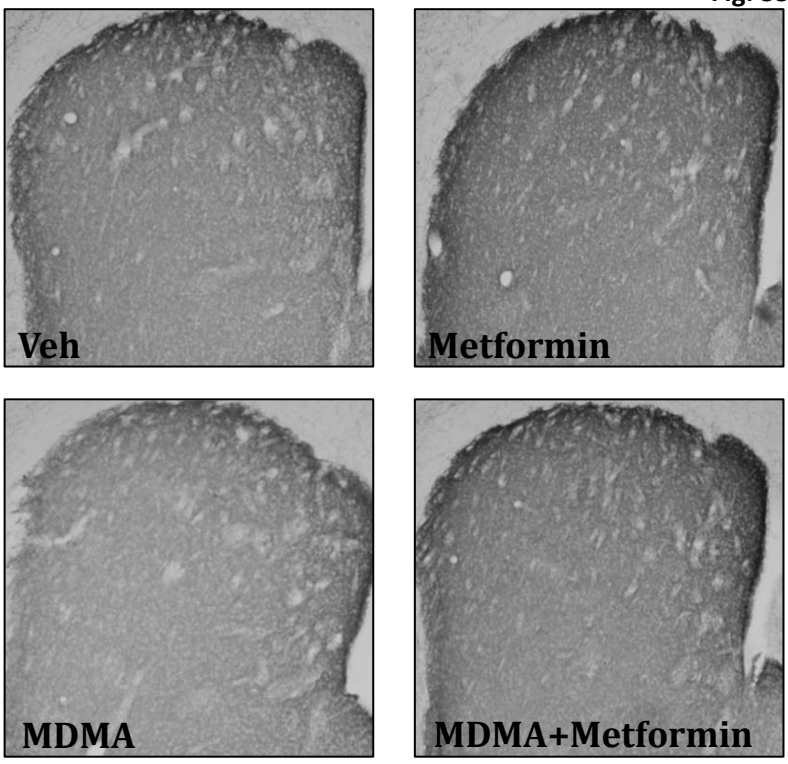

Representative coronal sections of the CPu immunostained for TH.

Fig. 34

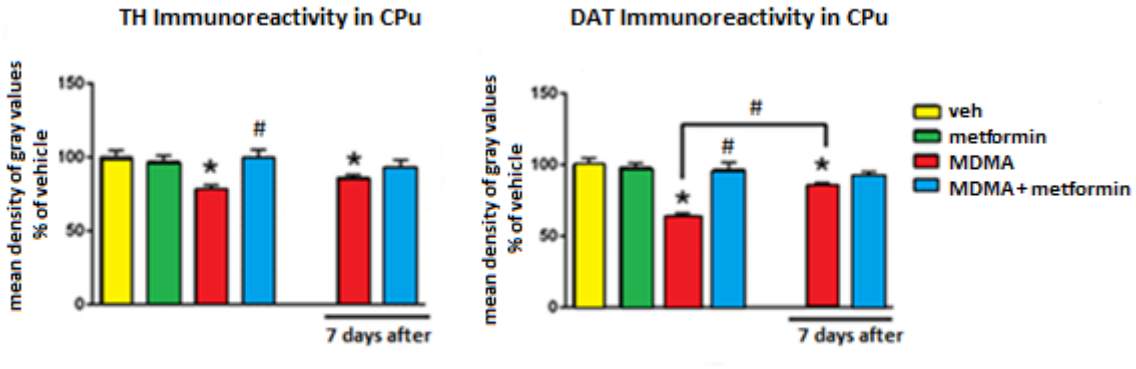

Immunoreactivity for TH and DAT in the CPu. *Mice were treated with vehicle (n=7), metformin (2X200 mg/kg, o.s., n=7), MDMA (4X20 mg/kg, i.p., n=11), and MDMA plus metformin (n=12), and sacrificed 48 hours and 7 days after the last MDMA administration. The graphs show the mean density of gray value of TH and DAT expressed as a percentage with respect to vehicle-treated mice. *p<0.05 compared with vehicle-treated mice. $^{\#}$p<0.05 compared with MDMA-treated mice sacrificed at 48 hours. Data were statistically compared with two-way ANOVA, followed by Tukey's post hoc test.*

- **Body temperature**

Baseline temperature was recorded prior to the first metformin or vehicle administration, to ascertain whether or not differences in this parameter occurred among the experimental groups, and then 1 hour after each administration of metformin, MDMA, or vehicle (**Figure 35**). There were no differences from the basal values measured before the beginning of the experiment in the metformin group or vehicle (**Figure 35**). There was a significant variation of the body temperature after each MDMA administration and also after 5 hours from the last dose of MDMA injected; this change was significant respect to basal values of the same group (**Figure 35**). Metformin is not able to counteract the hyperthermic effect induced by MDMA **(Figure 35).**

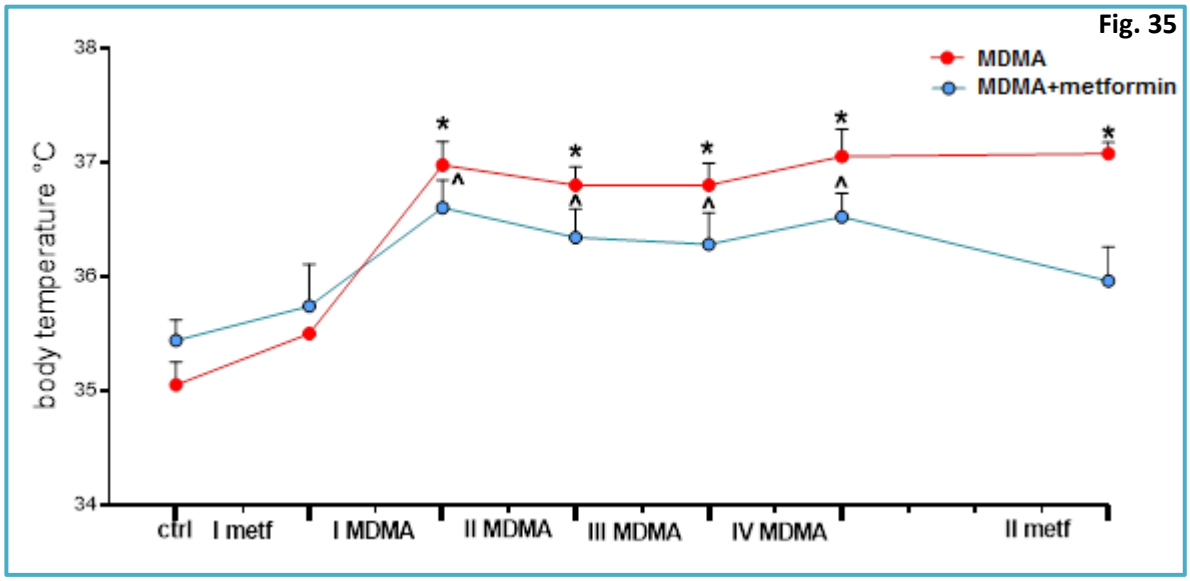

Effect of metformin on hyperthermia induced by MDMA: values of body temperature. *The graph reports the changes in body temperature induced by the administration of MDMA (4X20 mg/kg, i.p.) and metformin (2X200 mg/kg, o.s.). Baseline temperature was recorded prior to the first metformin or vehicle administration and then 1 hour after each administration of metformin, MDMA, or vehicle. The bold tick marks represent the measurements of body temperature 1 hour after each administration of metformin, MDMA, or vehicle. Values are expressed as mean ± SEM. *p<0.05 compared with basal values of MDMA group. ^p<0.05 compared with basal values of MDMA+metformin group. Data were statistically compared with ANOVA repeated measures, followed by Tukey's post hoc test.*

5. Discussion

ATS are the most abused drugs in the USA and throughout the world (UNODC report 2017). ATS addiction is correlated to severe neurologic and psychiatric adverse events including cognitive and behavior deficits. The repeated exposure to these substances also leads to drug craving. Moreover, experimental studies of these drugs confirmed that ATS drug-induced changes in gene expression in the PFC and NAc (Mychasiuk et al., 2013; Martin et al., 2012) as well as neurodegeneration processes in CPu and SNc (Costa et al., 2017; Moratalla, 2017). The neuropsychiatric complications are supposed to be partly related to drug-induced neurotoxic effects including damage to DAergic and 5-HTergic terminals as well as neuronal apoptosis (Cadet et al., 2007; Yamamoto et al., 2010).

Experiment I: METH SA

In the first set of experiments, in order to identify the molecular basis of compulsive METH taking, we have started to use footshocks as adverse events during METH SA.

Our results are consistent with other publications based on the footshock paradigm within SA, to identify rats with persistent drug taking behaviors despite contingent punishment to METH intake (Cadet et al., 2016; Cadet et al., 2017). The footshock paradigm is important not only to investigate the transition from recreation to addiction in drug abuse, but also to understand and identify the possible molecular substrates involved in compulsive drug use. Other studies showed that due to the different vulnerability to behavior relapse, after a withdrawal phase of a few days, M-SR rats increased METH seeking as compared to M-SS rats (Torres et al., 2017). Similar results have been reported in studies of cocaine SA, where a sub-population of rats showed resistance to punishment (Economidou et al., 2009; Pelloux et al., 2015).

METH SA is associated with persistent biochemical alterations in striatal and cortical DAergic terminals in the rat, with changes on monoaminergic systems (Krasnova et al., 2010; McFadden et al., 2012), GLUergic alterations (Schwendt et al., 2012) and/or with gene expression changes as well as c-Fos (Cornish et al., 2012; Jayanthi et al., 2014).

Furthermore, one of the most important findings from this work demonstrates that M-SR rats showed significant increases in several IEGs such as c-Fos, FosB, Fra2, and JunB mRNA levels with different responses within PFC and NAc. Moreover, Y-SR compared to M-SR rats showed no changes in the expression of these IEGs, suggesting that, the stress stimuli are not able to induce genetic

variations, since their effects are specific to compulsive METH taking (McCoy et al., 2011). METH alters the expression of a large number of transcripts (first step of gene expression) that are components of gene networks involved in the processes of METH abuse (Cadet et al., 2015). Indeed, previous data revealed that 543 mRNA expression of the transcription factors (e.g. c-fos, c-Jun, fosB, Nr4A1 etc.) were differentially expressed in the CPu within METH SA paradigm (Krasnova et al., 2013), inducing changes in the expression of several IEGs, (Martin et al., 2012). To date, few studies have conducted on the transcriptional or epigenetic effects of METH SA, whereas several others focused on cocaine and on gene expression in many brain regions (Feng et al., 2014; Ferguson et al., 2013).

Advances over the last decade have identified the brain circuits more vulnerable to molecular and behavioral changes associated with drug abuse such as METH. The NAc is an important interface between motivation and action (Di Chiara et al., 1999) in the circuit of addiction, since it is connected to areas such as CPu and midbrain DA systems, that control decision making behaviors and positive memory (Britt et al., 2012; Parkes et al., 2015). These are two cognitive processes that regulate drug-taking behaviors in rodents and humans (Orsini et al., 2015; Everitt 2014). In the role played by the NAc on drug addiction, beside the brain areas with extensive DAergic projections (CPu and DA midbrain), other different pathways seem to be involved (Kalivas & O'Brien, 2008; Koob et al., 2016; Koob 2010), including the GLUergic projections from the PFC. Moreover, NAc receives important limbic information from the amygdala, hippocampus and frontal cortex, and these information could be converted to motivational action through its connections with the extrapyramidal motor system (Koob & Volkow 2010). On this basis, we have analyzed gene expression change during SA not only in the NAc, but also in the PFC. Previous report showed that METH injection induces significant increases in IEGs expression such as c-fos, fosB, fra2, junB, Egr1-3, Nr4A1 and Nr4A3 in the CPu of rats, sub-chronically pretreated with METH and after one day of withdrawal, with a challenge of METH (5 mg/kg), (McCoy et al., 2011). In agreement, our results showed a similar increase of IEGs expression in M-SR group in the NAc, but not in PFC. Thus, our data are in line with the major role of NAc in the drug addiction and the main source of epigenetic modulation following chronic exposure to drugs of abuse (Mychasiuk et al., 2013), as compared to other brain regions. When taken together with our current observations, drug-induced gene expression changes seem to be region-specific (Meinhardt et al., 2013; Mychasiuk et al., 2013; Osterndorff-Kahanek et al., 2015). Such specificity likely reflects differential regulations occurring within distinct neuronal cell populations (Mychasiuk et al., 2013). Furthermore, drug-induced long-term transcriptional adaptations differ depending on

the drug used particularly for narcotics and psychostimulants (Becker et al., 2016; Mychasiuk et al., 2013). For example, previous studies revealed changes in the expression of 16 or 25 genes, after nicotine or AMPH exposure, respectively, in both NAc and PFC (Mychasiuk et al., 2013). At the same time, chronic treatment with different drugs such as METH and heroin, showed a dose-dependent induction of genes in CPu (Le Merrer et al., 2012; Piechota et al., 2012).

The specific gene expression changes lead to the development of different phenotypic features, suggesting a potential molecular explanation for the addiction to METH (McCoy et al., 2011). Understanding gene regulation and their consequences on synaptic plasticity, cellular morphology, and, ultimately, behavior, will represent a major challenge for this promising emerging field of research.

Experiment II: MDMA in Rhes mice

In the second set of experiments, we investigated the role of another ATS drug, MDMA, in order to evaluate any possible difference in the neurodegenerative processes as well as the effects of this drug treatment in the motor behavior of male and female Rhes$^{-/-}$ and Rhes$^{+/+}$, 3 and 12 month old mice. Our first results showed that Rhes$^{-/-}$ mice display an age dependent loss of DA neurons. Moreover, Rhes$^{-/-}$ male mice showed a high vulnerability to the neurotoxic effects of MDMA and a high sensitivity to its motor stimulant effects. In addition, our studies showed the differences between male and female Rhes$^{+/+}$ also in the basal conditions in vehicle-treated mice.

We observed that Rhes$^{-/-}$ male mice showed a significant decrease in the density of TH (+) fibers in CPu as well as in the total number of TH (+) neurons in SNc with aging. These results are consistent with our previous report that showed for the first time a decrease in TH (+) neurons in the SNc of Rhes$^{-/-}$ mice (Pinna et al., 2016). The decrease in DA nigrostriatal neurons may represent a specific vulnerability associated to these Rhes$^{-/-}$ mice, thus being one of factors related to neurodegenerative diseases such as PD, where a degeneration of DA nigrostriatal neurons turns out to be a peculiarity. The decrease of the total number of neurons in the SNc evidenced by Nissl staining provides further support to the existence of a real damage of DA neurons and not just a reduction of DA synthesis.

Additionally, evidence of this study shows that the vulnerability of DA nigrostriatal neurons of Rhes$^{-/-}$ female mice is significantly lower in CPu and SNc than Rhes$^{-/-}$ male mice. This may mean that the DAergic neurons of female mice are protected, in general, from neurodegeneration and, as suggested by several researchers (Sawada et al., 2002; Leranth et al., 2000), estrogens are implicated in this difference. In fact, in physiological conditions, estrogens have neurotrophic effects on nigrostriatal DAergic neurons, promoting the growth of neurites that expresses TH (Beyer et al., 2000; Reisert et al., 1987), increasing the TH expression in the neonate mouse midbrain (Ivanova et al., 2003), and enhancing differentiation and survival of DAergic neurons derived from human neuronal stem cells (Kishi et al., 2015). Moreover, this is consistent with the different incidence of PD between women and men (Smith & Dahodwala, 2014), thus adding further interest in this specific model.

Unlike the experimental models of DA neuron degeneration based on toxic insults, where a toxin is injected locally, this genetic animal model might provide new insights helping to clarify the mechanism of idiopathic PD in patients, since the mechanism of neurodegeneration of DA neurons is still under debate (Bellucci et al., 2016).

The mechanism at the basis of DA neuron degeneration in Rhes$^{-/-}$ mice needs further elucidation. However, on the basis of previous studies, we may suppose that Rhes signal pathways involved in neuronal survival, such as mTOR (Laplante & Sabatini 2012; Lee et al., 2015) and the influence of Rhes on G-alpha proteins of the i class (Gαi) coupled with G protein receptors (GPCR), signaling affecting the voltage-dependent inhibition of voltage-gated calcium channels 2 (Cav2.2), regulating calcium homeostasis (Thapliyal et al., 2008) and neurosecretion (Lipscombe et al., 1989), might be heavily implicated.

The DAergic neurotoxicity induced by MDMA in mice has been demonstrated by several studies (Granado et al., 2008, 2011; Costa et al., 2013) related to neurotoxicity effects in the nigrostriatal DAergic system of mice (Iravani et al., 2000; Green et al., 2003; Cadet et al., 2007; Halpin et al., 2014), with a decreased levels of both DA and DAT.

The study of MDMA neurotoxicity is particularly relevant since several reports showed that ATS might be part of the multiple factors leading to the DAergic neuron degeneration that causes PD (Costa et al., 2013; Cadet et al., 1998; Ares-Santos et al., 2014; Sulzer 2007). Indeed, preclinical studies and clinical observations have demonstrated that MDMA, similarly to METH and other ATS, induce long-lasting toxicity to DAergic neurons (Sonsalla et al., 1996; Granado et al., 2008, 2011; Costa et al., 2013; Ares-Santos et al., 2014). However, ad hoc studies for the occurrence of MDMA-induced neurotoxicity damage in humans are limited by the illegality of ATS drugs and their psychotic-like behavior effect (Moratalla et al., 2017).

Moreover, previous studies on Rhes$^{-/-}$ mice showed an enhanced response of locomotor activity and stereotypies induced by AMPH (Shahani et al., 2016; Vitucci et al., 2016). On the basis of these studies, we evaluated the motor response of Rhes$^{-/-}$ and Rhes$^{+/+}$ male and female mice along with neurotoxic effects of MDMA. In our results, Rhes$^{-/-}$ male mice display a higher motor stimulant effect in response to MDMA as compared to Rhes$^{+/+}$ male mice and during the first two administrations of the drug.

Furthermore, compared to Rhes$^{-/-}$ male mice, Rhes$^{-/-}$ female mice did not show a higher response to MDMA, both on locomotor and total (locomotor plus stereotypies) motor activity, suggesting once again a differential response between male and female Rhes$^{-/-}$ mice. Our findings are consistent with data showed by Shahani's laboratory (2016), stating that partially Rhes-deficient (Rhes$^{+/-}$) mice had an enhanced locomotor response to AMPH, though this report didn't show the differential effect

induced by AMPH in male and female mice. Moreover, our results are in line with the finding showing that Apomorphine, that is a D_1/D_2 receptor agonist, induced higher level of stereotypies in male $Rhes^{-/-}$ mice, as compared to female $Rhes^{-/-}$ mice (Quintero & Spano, 2011).

However, as reported by Ghiglieri and coworkers (2015), it should be noted that the locomotor activity induced by the DA D_1 agonist, SKF 81297, is higher in female $Rhes^{-/-}$ mice than in male $Rhes^{-/-}$ mice, thus suggesting a different response to DA D_1 receptor in $Rhes^{-/-}$ mice. However, in addition to increasing DA release, MDMA stimulates both D_1 and D_2 DA receptors, so we cannot discriminate the response of the two receptors in our study as in the one examined by Ghiglieri et al., 2015.

Experiment III: Metformin plus MDMA in mice

In the third set of experiments, we investigated the possible neuroprotective effect of metformin against, in short and long-term, MDMA-induced neurotoxicity as well as its role on hyperthermia. Our short (48 hours) and long-term evaluation (7 days) study showed that repeated MDMA administrations induced a significant loss of TH (+) neurons and fibers, respectively, in the SNc and CPu of adult mice. Nissl staining method confirmed a 30% reduction in the number of neurons in the SNc of MDMA-treated mice, thus showing that MDMA did not reduce TH expression or function, but induced DAergic neurodegeneration. Moreover, the striatal fibers degeneration induced by MDMA was confirmed by DAT immunoreactivity.

Metformin treatment completely prevented the MDMA induced nigrostriatal neuron death. In addition, Nissl (+) neurons revealed a recovery in the number of neurons in the SNc of mice treated with MDMA plus metformin.

The MDMA neurotoxicity is known to persist after its administration (Granado et al., 2008; Capela et al., 2009; Costa et al., 2013); therefore, we investigated the long lasting neuroprotective effect of metformin on neurodegeneration induced by MDMA effect, 7 days after the MDMA treatment. The results confirmed both the long-term neurotoxicity induced by MDMA, and the long-lasting neuroprotective effect of metformin in the SNc and in the CPu. According to previous studies (Granado et al., 2008), we observed in SNc a similar degeneration at 48 hours and 7 days after the MDMA administration; whereas, a slight recovery of DAergic fibers was detected in MDMA-treated mice sacrificed at 7 days, compared with mice of the same group sacrificed at 48 hours. Therefore, this study confirmed the persistent loss of DAergic cell bodies in the SNc following MDMA exposure, an effect that seems to involve cell death, and which is also accompanied by a decrease of TH and DAT fibers in the CPu.

On the basis of these long-term neurotoxic effects of MDMA, it is possible to speculate that exposure to MDMA may render the DAergic neurons more vulnerable to the detrimental effects of other insults in the neurodegenerative diseases (Moratalla et al., 2017). This hypothesis is proved by the higher incidence of PD reported in ATS abusers (Brust 2010; Christine et al., 2010; Callaghan et al., 2012; Curtin et al., 2015).

The neuroprotective effect of metformin on the neurodegenerative processes induced by MDMA could be particularly useful and in line with the neuroprotective properties of metformin

demonstrated in neurodegenerative disease models, such as PD (Patil et al., 2014), Alzheimer's disease (Potts & Lim 2012), and Huntington's disease (Ma et al., 2007).

Treatment with metformin for 5 weeks significantly ameliorated the degeneration of DAergic neurons in SNc, increased striatal DAergic levels, and improved motor impairment induced by MPTP toxin (Lu al., 2016).

On the other side, 2016 Ismaiel's study underlines that in mice, metformin did not prevent the negative effect of MPTP on DAergic neurons in SNc with a decrease in TH (+) neurons in an animal injected with MPTP for two days and treated with two daily doses of metformin for seven days (Ismaiel et al., 2016).

Furthermore, several reports proposed the hyperthermia as a mechanism related to the MDMA neurotoxicity (Green et al., 2004). In particular, several studies in experimental animals have indicated that MDMA-induced hyperthermia. Besides being harmful per se and causing dehydration and altered hydrosaline homeostasis (Green et al., 2004; Baylen & Rosenberg 2006), may also be one of the factors promoting glial activation and neurotoxicity, induced by this ATS (Miller & O'Callaghan 1995; Colado et al., 1999; Mechan et al., 2001).

Considering that one of the first effects of metformin intoxication is a drastic decrease in body temperature (Portela et al., 2015), we evaluated the ability of metformin to counteract the hyperthermic effects of MDMA. Therefore, we measured the animal body temperature 1 hour after each MDMA and metformin administration. The increase of body temperature showed by MDMA-treated mice confirmed the hyperthermic effect induced by the drug. However, the body temperature of metformin group did not change after the administrations, showing that lower doses of this antidiabetic drug are not able to induce hypothermia.

In addition, mice treated with MDMA plus metformin showed an increased body temperature induced after each MDMA administration, although we observed a significant decrease after the second metformin administration. Therefore, metformin pre-treatment is not able to prevent the hyperthermic effects of MDMA, not being able to exclude though that higher doses of metformin may decrease the MDMA-induced hyperthermia. At the same time, as suggested by the lower core temperature detected after the second dose of metformin, we cannot rule out that repeated metformin administration may cause MDMA-induced hyperthermia reduction. On this basis, we speculated that the neuroprotective effect of metformin in our experimental conditions does not appear mediated by a decrease of the MDMA-induced hyperthermic effects in mice during MDMA repeated administrations. Nevertheless, considering that the hyperthermic effects appear to be

correlated mainly with the 5-HT system, as shown by the administration of MDMA in rats (Commins et al., 1987), we cannot exclude that in different species the metformin could have a different effect on MDMA-induced hyperthermia and neurotoxicity.

One of the mechanisms proposed for the neuroprotection of metformin in the CNS is the activation of AMP-activated protein kinase (AMPK), which is a key regulator of cellular energy metabolism. On the other hand, in drosophila models of PD, AMPK activation, induced by metformin, alleviates DAergic dysfunction and mitochondrial abnormalities (Ng et al., 2012). However, the activation of AMPK exerts a protective effect against the neurotoxicity of 1-methyl-4-phenylpyridinium (MPP^+, neurotoxin that causes permanent symptoms of PD), and it has been proposed as a survival factor for DAergic neurons in PD (Choi et al., 2010). In particular, previous studies reported that metformin (Chakraborty et al., 2011; Patil et al., 2014) is able to counteract the oxidative stress, one of the principal mechanisms involved in neurodegenerative disease and MPTP neurotoxicity (Meredith & Kang 2006; Puerta et al., 2010).

Similarly, the increase in the antioxidant enzymes activity induced by metformin (Patil et al., 2014; Chakraborty et al., 2011) may lessen MDMA-induced ROS and NO species generation (Green et al., 2003; Puerta et al., 2010; Gorska et al., 2014). Finally, as shown by studies performed *in vivo* and *in vitro*, drugs that alter DA transmission, such as ATS, may affect neurogenesis and synaptogenesis (Rice & Barone 2000; Fasano et al., 2008; Goffin et al., 2010).

Wang et al. (2012) suggested that metformin promotes neurogenesis by activating an atypical protein kinase c (aPKC) CREB-binding protein (CBP) pathway. Moreover, CREB played a major role in neurodevelopment, synaptic plasticity, and neuroprotection (Sakamoto et al., 2011), promoting the transcription of brain-derived neurotrophic factor and TH (Piech-Dumas & Tank 1999). On this basis, restorative levels of TH immunoreactivity in mice treated with MDMA plus metformin suggest that one of the protective effects of metformin may be mediated by enhanced neurogenesis. In conclusion, the findings of this study showed that metformin treatment prevents the short- and long-term neurodegenerative effects of repeated MDMA administrations in adult mice, suggesting a therapeutic potential of this antidiabetic medication in the treatment of neurodegenerative processes.

Conclusions

In conclusion, the rapid escalation and maintenance of METH intake, inducing a significant increase in the expression of several IEGs in the NAc, but not in PFC, support the important role played by NAc in drug's addiction. The changes related to many clinical manifestations in METH-addicted patients include deficits in executive and memory functions, depression, and psychosis (Dean et al., 2013). Our gene expression data, thus, raise the possibility of the existence of some subpopulations of METH addicts, who might differentiate their response to pharmacological therapeutic approaches. However, further studies of the specific roles of individual genes will be necessary, in order to better understand the molecular and cellular processes involved in METH abuse. In addition, the punishment-based procedure proposed in our studies too, can be used to investigate mechanisms of relapse to drug abuse under conditions that more closely approximate the human condition.

Furthermore, the results on DA neuron degeneration by disclosing a higher vulnerability to MDMA of male Rhes$^{-/-}$ as compared with female, draws attention to the different response of the two genders to ATS drugs, suggesting a further concern on the use of these substances as recreational drugs. A previous paper (Pinna et al., 2016) suggests that Rhes$^{-/-}$ mice might represent a genetic model of PD, where to study mechanisms and vulnerability factors in PD. The results of a higher vulnerability to DAergic neurodegeneration of Rhes$^{-/-}$ male mice, as compared to female, reported in this thesis give support to the notion that these mice may represent a model of PD.

Moreover, findings of this thesis showed that metformin treatment prevents the short- and long-term neurodegenerative effects of repeated MDMA administrations in adult mice, suggesting a therapeutic potential of this antidiabetic medication in the treatment of neurodegenerative processes.

All together, these studies add important information to clarify cellular and molecular mechanisms involved in ATS-mediated abuse and neurotoxic effects, and the possible implications on neurodegenerative diseases such as PD.

References

- Abd-Elsameea AA, Moustaf AA, Mohamed AM. Modulation of the oxidative stress by metformin in the cerebrum of rats exposed to global cerebral ischemia and ischemia/reperfusion. Eur Rev Med Pharmacol Sci. 2014.
- Abekawa T, Ohmori T, Koyama T. Effects of repeated administration of a high dose of methamphetamine on dopamine and glutamate release in rat striatum and nucleus accumbens. Brain Res. 1994.
- Adinoff B. Neurobiologic processes in drug reward and addiction. Harv Rev Psychiatry. 2004.
- Afanador L, Mexhitaj I, Diaz C, Ordonez D, Baker L, Angulo JA. The role of the neuropeptide somatostatin on methamphetamine and glutamate-induced neurotoxicity in the striatum of mice. Brain Res. 2013.
- Altman J, Everitt BJ, Glautier S, Markou A, Nutt D, Oretti R, Phillips GD, Robbins TW. The biological, social and clinical bases of drug addiction: commentary and debate Psychopharmacology (Berl). 1996.
- Ares-Santos S, Granado N, Espadas I, Martinez-Murillo R, Moratalla R. Methamphetamine causes degeneration of dopamine cell bodies and terminals of the nigrostriatal pathway evidenced by silver staining. Neuropsychopharmacology. 2014.
- Ares-Santos S, Granado N, Oliva I, O'Shea E, Martin ED, Colado MI, Moratalla R. Dopamine D (1) receptor deletion strongly reduces neurotoxic effects of methamphetamine. Neurobiol Dis.2012.
- Axt KJ, Commins DL, Vosmer G, Seiden LS. alpha-Methyl-p-tyrosine pretreatment partially prevents methamphetamine-induced endogenous neurotoxin formation. Brain Res. 1990.
- Bae M.H., C.H. Jeong, S.H. Kim, M.K. Bae, J.W. Jeong, M.Y. Ahn, et al.Regulation of Egr-1 by association with the proteasome component C8 Biochim. Biophys. 2002.
- Baggott M, Mendelson J, Jones R. More about parkin- sonism after taking Ecstasy. N Engl J Med. 1999.
- Bahrami S, Drabløs F. Gene regulation in the immediate-early response process. Adv Biol Regul. 2016.
- Bali A, Jaggi AS. Electric foot shock stress: a useful tool in neuropsychiatric studies. Rev Neurosci. 2015.
- Bali A, Jaggi AS. Electric foot shock stress: a useful tool in neuropsychiatric studies. Rev Neurosci. 2015.
- Bang S, Steenstra C, Kim SF. Striatum specific protein, Rhes regulates AKT pathway. Neurosci Lett. 2012.
- Banks ML, Czoty PW, Gage HD, Bounds MC, Garg PK, Garg S, Nader MA. Effects of cocaine and MDMA self-administration on serotonin transporter availability in monkeys. Neuropsychopharmacology. 2008.
- Baylen CA, Rosenberg H. A review of the acute subjective effects of MDMA/ecstasy. Addiction. 2006.
- Becker, J. A. J., Kieffer, B. L., & Le Merrer, J. Differential behavioral and molecular alterations upon protracted abstinence from cocaine versus morphine, nicotine, THC and alcohol. Addiction Biology. 2016.
- Bellucci A, Mercuri NB, Venneri A, Faustini G, Longhena F, Pizzi M, Missale C, Spano P. Review: Parkinson's disease: from synaptic loss to connectome dysfunction. Neuropathol Appl Neurobiol. 2016.
- Bergers G, Graninger P, Braselmann S, Wrighton C, Busslinger M. Transcriptional activation of

the fra-1 gene by AP-1 is mediated by regulatory sequences in the first intron. Mol Cell Biol. 1995.
- Bernal, J., J. Numez. Thyroid hormones and brain development. Eur. J. Endocrinol. 1995.
- Beyer C, Karolczak M. Estrogenic stimulation of neurite growth in midbrain dopaminergic neurons depends on cAMP/protein kinase A signalling. J Neurosci Res. 2000.
- Björklund A, Dunnett SB. Dopamine neuron systems in the brain: an update. Trends Neurosci. 2007.
- Blech-Hermoni Y, Kiyatkin EA. State-dependent action of cocaine on brain temperature and movement activity: implications for movement sensitization. Pharmacol Biochem Behav. 2004.
- Borg GJ. More about parkinsonism after taking Ecstasy. N Engl J Med. 1999.
- Bowyer JF, Davies DL, Schmued L, Broening HW, Newport GD, Slikker W Jr, Holson RR. Further studies of the role of hyperthermia in methamphetamine neurotoxicity. J Pharmacol Exp Ther.; 1994.
- Bray GA. Use and abuse of appetite-suppressant drugs in the treatment of obesity. Ann Intern Med. 1993.
- Britt JP, Benaliouad F, McDevitt RA, Stuber GD, Wise RA, Bonci A. Synaptic and behavioral profile of multiple glutamatergic inputs to the nucleus accumbens. Neuron. 2012.
- Brodie, B. B., Cho, A. K. & Gessa, G. L. In Amphetamines and Related Compounds. Raven Press, New York; 1970.
- Brown JM, Hanson GR, Fleckenstein AE. Methamphetamine rapidly decreases vesicular dopamine uptake. J. Neurochem. 2000.
- Brown PL, Kiyatkin EA. Brain hyperthermia induced by MDMA (ecstasy): modulation by environmental conditions. Eur J Neurosci. 2004.
- Brown TA. Genomes. Bios Scientific Publishers Ltd. 2002.
- Brust JC. Substance abuse and movement disorders. Mov Disord. 2010.
- Cadet J. L., Jayanthi S., and Deng X., “Speed kills: cellular and molecular bases of methamphetamine-induced nerve terminal degeneration and neuronal apoptosis,” The FASEB Journal. 2003.
- Cadet JL, Brannock C, Jayanthi S, Krasnova IN. Transcriptional and epigenetic substrates of methamphetamine addiction and withdrawal: evidence from a long-access self-administration model in the rat. Mol Neurobiol. 2015.
- Cadet JL, Brannock C, Krasnova IN, Jayanthi S, Ladenheim B, McCoy MT, Walther D, Godino A, Pirooznia M, Lee RS. Genome-wide DNA hydroxymethylation identifies potassium channels in the nucleus accumbens as discriminators of methamphetamine addiction and abstinence. Mol Psychiatry. 2017.
- Cadet JL, Brannock C. Free radicals and the pathobiology of brain dopamine systems. Neurochem Int. 1998.
- Cadet JL, Krasnova IN, Jayanthi S, Lyles J. Neurotoxicity of substituted amphetamines: molecular and cellular mechanisms. Neurotox Res. 2007.
- Cadet JL, Krasnova IN, Walther D, Brannock C, Ladenheim B, McCoy MT, Collector D, Torres OV, Terry N, Jayanthi S. Increased expression of proenkephalin and prodynorphin mRNAs in the nucleus accumbens of compulsive methamphetamine taking rats. Sci Rep. 2016.
- Cadet JL, McCoy MT, Cai NS, Krasnova IN, Ladenheim B, Beauvais G, Wilson N, Wood W, Becker KG, Hodges AB. Methamphetamine preconditioning alters midbrain transcriptional responses to methamphetamine-induced injury in the rat striatum. PLoS One. 2009.
- Cahova M, Palenickova E, Dankova H, Sticova E, Burian M, Drahota Z, Cervinkova Z, Kucera O, Gladkova C, Stopka P, Krizova J, Papackova Z, Oliyarnyk O, Kazdova L. Metformin prevents

ischemia reperfusion-induced oxidative stress in the fatty liver by attenuation of reactive oxygen species formation. Am J Physiol Gastrointest Liver Physiol. 2015.
- Caldwell J, Dring LG, Williams RT. Metabolism of (14 C) methamphetamine in man, the guinea pig and the rat. Biochem J. 1972.
- Callaghan RC, Cunningham JK, Sykes J, Kish SJ. Increased risk of Parkinson's disease in individuals hospitalized with conditions related to the use of methamphetamine or other amphetamine-type drugs. Drug Alcohol Depend. 2012.
- Camarero J, Sanchez V, O'Shea E, Green AR, and Colado MI. Studies, using in vivo microdialysis, on the effect of the dopamine uptake inhibitor GBR 12909 on 3, 4-methylenedioxymethamphetamine (MDMA, "ecstasy")-induced dopamine release and free radical formation in the mouse striatum. *J Neurochem. 2002.*
- Cameron AR, Morrison VL, Levin D, Mohan M, Forteath C, Beall C, McNeilly AD, Balfour DJ, Savinko T, Wong AK, Viollet B, Sakamoto K, Fagerholm SC, Foretz M, Lang CC, Rena G. Anti-Inflammatory Effects of Metformin Irrespective of Diabetes Status. Circ Res. 2016.
- Capela JP, Carmo H, Remião F, Bastos ML, Meisel A, Carvalho F. Molecular and cellular mechanisms of ecstasy-induced neurotoxicity: an overview. Mol Neurobiol. 2009.
- Cardoso FE, Jankovic J. Cocaine-related movement disorders. Mov Disord. 1993.
- Chakraborty A, Chowdhury S, Bhattacharyya M. Effect of metformin on oxidative stress, nitrosative stress and inflammatory biomarkers in type 2 diabetes patients. Diabetes Res Clin Pract. 2011.
- Chiu R, Angel P, Karin M. Jun-B differs in its biological properties from, and is a negative regulator of, c-Jun. Cell. 1989.
- Choi JS, Park C, Jeong JW. AMP-activated protein kinase is activated in Parkinson's disease models mediated by 1-methyl-4- phenyl-1, 2, 3, 6-tetrahydropyridine. Biochem Biophys Res Commun. 2010.
- Christine CW, Garwood ER, Schrock LE, Austin DE, McCulloch CE. Parkinsonism in patients with a history of amphetamine exposure. Mov Disord. 2010.
- Colado MI, Camarero J, Mechan AO, Sanchez V, Esteban B, Elliott JM, and Green AR. A study of the mechanisms involved in the neurotoxic action of 3, 4-methylenedioxymethamphetamine (MDMA, "ecstasy") on dopamine neurones in mouse brain. Br J Pharmacol. 2001.
- Colado MI, O'Shea E, Granados R, Esteban B, Martín AB, Green AR. Studies on the role of dopamine in the degeneration of 5-HT nerve endings in the brain of Dark Agouti rats following 3, 4-methylenedioxymethamphetamine (MDMA or 'ecstasy') administration. Br J Pharmacol. 1999.
- Colado MI, Williams JL, Green AR. The hyperthermic and neurotoxic effects of 'Ecstasy' (MDMA) and 3, 4 methylenedioxyamphetamine (MDA) in the Dark Agouti (DA) rat, a model of the CYP2D6 poor metabolizer phenotype. Br J Pharmacol. 1995.
- Commins DL, Vosmer G, Virus RM, Woolverton WL, Schuster CR, Seiden LS. Biochemical and histological evidence that methylenedioxymethylamphetamine (MDMA) is toxic to neurons in the rat brain. J Pharmacol Exp Ther. 1987.
- Connor TJ, O'Shaughnessy D, Kelly JP. Methylenedioxymethamphetamine ('MDMA; Ecstasy') suppresses zymozan-induced oxidative burst in neutrophils. Ir J Med Sci. 2004.
- Cornish JL, Hunt GE, Robins L, McGregor IS. Regional c-Fos and FosB/ΔFosB expression associated with chronic methamphetamine self-administration and methamphetamine-seeking behavior in rats. Neuroscience. 2012.
- Costa A, Caltagirone C. Malattia di Parkinson e parkinsonismi - La prospettiva delle neuroscienze cognitive. Springer. 2009.

- Costa G, Frau L, Wardas J, Pinna A, Plumitallo A, Morelli M. MPTP-induced dopamine neuron degeneration and glia activation is potentiated in MDMA-pretreated mice. Mov Disord. 2013.
- Costa G, Morelli M, Simola N. Progression and Persistence of Neurotoxicity Induced by MDMA in Dopaminergic Regions of the Mouse Brain and Association with Noradrenergic, GABAergic, and Serotonergic Damage. Neurotox Res. 2017.
- Curran T, Franza BR Jr. Fos and Jun: the AP-1 connection. Cell. 1988.
- Curtin Karen, Annette E. Fleckenstein, Reid J. Robison Michael J. Crookston, Ken R. Smith, and Glen R. Hansonc. Methamphetamine/amphetamine abuse and risk of Parkinson's disease in Utah: a population-based assessment. Drug Alcohol Depend. 2015.
- Dao CK, Nowinski SM, Mills EM. The heat is on: molecular mechanisms of drug-induced hyperthermia. Temp Jour. 2014.
- de la Torre R, Yubero-Lahoz S, Pardo-Lozano R, Farré M. MDMA, methamphetamine, and CYP2D6 pharmacogenetics: what is clinically relevant? Front Genet. 2012.
- Dean AC, Groman SM, Morales AM, London ED. An evaluation of the evidence that methamphetamine abuse causes cognitive decline in humans. Neuropsychopharmacology. 2013.
- DeMaagd G, Philip A. Parkinson's Disease and Its Management: Part 1: Disease Entity, Risk Factors, Pathophysiology, Clinical Presentation, and Diagnosis. P T. 2015.
- Deng X, Ladenheim B, Tsao LI, Cadet JL. Null mutation of c-fos causes exacerbation of methamphetamine-induced neurotoxicity. J. Neurosci. 1999.
- Deng X, Wang Y, Chou J, Cadet JL. Methamphetamine causes widespread apoptosis in the mouse brain: evidence from using an improved TUNEL histochemical method. Brain Res. Mol. Brain Res. 2001.
- Deroche-Gamonet V, Belin D, Piazza PV. Evidence for addiction-like behavior in the rat. Science. 2004.
- Economidou D, Pelloux Y, Robbins TW, Dalley JW, Everitt BJ. High impulsivity predicts relapse to cocaine-seeking after punishment-induced abstinence. Biol Psychiatry. 2009.
- Errico F, Santini E, Migliarini S, Borgkvist A, Centonze D, Nasti V, Carta M, De Chiara V, Prosperetti C, Spano D, Herve D, Pasqualetti M, Di Lauro R, Fisone G, Usiello A. The GTP-binding protein Rhes modulates dopamine signalling in striatal medium spiny neurons. Mol Cell Neurosci. 2008.
- Everitt BJ. Neural and psychological mechanisms underlying compulsive drug seeking habits and drug memories--indications for novel treatments of addiction. Eur J Neurosci. 2014.
  exposure. Behav Brain Res. 2013.
- Falk JD, Vargiu P, Foye PE, Usui H, Perez J, Danielson PE, Lerner DL, Bernal J, Sutcliffe JG. Rhes: A striatal-specific Ras homolog related to Dexras1. J Neurosci Res. 1999.
- Fasano C, Poirier A, DesGroseillers L, Trudeau LE. Chronic activation of the D2 dopamine autoreceptor inhibits synaptogenesis in mesencephalic dopaminergic neurons in vitro. Eur J Neurosci. 2008.
- Feng J, Wilkinson M, Liu X, Purushothaman I, Ferguson D, Vialou V, Maze I, Shao N, Kennedy P, Koo J, Dias C, Laitman B, Stockman V, LaPlant Q, Cahill ME, Nestler EJ, Shen L. Chronic cocaine-regulated epigenomic changes in mouse nucleus accumbens. Genome Biol. 2014.
- Ferguson D, Koo JW, Feng J, Heller E, Rabkin J, Heshmati M, Renthal W, Neve R, Liu X, Shao N, Sartorelli V, Shen L, Nestler EJ. Essential role of SIRT1 signaling in the nucleus accumbens in cocaine and morphine action. J Neurosci. 2013.
- Fleckenstein AE, Volz TJ, Riddle EL, Gibb JW, Hanson GR. New insights into the mechanism of action of amphetamines. Annu Rev Pharmacol Toxicol. 2007.

- Foletta, V.C., D.H. Segal, and D.R. Cohen. Transcriptional regulation in the immune system: all roads lead to AP-1. J. Leukoc. Biol. 1998.
- Fox SH, Visanji N, Reyes G, Huot P, Gomez-Ramirez J, Johnston T, Brotchie JM. Neuropsychiatric behaviors in the MPTP marmoset model of Parkinson's disease. Can J Neurol Sci. 2010.
- Frau L, Simola N, Plumitallo A, Morelli M. Microglial and astroglial activation by 3, 4-methylenedioxymethamphetamine (MDMA) in mice depends on S (+) enantiomer and is associated with an increase in body temperature and motility. J Neurochem. 2013.
- Frau L, Simola N, Porceddu PF, Morelli M. Effect of crowding, temperature and age on glia activation and dopaminergic neurotoxicity induced by MDMA in the mouse brain. Neurotoxicology. 2016.
- Freudenmann RW, Oxler F, Bernschneider-Reif S. The origin of MDMA (ecstasy) revisited: the true story reconstructed from the original documents. Addiction. 2006.
- Fumagalli F, Gainetdinov RR, Valenzano KJ, Caron MG. Role of dopamine transporter in methamphetamine-induced neurotoxicity: evidence from mice lacking the transporter. J. Neurosci. 1998.
- Gao X, Chen H. Hyperthermia on skin immune system and its application in the treatment of human papillomavirus-infected skin diseases. Front Med. 2014.
- Gerfen CR, Keefe KA, Gauda EB. D1 and D2 dopamine receptor function in the striatum: coactivation of D1- and D2-dopamine receptors on separate populations of neurons results in potentiated immediate early gene response in D1-containing neurons. J Neurosci. 1995.
- Ghiglieri V, Napolitano F, Pelosi B, Schepisi C, Migliarini S, Di Maio A, Pendolino V, Mancini M, Sciamanna G, Vitucci D, Maddaloni G, Giampà C, Errico F, Nisticò R, Pasqualetti M, Picconi B, Usiello A. Rhes influences striatal cAMP/PKA-dependent signaling and synaptic plasticity in a gender-sensitive fashion. Sci Rep. 2015.
- Go´rska AM, Noworyta-Sokołowska K, Gołembiowska K. The effect of caffeine on MDMA-induced hydroxyl radical production in the mouse striatum. Pharmacol Rep. 2014.
- Goffin D, Ali AB, Rampersaud N, Harkavyi A, Fuchs C, Whitton PS, Nairn AC, Jovanovic JN. Dopamine-dependent tuning of striatal inhibitory synaptogenesis. J Neurosci. 2010.
- Gołembiowska K., Górska A.M., Kamińska K. Effect of caffeine on the release of DA, 5-HT and production of hydroxyl radical induced by methamphetamine and 3,4-methylenedioxymethamphetamine in the mouse striatum Dopamine, Alghero, 2013.
- Górska AM, Noworyta-Sokołowska K, Gołembiowska K. The effect of caffeine on MDMA-induced hydroxyl radical production in the mouse striatum. Pharmacol Rep. 2014.
- Granado N, Ares-Santos S, Moratalla R. Methamphetamine and Parkinson's disease. Parkinsons Dis. 2013.
- Granado N, Ares-Santos S, Oliva I, O'Shea E, Martin ED, Colado MI, Moratalla R. Dopamine D2-receptor knockout mice are protected against dopaminergic neurotoxicity induced by methamphetamine or MDMA. Neurobiol Dis. 2011.
- Granado N, Ares-Santos S, O'Shea E, Vicario-Abejón C, Colado MI, Moratalla R. Selective vulnerability in striosomes and in the nigrostriatal dopaminergic pathway after methamphetamine administration : early loss of TH in striosomes after methamphetamine. Neurotox Res. 2010.
- Granado N, Escobedo I, O'Shea E, Colado I, Moratalla R. Early loss of dopaminergic terminals in striosomes after MDMA administration to mice. Synapse. 2008.
- Graybiel AM, Moratalla R, Robertson HA. Amphetamine and cocaine induce drug-specific activation of the c-fos gene in striosome-matrix compartments and limbic subdivisions of the

striatum. Proc Natl Acad Sci U S A. 1990.
- Green AR, Mechan AO, Elliott JM, O'Shea E, Colado MI (2003) The pharmacology and clinical pharmacology of 3,4-methylenedioxymethamphetamine (MDMA, 'ecstasy'). Pharmacol Rev. 2003.
- Green AR, O'shea E, Colado MI. A review of the mechanisms involved in the acute MDMA (ecstasy)-induced hyperthermic response. Eur J Pharmacol. 2004.
- Greenberg ME, Ziff EB. Stimulation of 3T3 cells induces transcription of the c-fos proto-oncogene. Nature. 1984.
- Grob CS, Poland RE, Chang L, Ernst T. Psychobiologic effects of 3, 4 methylenedioxymethamphetamine in humans: methodological considerations and preliminary observations. Behav Brain Res. 1996.
- Grzanna and Brown. "Activation of immediate early genes by drugs of abuse" 2007, Nida research, monograph series. 2007.
- Guilarte T. R., "Is methamphetamine abuse a risk factor in Parkinsonism?" NeuroToxicology, 2001.
- Guilarte TR, Nihei MK, McGlothan JL, Howard AS. Methamphetamine-induced deficits of brain monoaminergic neuronal markers: distal axotomy or neuronal plasticity. Neuroscience. 2003.
- Halpin LE, Collins SA, Yamamoto BK. Neurotoxicity of methamphetamine and 3, 4 methylenedioxymethamphetamine Life Sci. 2014.
- Hansen JP, Riddle EL, Sandoval V, Brown JM, Gibb JW, Hanson GR, Fleckenstein AE. "Methylenedioxymethamphetamine decreases plasmalemmal and vesicular dopamine transport: mechanisms and implications for neurotoxicity". J. Pharmacol. Exp. Ther. 2002.
- Harrison LM, Lahoste GJ. The role of Rhes, Ras homolog enriched in striatum, in neurodegenerative processes. Exp Cell Res. 2013.
- Herdegen T, Leah JD. Inducible and constitutive transcription factors in the mammalian nervous system: control of gene expression by Jun, Fos and Krox, and CREB/ATF proteins. Brain Res Brain Res Rev. 1998.
- Hess J, Angel P, Schorpp-Kistner M. AP-1 subunits: quarrel and harmony among siblings. J Cell Sci. 2004.
- Hill CS, Treisman R. Transcriptional regulation by extracellular signals: mechanisms and specificity. Cell. 1995.
- Hirai SI, Ryseck RP, Mechta F, Bravo R, Yaniv M. Characterization of junD: a new member of the jun proto-oncogene family. EMBO J. 1989.
- Hyman S. The science of mental health. Volume 9. Routledge. 2001.
- Iravani MM, Asari D, Patel J, Wieczorek WJ, Kruk ZL. Direct effects of 3,4-methylenedioxymethamphetamine (MDMA) on serotonin or dopamine release and uptake in the caudate putamen, nucleus accumbens, substantia nigra pars reticulata, and the dorsal raphé nucleus slices. Synapse. 2000.
- Ismaiel AA, Espinosa-Oliva AM, Santiago M, García-Quintanilla A, Oliva-Martín MJ, Herrera AJ, Venero JL, de Pablos R. Metformin, besides exhibiting strong in vivo anti-inflammatory properties, increases mptp-induced damage to the nigrostriatal dopaminergic system. Toxicol Appl Pharmacol. 2016.
- Ivanova T, Beyer C. Estrogen regulates tyrosine hydroxylase expression in the neonate mouse midbrain. J Neurobiol. 2003.
- Jayanthi S, Deng X, Ladenheim B, McCoy MT, Cluster A, Cai NS, Cadet JL. Calcineurin/NFAT-induced up-regulation of the Fas ligand/Fas death pathway is involved in methamphetamine-induced neuronal apoptosis. Proceedings of the National Academy of Sciences of the United

States of America. 2005.
- Jayanthi S, McCoy MT, Chen B, Britt JP, Kourrich S, Yau HJ, Ladenheim B, Krasnova IN, Bonci A, Cadet JL. Methamphetamine downregulates striatal glutamate receptors via diverse epigenetic mechanisms. Biol Psychiatry. 2014.
- Jentsch JD, Taylor JR. Impulsivity resulting from frontostriatal dysfunction in drug abuse: implications for the control of behavior by reward-related stimuli. Psychopharmacology (Berl). 1999.
- Johnson MP, Hoffman AJ, Nichols DE. Effects of the enantiomers of MDA, MDMA and related analogues on [3H]serotonin and [3H]dopamine release from superfused rat brain slices. Eur J Pharmacol. 1986.
- Kagaya S, Hashida R, Ohkura N, Tsukada T, Sugita Y, Terakawa M, Tsujimoto G, Katsunuma T, Akasawa A, Matsumoto K, Saito H. NR4A orphan nuclear receptor family in peripheral blood eosinophils from patients with atopic dermatitis and apoptotic eosinophils in vitro. Int Arch Allergy Immunol. 2005.
- Kalant H. The pharmacology and toxicology of "ecstasy" (MDMA) and related drugs. CMAJ. 2001.
- Kalivas PW, O'Brien C. Drug addiction as a pathology of staged neuroplasticity. Neuropsychopharmacology. 2008.
- Kikuchi-Utsumi K, Ishizaka M, Matsumura N, Nakaki T. Alpha(1A)-adrenergic control of piloerection and palpebral fissure width in rats. Auton Neurosci. 2013.
- Kiyatkin EA, Ren S, Wakabayashi KT, Baumann MH, Shaham Y. Clinically Relevant Pharmacological Strategies That Reverse MDMA-Induced Brain Hyperthermia Potentiated by Social Interaction. Neuropsychopharmacology. 2016.
- Kiyatkin EA, Sharma HS. Expression of heat shock protein (HSP 72 kDa) during acute methamphetamine intoxication depends on brain hyperthermia: neurotoxicity or neuroprotection? J Neural Transm (Vienna). 2011.
- Kishi Y, Takahashi J, Koyanagi M, Morizane A, Okamoto Y, Horiguchi S, et al. Estrogen promotes differentiation and survival of dopaminergic neurons derived from human neural stem cells. J Neurosci Res. 2005.
- Koch S, Galloway MP. MDMA induced dopamine release in vivo: role of endogenous serotonin. J Neural Transm. 1997.
- Koob GF, Le Moal M. Drug abuse: hedonic homeostatic dysregulation. Science. 1997.
- Koob GF, Sanna PP, Bloom FE. Neuroscience of addiction. Neuron. 1998.
- Koob GF, Volkow ND. Neurobiology of addiction: a neurocircuitry analysis. Lancet Psychiatry. 2016.
- Koob GF, Volkow ND. Neurocircuitry of addiction. Neuropsychopharmacology. 2010.
- Koob GF. A role for brain stress systems in addiction. Neuron. 2008.
- Kousik SM, Graves SM, Napier TC, Zhao C, Carvey PM. Methamphetamine-induced vascular changes lead to striatal hypoxia and dopamine reduction. Neuroreport. 2011.
- Krasnova IN, Cadet JL. Methamphetamine toxicity and messengers of death. Brain Res Rev. 2009.
- Krasnova IN, Chiflikyan M, Justinova Z, McCoy MT, Ladenheim B, Jayanthi S, Quintero C, Brannock C, Barnes C, Adair JE, Lehrmann E, Kobeissy FH, Gold MS, Becker KG, Goldberg SR, Cadet JL. CREB phosphorylation regulates striatal transcriptional responses in the self-administration model of methamphetamine addiction in the rat. Neurobiol Dis. 2013.
- Krasnova IN, Justinova Z, Ladenheim B, Jayanthi S, McCoy MT, Barnes C, et al. Methamphetamine self-administration is associated with persistent biochemical alterations in

striatal and cortical dopaminergic terminals in the rat. PLoS ONE. 2010.
- Kuan YC, Huang KW, Lin CL, Hu CJ, Kao CH. Effects of metformin exposure on neurodegenerative diseases in elderly patients with type 2 diabetes mellitus. Prog Neuropsychopharmacol Biol Psychiatry. 2017.
- Kuhn DM, et al. Dopamine quinones activate microglia and induce a neurotoxic gene expression profile: relationship to methamphetamine-induced nerve ending damage. Ann N Y Acad Sci. 2006.
- Kukushkin A.N., Svetlikova S.B., Pospelov V.A. Effect of anisomycin on activation of early response genes c-fos, c-jun, Egr-1 in cells transformed by E1A and cHa-ras oncogenes Mol. Biol. 2005.
- Kuniyoshi SM, Jankovic J. MDMA and Parkinsonism. N Engl J Med. 2003.
- Kupferschmidt DA, Newman AE, Boonstra R, Erb S. Antagonism of cannabinoid 1 receptors reverses the anxiety-like behavior induced by central injections of corticotropin-releasing factor and cocaine withdrawal. 2011.
- Łabuzek K, Liber S, Gabryel B, Okopień B. Metformin has adenosine-monophosphate activated protein kinase (AMPK)-independent effects on LPS-stimulated rat primary microglial cultures. Pharmacol Rep. 2010.
- Laplante M, Sabatini DM. mTOR signaling in growth control and disease. Cell. 2012.
- Lee DY. Roles of mTOR Signaling in Brain Development. Exp Neurobiol. 2015.
- Le Merrer J., Befort K., Gardon O., Filliol D., Darcq E., Dembele D., Kieffer B. L. Protracted abstinence from distinct drugs of abuse shows regulation of a common gene network. Addiction Biology. 2012.
- Leranth C, Roth RH, Elsworth JD, Naftolin F, Horvath TL, Redmond DE Jr. Estrogen is essential for maintaining nigrostriatal dopamine neurons in primates: implications for Parkinson's disease and memory. J Neurosci. 2000.
- Lin LY, Di Stefano EW, Schmitz DA, Hsu L, Ellis SW, Lennard MS, Tucker GT, Cho AK. Oxidation of methamphetamine and methylenedioxymethamphetamine by CYP2D6. Drug Metab Dispos. 1997.
- Lipscombe D, Kongsamut S, Tsien RW. Alpha-adrenergic inhibition of sympathetic neurotransmitter release mediated by modulation of N-type calcium-channel gating. Nature. 1989.
- Liu J., L. Grogan, M.M. Nau, C.J. Allegra, E. Chu, J.J. WrightPhysical interaction between p53 and primary response gene Egr-1, Int. J. Oncol. 2001.
- Logan BJ, Laverty R, Sanderson WD, and Yee YB. Differences between rats and mice in MDMA (methylenedioxymethamphetamine) neurotoxicity. Eur J Pharmacol. 1988.
- Long X, Lin Y, Ortiz-Vega S, Yonezawa K, Avruch J. Rheb binds and regulates the mTOR kinase. Curr Biol. 2005.
- Lu M, Su C, Qiao C, Bian Y, Ding J, Hu G. Metformin Prevents Dopaminergic Neuron Death in MPTP/P-Induced Mouse Model of Parkinson's Disease via Autophagy and Mitochondrial ROS Clearance. Int J Neuropsychopharmacol. 2016.
- Lynch WJ, Nicholson KL, Dance ME, Morgan RW, Foley PL. Animal models of substance abuse and addiction: implications for science, animal welfare, and society. Comp Med. 2010.
- Ma TC, Buescher JL, Oatis B, Funk JA, Nash AJ, Carrier RL, Hoyt KR. Metformin therapy in a transgenic mouse model of Huntington's disease. Neurosci Lett. 2007.
- Maki Y, Bos TJ, Davis C, Starbuck M, Vogt PK. Avian sarcoma virus 17 carries the jun oncogene. Proc Natl Acad Sci U S A. 1987.
- Mariani JJ, Levin FR. Treatment strategies for co-occurring ADHD and substance use disorders.

Am J Addict. 2007.
- Mark KA, Soghomonian JJ, Yamamoto BK. High-dose methamphetamine acutely activates the striatonigral pathway to increase striatal glutamate and mediate long-term dopamine toxicity. J Neurosci. 2004.
- Martin TA, Jayanthi S, McCoy MT, Brannock C, Ladenheim B, Garrett T, Lehrmann E, Becker KG, Cadet JL. Methamphetamine causes differential alterations in gene expression and patterns of histone acetylation/hypoacetylation in the rat nucleus accumbens. PLoS One. 2012.
- Mazzoni P, Shabbott B, Cortés JC. Motor control abnormalities in Parkinson's disease. Cold Spring Harb Perspect Med. 2012.
- McCoy MT, Jayanthi S, Wulu JA, Beauvais G, Ladenheim B, Martin TA, Krasnova IN, Hodges AB, Cadet JL. Chronic methamphetamine exposure suppresses the striatal expression of members of multiple families of immediate early genes (IEGs) in the rat: normalization by an acute methamphetamine injection. Psychopharmacology (Berl). 2011.
- McFadden LM, Hadlock GC, Allen SC, Vieira-Brock PL, Stout KA, Ellis JD, Hoonakker AJ, Andrenyak DM, Nielsen SM, Wilkins DG, Hanson GR, Fleckenstein AE. Methamphetamine self-administration causes persistent striatal dopaminergic alterations and mitigates the deficits caused by a subsequent methamphetamine exposure. J Pharmacol Exp Ther. 2012.
- McGuinness T. Methamphetamine abuse. Am J Nurs. 2006.
- Mechan AO, Esteban B, O'Shea E, Elliott JM, Colado MI, and Green AR. The pharmacology of the acute hyperthermic response that follows administration of 3,4-methylenedioxymethamphetamine (MDMA, “ecstasy”) to rats. Br J Pharmacol. 2002.
- Mechan AO, O'Shea E, Elliott JM, Colado MI, Green AR. A neurotoxic dose of 3,4-methylenedioxymethamphetamine (MDMA; ecstasy) to rats results in a long-term defect in thermoregulation. Psychopharmacology (Berl). 2001.
- Meinhardt, M. W., Hansson, A. C., Perreau-Lenz, S., Bauder-Wenz, C., Stählin, O., Heilig, M., Sommer, W. H. Rescue of infralimbic mGluR2 deficit restores control over drug-seeking behavior in alcohol dependence. Journal of Neuroscience. 2013.
- Meredith CW, Jaffe C, Ang-Lee K, Saxon AJ. Implications of chronic methamphetamine use: a literature review. Harv Rev Psychiatry. 2005.
- Meredith GE, Kang UJ. Behavioral models of Parkinson’s disease in rodents: a new look at an old problem. Mov Disord. 2006.
- Metzger RR, Haughey HM, Wilkins DG, Gibb JW, Hanson GR, Fleckenstein AE. Methamphetamine-induced rapid decrease in dopamine transporter function: role of dopamine and hyperthermia. J Pharmacol Exp Ther. 2000.
- Mychasiuk, R., Muhammad, A., Ilnytskyy, S., & Kolb, B. Persistent gene expression changes in NAc, mPFC, and OFC associated with previous nicotine or amphetamine exposure. Behavioural Brain Research. 2013.
- Miller DB, O'Callaghan JP. Elevated environmental temperature and methamphetamine neurotoxicity. Environ Res. 2003.
- Miller DB, O'Callaghan JP. Environment-, drug- and stress-induced alterations in body temperature affect the neurotoxicity of substituted amphetamines in the C57BL/6J mouse. J Pharmacol Exp Ther. 1994.
- Miller DB, O'Callaghan JP. The role of temperature, stress, and other factors in the neurotoxicity of the substituted amphetamines 3,4-methylenedioxymethamphetamine and fenfluramine. Mol Neurobiol. 1995.
- Mintzer S, Hickenbottom S, Gilman S. Parkinsonism after taking Ecstasy . N Engl J Med. 1999.

- Miyazaki I., Asanuma M., Diaz-Corrales F. J. et al., “Methamphetamine-induced dopaminergic neurotoxicity is regulated by quinone formation-related molecules,” The FASEB Journal. 2006.
- Mooney ME, Herin DV, Schmitz JM, Moukaddam N, Green CE, Grabowski J. Effects of oral methamphetamine on cocaine use: a randomized, double-blind, placebo-controlled trial. Drug Alcohol Depend. 2009.
- Moratalla R, Khairnar A, Simola N, Granado N, Garcı´a-Montes JR, Porceddu PF, Tizabi Y, Costa G, Morelli M (2015) Amphetamine-related drugs neurotoxicity in humans and experimental animals: Main mechanisms. Prog Neurobiol 2015.
- Moratalla R, Robertson HA, Graybiel AM. Dynamic regulation of NGFI-A (zif268, egr1) gene expression in the striatum. J Neurosci. 1992.
- Morton J. Ecstasy: pharmacology and neurotoxicity. Curr Opin Pharmacol. 2005.
- Mychasiuk R, Muhammad A, Ilnytskyy S, Kolb B. Persistent gene expression changes in NAc, mPFC, and OFC associated with previous nicotine or amphetamine. 2013.
- Nagai T, Kamiyama S, Nagai T. Forensic toxicologic analysis of methamphetamine and amphetamine optical isomers by high performance liquid chromatography. Z Rechtsmed. 1988.
- Nash JF, Yamamoto BK. Methamphetamine neurotoxicity and striatal glutamate release: comparison to 3,4-methylenedioxymethamphetamine. Brain Res. 1992.
- Neale A, Abraham S, Russell J. "Ice" use and eating disorders: a report of three cases. Int J Eat Disord. 2009.
- Nestler EJ, Barrot M, Self DW. DeltaFosB: a sustained molecular switch for addiction. Proc Natl Acad Sci. 2001.
- Nestler EJ. Molecular mechanisms of drug addiction. J Neurosci. 1992.
- Ng CH, Guan MS, Koh C, Ouyang X, Yu F, Tan EK, O’Neill SP, Zhang X, Chung J, Lim KL. AMP kinase activation mitigates dopaminergic dysfunction and mitochondrial abnormalities in Drosophila models of Parkinson’s disease. J Neurosci. 2012.
- Nicholls DG. Mitochondrial dysfunction and glutamate excitotoxicity studied in primary neuronal cultures. Curr Mol Med. 2004.
- O'Connor MN, Gallagher P, Byrne S, O'Mahony D. Adverse drug reactions in older patients during hospitalisation: are they predictable? Age Ageing. 2012.
- O'Donnell A, Odrowaz Z, Sharrocks AD. Immediate-early gene activation by the MAPK pathways: what do and don't we know? Biochem Soc Trans. 2012.
- Okuno H. Regulation and function of immediate-early genes in the brain: beyond neuronal activity markers. Neurosci. Res. 2011.
- Orsini CA, Moorman DE, Young JW, Setlow B, Floresco SB. Neural mechanisms regulating different forms of risk-related decision-making: insights from animal models. Neurosci Biobehav Rev. 2015.
- O'Shea E, Esteban B, Camarero J, Green AR, and Colado MI. Effect of GBR 12909 and fluoxetine on the acute and long term changes induced by MDMA (“ecstasy”) on the 5-HT and dopamine concentrations in mouse brain. Neuropharmacology. 2001.
- O'Shea E, Granados R, Esteban B, Colado MI, Green AR. The relationship between the degree of neurodegeneration of rat brain 5-HT nerve terminals and the dose and frequency of administration of MDMA ('ecstasy'). Neuropharmacology. 1998.
- Osterndorff-Kahanek, E. A., Becker, H. C., Lopez, M. F., Farris, S. P., Tiwari, G. R., Nunez, Y. O. Mayfield, R. D. Chronic ethanol exposure produces time- and brain region-dependent changes in gene coexpression networks. PLoS ONE. 2015.
- O'Suilleabhain P, Giller C. Rapidly progressive parkinsonism in a self-reported user of ecstasy

and other drugs. Mov Disord. 2003.
- Panlilio LV, Goldberg SR. Self-administration of drugs in animals and humans as a model and an investigative tool. Addiction. 2007.
- Parkes SL, Bradfield LA, Balleine BW. Interaction of insular cortex and ventral striatum mediates the effect of incentive memory on choice between goal-directed actions. J Neurosci. 2015.
- Patil SP, Jain PD, Ghumatkar PJ, Tambe R, Sathaye S. Neuroprotective effect of metformin in MPTP-induced Parkinson's disease in mice. Neuroscience. 2014.
- Paxinos and Franklin's the Mouse Brain in Stereotaxic Coordinates 3th Edition. Neur 2008.
- Pelloux Y, Murray JE, Everitt BJ. Differential vulnerability to the punishment of cocaine related behaviours: effects of locus of punishment, cocaine taking history and alternative reinforcer availability. Psychopharmacology (Berl). 2015.
- Piech-Dumas KM, Tank AW. CREB mediates the cAMPresponsiveness of the tyrosine hydroxylase gene: use of an antisense RNA strategy to produce CREB-deficient PC12 cell lines. Brain Res Mol Brain Res. 1999.
- Piechota, M., Korostynski, M., Sikora, M., Golda, S., Dzbek, J., & Przewlocki, R. Common transcriptional effects in the mouse striatum following chronic treatment with heroin and methamphetamine. *Genes, Brain & Behavior*. 2012.
- Pinna A, Napolitano F, Pelosi B, Di Maio A, Wardas J, Casu MA, Costa G, Migliarini S, Calabresi P, Pasqualetti M, Morelli M, Usiello A. The Small GTP-Binding Protein Rhes Influences Nigrostriatal-Dependent Motor Behavior During Aging. Mov Disord. 2016.
- Portela LV, Gnoatto J, Brochier AW, Haas CB, de Assis AM, de Carvalho AK, Hansel G, Zimmer ER, Oses JP, Muller AP. Intracerebroventricular metformin decreases body weight but has pro-oxidant effects and decreases survival. Neurochem Res. 2015.
- Potts MB, Lim DA. An old drug for new ideas: metformin promotes adult neurogenesis and spatial memory formation. Cell Stem Cell. 2012.
- Puerta E, Hervias I, Gon˜i-Allo B, Zhang SF, Jorda´n J, Starkov AA, Aguirre. Methylenedioxymethamphetamine inhibits mitochondrial complex I activity in mice: a possible mechanism underlying neurotoxicity. Br J Pharmacol. 2010.
- Quintero GC, Spano D, Lahoste GJ, Harrison LM. The Ras homolog Rhes affects dopamine D1 and D2 receptor-mediated behavior in mice. Neuroreport. 2008.
- Quintero GC, Spano D. Exploration of sex differences in Rhes effects in dopamine mediated behaviors. Neuropsychiatr Dis Treat. 2011.
- Radi, R, Beckman JS, Bush KM, Freeman BA “Peroxynitrite oxidation of sulfhydryls. The cytotoxic potential of superoxide and nitric oxide. J. Biol. Chem. 1991.
- Rahmani SH, Ahmadi S and Moghaddam HH. Serotonin Syndrome Following Single Ingestion of High Dose Methamphetamine. J Clinic Toxicol. 2011.
- Rani A, Greenlaw R, Runglall M, Jurcevic S, John S. FRA2 is a STAT5 target gene regulated by IL-2 in human CD4 T cells. PLoS One. 2014.
- Reisert I, Han V, Lieth E, Toran-Allerand D, Pilgrim C, Lauder J. Sex steroids promote neurite growth in mesencephalic tyrosine hydroxylase immunoreactive neurons in vitro. Int J Dev Neurosci. 1987.
- Ricaurte GA, McCann UD. Neurotoxic amphetamine analogues: effects in monkeys and implications for humans. Ann N Y Acad Sci. 1992.
- Ricaurte GA, Schuster CR, Seiden LS. Long-term effects of repeated methylamphetamine administration on dopamine and serotonin neurons in the rat brain: a regional study. Brain Res. 1980.

- Ricaurte GA, Yuan J, Hatzidimitriou G, Cord BJ, McCann UD. Severe dopaminergic neurotoxicity in primates after a common recreational dose regimen of MDMA ("ecstasy"). Science. 2002. Retracted Article.
- Rice D, Barone S Jr. Critical periods of vulnerability for the developing nervous system: evidence from humans and animal models. Environ Health Perspect. 2000.
- Riddle EL, Topham MK, Haycock JW, Hanson GR, Fleckenstein AE. "Differential trafficking of the vesicular monoamine transporter-2 by methamphetamine and cocaine". Eur. J. Pharmacol. 2002.
- Robertson HA, Peterson MR, Murphy K, Robertson GS. D1-dopamine receptor agonists selectively activate striatal c-fos independent of rotational behaviour. Brain Res. 1989.
- Robinson TE, Berridge KC. The neural basis of drug craving: an incentive-sensitization theory of addiction. Brain Res Brain Res Rev. 1993.
- Rothman RB, Baumann MH. Monoamine transporters and psychostimulant drugs. Eur J Pharmacol. 2003.
- Rubio I, Wittig U, Meyer C, Heinze R, Kadereit D, Waldmann H, Downward J, Wetzker R. Farnesylation of Ras is important for the interaction with phosphoinositide 3-kinase gamma. Eur J Biochem. 1999.
- Rudnick G, Wall SC. The molecular mechanism of "ecstasy" [3,4-methylenedioxy-methamphetamine (MDMA)]: serotonin transporters are targets for MDMA-induced serotonin release. Proc Natl Acad Sci U S A. 1992.
- Rusyniak DE. Neurologic manifestations of chronic methamphetamine abuse. Neurol Clin. 2011.
- Ryder K, Lanahan A, Perez-Albuerne E, Nathans D. jun-D: a third member of the jun gene family. Proc Natl Acad Sci U S A. 1989.
- Saisho Y. Metformin and Inflammation: Its Potential Beyond Glucose-lowering Effect. Endocr Metab Immune Disord Drug Targets. 2015.
- Saito M, Terada M, Saito TR, Takahashi KW. Effects of the long-term administration of methamphetamine on body weight, food intake, blood biochemistry and estrous cycle in rats. Exp Anim. 1995.
- Sakamoto K, Karelina K, Obrietan K. CREB: a multifaceted regulator of neuronal plasticity and protection. J Neurochem. 2011.
- Sandoval V, Hanson GR, Fleckenstein AE. Methamphetamine decreases mouse striatal dopamine transporter activity: roles of hyperthermia and dopamine. Eur J Pharmacol. 2000.
- Sawada H, Ibi M, Kihara T, Honda K, Nakamizo T, Kanki R, et al. Estradiol protects dopaminergic neurons in a MPP^+ Parkinson's disease model. Neuropharmacology. 2002.
- Schepers RJ, Oyler JM, Joseph RE Jr, Cone EJ, Moolchan ET, Huestis MA. Methamphetamine and amphetamine pharmacokinetics in oral fluid and plasma after controlled oral methamphetamine administration to human volunteers. Clin Chem. 2003.
- Schmidt CJ, Levin JA, Lovenberg W. In vitro and in vivo neurochemical effects of methylenedioxymethamphetamine on striatal monoaminergic systems in the rat brain. Biochem Pharmacol. 1987.
- Schwendt M, Reichel CM, See RE. Extinction-dependent alterations in corticostriatal mGluR2/3 and mGluR7 receptors following chronic methamphetamine self-administration in rats. PLoS One. 2012.
- Sciamanna G, Napolitano F, Pelosi B, Bonsi P, Vitucci D, Nuzzo T, Punzo D, Ghiglieri V, Ponterio G, Pasqualetti M, Pisani A, Usiello A. Rhes regulates dopamine D2 receptor transmission in striatal cholinergic interneurons. Neurobiol Dis. 2015.

- Shaham Y, Stewart J. Stress reinstates heroin-seeking in drug-free animals: an effect mimicking heroin, not withdrawal. Psychopharmacology. 1995.
- Shahani N, Swarnkar S, Giovinazzo V, Morgenweck J, Bohn LM, Scharager-Tapia C, Pascal B, Martinez-Acedo P, Khare K, Subramaniam S. RasGRP1 promotes amphetamine-induced motor behavior through a Rhes interaction network ("Rhesactome") in the striatum. Sci Signal. 2016.
- Shankaran M, Gudelsky GA. A neurotoxic regimen of MDMA suppresses behavioral, thermal and neurochemical responses to subsequent MDMA administration. Psychopharmacology (Berl). 1999.
- Shepard JD, Bossert JM, Liu SY, Shaham Y. The anxiogenic drug yohimbine reinstates methamphetamine seeking in a rat model of drug relapse. Biol Psychiatry. 2004.
- Smith KM, Dahodwala N. Sex differences in Parkinson's disease and other movement disorders. Exp Neurol. 2014.
- Sonsalla PK, Jochnowitz ND, Zeevalk GD, Oostveen JA, Hall ED. Treatment of mice with methamphetamine produces cell loss in the substantia nigra. Brain Res. 1996.
- Sonsalla, P.K., Riordan, D.E., and Heikkila, R.E. Competitive and noncompetitive antagonists an N-methyl-D-aspartate receptors protect against methamphetamine-induced dopaminergic damage in mice. J. Pharm. Exp. Therm. 1991.
- Spano D, Branchi I, Rosica A, Pirro MT, Riccio A, Mithbaokar P, Affuso A, Arra C, Campolongo P, Terracciano D, Macchia V, Bernal J, Alleva E, Di Lauro R. Rhes is involved in striatal function. Mol Cell Biol. 2004.
- Sprague J., Everman S. L., & Nichols D. E. An integrated hypothesis for the serotonergic axonal loss induced by 3, 4-methylenedioxymethamphetamine. Neurotoxicology. 1998.
- Stephans SE, Whittingham TS, Douglas AJ, Lust WD, Yamamoto BK. Substrates of energy metabolism attenuate methamphetamine-induced neurotoxicity in striatum. Journal of neurochemistry. 1998.
- Stone DM, Hanson GR, Gibb JW. Differences in the central serotonergic effects of methylenedioxymethamphetamine (MDMA) in mice and rats. Neuropharmacology. 1987.
- Stone DM, Johnson M, Hanson GR, Gibb JW. Role of endogenous dopamine in the central serotonergic deficits induced by 3,4-methylenedioxymethamphetamine. J Pharmacol Exp Ther. 1988.
- Sulzer D, Schmitz Y. Parkinson's disease: return of an old prime suspect. Neuron. 2007.
- Sulzer D, Sonders MS, Poulsen NW, Galli A. Mechanisms of neurotransmitter release by amphetamines: a review. Prog Neurobiol. 2005.
- Tansey MG, McCoy MK, Frank-Cannon TC. Neuroinflammatory mechanisms in Parkinson's disease: potential environmental triggers, pathways, and targets for early therapeutic intervention. Exp Neurol. 2007.
- Tetradis S, Bezouglaia O, Tsingotjidou A, Vila A. Regulation of the nuclear orphan receptor Nur77 in bone by parathyroid hormone. Biochem Biophys Res Commun.2001.
- Thapliyal A, Bannister RA, Hanks C, Adams BA. The monomeric G proteins AGS1 and Rhes selectively influence Galphai-dependent signaling to modulate N-type (CaV2.2) calcium channels. Am J Physiol Cell Physiol. 2008.
- Theberge FR, Li X, Kambhampati S, Pickens CL, St Laurent R, Bossert JM, Baumann MH, Hutchinson MR, Rice KC, Watkins LR, Shaham Y. Effect of chronic delivery of the Toll-like receptor 4 antagonist (+)-naltrexone on incubation of heroin craving. Biol Psychiatry. 2013.
- Theberge FR, Pickens CL, Goldart E, Fanous S, Hope BT, Liu QR, Shaham Y. Association of time-dependent changes in mu opioid receptor mRNA, but not BDNF, TrkB, or MeCP2 mRNA and protein expression in the rat nucleus accumbens with incubation of heroin craving.

Psychopharmacology (Berl). 2012.
- Thiriet N, Jayanthi S, McCoy M, Ladenheim B, Cadet JL. Methamphetamine increases expression of the apoptotic c-myc and L-myc genes in the mouse brain. Brain Res Mol Brain Res. 2001.
- Thomas DM, Francescutti-Verbeem DM, Kuhn DM. The newly synthesized pool of dopamine determines the severity of methamphetamine-induced neurotoxicity. J Neurochem. 2008.
- Thrash B, Thiruchelvan K, Ahuja M, Suppiramaniam V, Dhanasekaran M. Methamphetamine-induced neurotoxicity: the road to Parkinson's disease. Pharmacol Rep. 2009.
- Todd G, Noyes C, Flavel SC, Della Vedova CB, Spyropoulos P, Chatterton B, Berg D, White JM. Illicit stimulant use is associated with abnormal substantia nigra morphology in humans. PLoS One. 2013.
- Torres OV, Jayanthi S, Ladenheim B, McCoy MT, Krasnova IN, Cadet JL. Compulsive methamphetamine taking under punishment is associated with greater cue-induced drug seeking in rats. Behav Brain Res. 2017.
- Towler MC, Hardie DG. AMP-activated protein kinase in metabolic control and insulin signaling. Circ Res. 2007.
- United Nations Office on Drugs and Crime (2000). World Drug Report. 2000.
- Vargiu P, Morte B, Manzano J, Perez J, de Abajo R, Gregor Sutcliffe J, Bernal J. Thyroid hormone regulation of rhes, a novel Ras homolog gene expressed in the striatum. Brain Res Mol Brain Res. 2001.
- Verrico CD, Miller GM, Madras BK. MDMA (Ecstasy) and human dopamine, norepinephrine, and serotonin transporters: implications for MDMA-induced neurotoxicity and treatment. Psychopharmacology (Berl). 2007.
- Vitucci D, Di Giorgio A, Napolitano F, Pelosi B, Blasi G, Errico F, Attrotto, MT, Gelao B, Fazio L, Taurisano P, Di Maio A, Marsili V, Pasqualetti M, BertolinoA, Usiello A. Rasd2 Modulates Prefronto-Striatal Phenotypes in Humans and 'Schizophrenia-Like Behaviors' in Mice. Neuropsychopharmacology. 2016.
- Volkow ND, Chang L, Wang GJ, Fowler JS, Franceschi D, Sedler M, Gatley SJ, Miller E, Hitzemann R, Ding YS, Logan J. Loss of dopamine transporters inmethamphetamine abusers recovers with protracted abstinence. J Neurosci. 2001.
- Volkow ND, Morales M. The Brain on Drugs: From Reward to Addiction. Cell. 2015.
- Volkow ND, Wang GJ, Fowler JS, Tomasi D. Addiction circuitry in the human brain. Annu Rev Pharmacol Toxicol. 2012.
- Wang J, Gallagher D, DeVito LM, Cancino GI, Tsui D, He L, Keller GM, Frankland PW, Kaplan DR, Miller FD. Metformin activates an atypical PKC-CBP pathway to promote neurogenesis and enhance spatial memory formation. Cell Stem Cell. 2012.
- Wang JQ, Smith AJ, McGinty JF. A single injection of amphetamine or methamphetamine induces dynamic alterations in c-fos, zif/268 and preprodynorphin messenger RNA expression in rat forebrain. Neuroscience. 1995.
- Westfall TC and Westfall DP “Adrenergic agonsists and antagonists”, in Goodman & Gilman's The
- Wilson JM, Levey AI, Rajput A, Ang L, Guttman M, Shannak K, Niznik HB, Hornykiewicz O, Pifl C, Kish SJ. Differential changes in neurochemical markers of striatal dopamine nerve terminals in idiopathic Parkinson's disease. Neurology. 1996.
- Xie T, Tong L, McCann UD, Yuan J, Becker KG, Mechan AO, Cheadle C, Donovan DM, Ricaurte GA. Identification and characterization of metallothionein-1 and -2 gene expression in the context of (+/-)3,4-methylenedioxymethamphetamine-induced toxicity to brain dopaminergic

neurons. J Neurosci. 2004.
- Yager LM, Garcia AF, Wunsch AM, Ferguson SM. The ins and outs of the striatum: role in drug addiction. Neuroscience. 2015.
- Yamamoto BK, Moszczynska A, Gudelsky GA. Amphetamine toxicities: classical and emerging mechanisms. Ann N Y Acad Sci.; 2010.
- Yamamoto BK, Moszczynska A, Gudelsky GA. Amphetamine toxicities: classical and emerging mechanisms. Ann N Y Acad Sci. 2010.
- Yamamoto BK, Zhu W. The effects of methamphetamine on the production of free radicals and oxidative stress. J Pharmacol Exp Ther. 1998.
- Young ST, Porrino LJ, Iadarola MJ. Cocaine induces striatal c-fos-immunoreactive proteins via dopaminergic D1 receptors. Proc Natl Acad Sci USA. 1991.
- Zhang F., M. Lin, P. Abidi, G. Thiel, J. LiuSpecific interaction of Egr1 and c/EBPbeta leads to the transcriptional activation of the human low density lipoprotein receptor gene J. Biol. Chem. 2003.